

**A GEOSTATISTICAL APPRAISAL OF THE RELATIONSHIPS
BETWEEN GROUNDWATER YIELDS AND SELECTED GEOELECTRIC
PARAMETERS AT DIFFERENT CONFIDENCE INTERVALS IN PARTS
OF THE BASEMENT COMPLEX OF OSUN STATE**

BY
MARIAM ALAKE KASALI
(GLY/2014/023)

**A THESIS SUBMITTED TO THE DEPARTMENT OF GEOLOGY,
OBAFEMI AWOLOWO UNIVERSITY, ILE-IFE, OSUN STATE, IN
PARTIAL FULFILMENT OF THE REQUIREMENTS FOR THE AWARD
OF BACHELOR OF SCIENCE IN APPLIED GEOPHYSICS**

JUNE 2019

CERTIFICATION

This is to certify that Kasali Mariam Alake (GLY/2014/023) carried out this Thesis under my supervision in accordance with the partial fulfilment for the award of the Bachelor of Science Degree in Applied Geophysics of the Department of Geology, Faculty of Science, Obafemi Awolowo University, Ile-Ife.

.....
Dr. D.E. Falebita

.....
Date:

Supervisor

DEDICATION

I want to dedicate this work to God Almighty, the beginning and the end of everything. Also to my parents, Dr. R. Kasali and Mrs. Fatimat Kasali. Thank you for being my support system.

ACKNOWLEDGEMENT

I wish to express my gratitude to God Almighty for the gift of life and privilege. My profound gratitude goes to my supervisor, Dr. D.E. Falebita for his guidance and assistance in spite of tight schedule towards the success of this project. He takes his time to supervise, brainstorm and make necessary corrections on the project. Thank you a million times sir.

I wish to appreciate all my lecturers in the Department of Geology, Obafemi Awolowo University, Ile-Ife, for their various and invaluable contributions to my academic pursuit. I want to specially appreciate Prof. M.O. Olorunfemi, Prof M.T. Olowookere, Prof. V.O. Olarewaju. Prof. M.A. Rahaman, Dr. A.A. Adepelumi, Dr. O.A Alao, Dr. O. Afolabi, Dr. S.A. Adekola (Head of Department), Dr. A.O. Olorunfemi, Dr B.M. Salami and Mr Fadahunsi for their contributions, teachings and support in the course of my studies, may God crown their efforts with success.

Furthermore, my sincere appreciation goes to my parents for never giving up on me, for always giving me their moral and financial support any time I needed it. And to my siblings Kasali Saheed and Kasali Ismael, thank you for your support.

Finally, I would not forget my colleagues Ejzie Karen, Ugbome Adaeze, Olufidipo Julius, Agbai Paul GodsWill and the entire students of the Department of Geology, Obafemi Awolowo University. Thank you for your friendship.

TABLE OF CONTENTS

TITLE	PAGES
TITLE PAGE	
CERTIFICATION	i
DEDICATION	ii
ACKNOWLEDGEMENTS	iii
TABLE OF CONTENTS	iv
LIST OF FIGURES	vii
LIST OF TABLES	ix
ABSTRACT	x
CHAPTER ONE: INTRODUCTION	
1.0 Background of the Study	1
1.2 Location of the Study Area	2
1.3 Relief, Climate and Vegetation of the Study Area	2
1.4 Aim and Objectives	4
1.5 Previous Work	4
1.6 Expected Contribution to Knowledge	4
CHAPTER TWO: GEOLOGY OF THE STUDY AREA	
2.1 General Introduction	6
2.1.1 The Migmatite-gneiss-quartzite Complex	8
2.1.2 Slightly Migmatized to Non-migmatized Metasedimentary and Metaigneous rocks.	8
2.1.3 Charnockitic, Gabbroic and Dioritic rocks.	8

2.1.4 Older Granite Suite	9
2.1.5 Metamorphosed to Un-metamorphosed Alkaline volcanic and Hyper-basal Rocks	9
2.1.6 Un-metamorphosed Dolerite Dykes, Syenite Dykes	9
2.2 Geology of the Study Area	10
2.3 PRINCIPLES AND THEORIES OF GEOSTATISTICS	12
2.3.1 Definition of Geostatistics	12
2.3.2 Geostatistics workflow	13
2.3.3 Methods used in Geostatistics	14
a) Semi Variogram	15
b) Kriging	19
c) Simulation	19

CHAPTER THREE: METHODOLOGY

3.1 Vertical Electrical Sounding Technique	21
3.1.1 Electrode Configuration	21
• Schlumberger Electrode Array	22
3.1.2 Data Presentation	22
3.1.3 Data Interpretation	26
3.2 Determination of the Coefficient of Anisotropy	32
3.3 Geostatistical Method: Introduction	33
3.3.1 Techniques used for Geostatistics Method	33
a) (Semi)Variogram	33
b) Kriging	33
3.4 Data Processing	34

3.4.1 Conversion of Krigged mean (m) and standard deviation (σ) values to three confidence intervals	34
---	----

3.4.2 Multivariate Regression Analysis of Yield and Geoelectric Parameters	34
--	----

3.4.3 Finding the Best Fit Yield Equation from the Confident Intervals	36
--	----

CHAPTER FOUR: RESULTS AND DISCUSSION

4.1 VES Results	37
-----------------	----

4.1.1 The VES Map.	37
--------------------	----

4.1.2 The VES Type Curves	37
---------------------------	----

4.1.3 The VES General Interpretation	43
--------------------------------------	----

4.1.4 Results from the Aquifer Zone	47
-------------------------------------	----

4.2 Geostatistics Results	48
---------------------------	----

4.2.1 Variogram Plots	48
-----------------------	----

4.2.2 Kriging	53
---------------	----

4.3 Result of the Multivariate Regression Analysis.	58
---	----

4.3.1 The Governing Regression Models at each Distribution Levels.	60
--	----

4.3.2 Relationship Between New and Original Yield Values.	61
---	----

4.3.3 Best Fit Yield Prediction Equation.	64
---	----

CHAPTER FIVE: CONCLUSION AND RECOMMENDATION

5.1 Conclusion	69
----------------	----

5.2 Recommendation	70
REFFERENCE S	71
APPENDIX	74

LIST OF FIGURES

FIGURES	CAPTIONS	PAGES
1.1	Map Showing Location of the Study Area.	3
2.1	The Geological Map of Nigeria. (Obaje 2009)	7
2.2	The Geology of the Study Area.	11
2.3	Parts of a Variogram (Bohling. 2007)	16
2.4	Types of Variogram Models. (Igel, 2007)	18
3.1	Schlumberger Electrode Configuration.	23
3.2	Other common Electrode Arrays.	24
3.3	Four Typical Three Layer Curves	25
3.4	Two layers Master curves	28
3.5	The Log-Log Paper	29
3.6	K and Q Type Auxiliary curve	30
3.7	The A and H Type Auxiliary Curve	31
3.8	Flow Chat of Steps in Performing a Geostatistical Estimation	35
4.1	Map Showing the 39 VES Positions	38
4.2	The Curve Types (A) HKH Curve, (B) H Curve and (C) HA Curves	40
4.3	The Curve Types (D) AKH Curve and (E) KH Curve	42
4.4	Variogram Plot for Coefficient of Anisotropy	50
4.5	Variogram Plot for Resistivity	51
4.6	Variogram Plot for Thickness	52

4.7	Variogram Plot for Yield	53
4.8	Kriged Contoured Coefficient of Anisotropy Map	51
4.9	Kriged Contoured Resistivity Map	56
4.10	Kriged Contoured Thickness Data	57
4.11	Kriged Contoured Yield Data	58
4.12	Superimposed Map of the Geologic Map and Kriged Mean Maps	59
4.13	Relationship Between Original Yield and Estimated Yield at 99.73%	63
4.14	Relationship Between Original Yield and Estimated Yield at 95.45%	66
4.15	Relationship Between Original Yield and Estimated Yield at 68.27%	68

LIST OF TABLES

TABLES	CAPTIONS	PAGES
4.1	A Summary of the VES Interpretation Results	47
4.2	The VES Results and Coefficient of Anisotropy the Aquifer Zone.	49
4.3	Relationship Between the Original and Estimated Yield Values at 99.73%	62
4.4	Relationship Between the Original and Estimated Yield Values at 95.45%	65
4.5	Relationship Between the Original and Estimated Yield Values at 68.27%	67

ABSTRACT

This study used geostatistics to appraise the relationships that exist between groundwater yields and three selected geoelectric parameters of thickness, resistivity and coefficient of anisotropy at different distribution levels in the basement complex of northeastern part of Osun State. This was done in other to know the levels at which we could have the highest correlation between geoelectric parameters and groundwater yield, also to know if geoelectric parameters are enough to predict groundwater yield.

The methodology involved collecting secondary VES data from the northeastern part of Osun State. The VES data were interpreted using partial curve matching technique and computer assisted 1D forward modelling. The coefficient of anisotropy was calculated from the geoelectric parameters (aquifer layer resistivity and thickness) using Dar-Zarrouk's method. Geostatistics and a multivariate regression analysis were subsequently carried out on the data. Geostatistics was used to extrapolate data beyond the 39 points, using SURFER for the variogram modelling and kriging of the data, these data were converted to three confidence intervals of 99.73%, 95.45% and 68.27% using the mean and standard deviation estimate derived from kriging. A multivariate regression analysis was done afterwards on the estimated data at the three confidence intervals and relationships between yield and the geoelectric parameters at the different distribution levels were obtained.

The results showed a linear relationship and correlation between the groundwater yields and the geoelectric parameters with the multivariate regression analysis model obtained. The confidence interval at 99.73% gave the highest correlation of 60%, followed by 95.45% (confidence

interval) which gave a correlation of 49% and 68.27% (confidence interval) which gave a correlation of 34% between groundwater yield and the geoelectric parameters. Also, correlating the original 39 yield to the newly estimated yield generated by applying the regression models/equations gotten by the multivariate regression analysis at the different confidence intervals gave us the highest correlation of 7% at 99.73% confidence interval and the lowest of 6.86% at 68.27% confidence interval.

In conclusion, the study showed a positive linear relationship of not more than 60% correlation between groundwater yield and geoelectric parameters in the study area. The remaining 40% is an indication that the three geoelectric parameters are not the only contributing factors to yield values of the area.

CHAPTER ONE

INTRODUCTION

1.0 BACKGROUND OF THE STUDY

The VES technique is a geophysical technique which measures the vertical variations in the resistivity of subsurface layers with depth (Telford *et al*, 1990). It usually involves the use of different kind of arrays such as Wenner, Schlumberger, Dipole-Dipole etc. in acquiring data. The VES data are processed by using the partial curve matching technique (Bhattacharya, 1968) and further interpreted with the use of software like WinResist and interpretVES. The parameters often gotten from the interpretation of VES data are thickness and resistivity of the different rock layers. The electrical anisotropy occurs when electric current flow within the earth varies with azimuth (Whitman, 2017). It is often determined from the longitudinal conductance, transverse resistance, thickness, resistivity, longitudinal resistivity and transverse resistivity of each layer.

Geostatistical method is an extremely important aspect of modern geosciences as it helps us in unsampled data estimation. It is used generally to populate area with no data by using available data. It involves methods like variogram which assumes a trend for the data and kriging which does the estimation (Bohling, 2007). Overtime, there has been increase in the use of this method as it saves time, money and energy used in going to acquire primary data. Also, with recent inventions, the method can now be carried out using computer software packages.

A multivariate regression analysis involves the prediction of a dependent variation (Y) from two or more Independent variables (Xi) (Liu, 2018). To perform an accurate multivariate regression

on our data, the R software has proved very useful in doing this. Mogaji, 2015 has successfully used the software to generate yield prediction equations.

Geostatistics is a reliable and fast method of prediction. It can be used to predict any regionalized variables by taking into consideration the condition surrounding the data.

1.2 LOCATION OF THE STUDY AREA

Geographically, the study area is located in the northeastern part of Osun State Nigeria, within latitudes $7^{\circ}48'150^{11}N$ to $8^{\circ}3'29^{11}N$ and longitudes $4^{\circ}36'22^{11}E$ to $4^{\circ}55'21^{11}E$. It covers Okuku, Ota, Ikorun, Iragbiji and Imesi-ile. Osun State is bounded in the west by Oyo State and Ogun State, in the north by Kwara State and in the east by Ekiti State and Ondo State (Fig 1.1).

1.3 RELIEF, CLIMATE AND VEGETATION OF THE STUDY AREA

The study area is situated in the tropical rain forest. It is found in a state which covers an area of approximately 14,875 sq. km. though situated in a landlocked area, it is drained by many rivers and streams which serve the water needs of the study area. The area has an elevation of 246 meters' average above sea level. The topography is uneven and characterized by ridges, hills and valleys. The uneven topography is caused by the crystalline nature of the rocks found in the area which make them resistant to weathering. The climate is tropical. The average annual temperature in the area is about $28^{\circ}C$. Precipitation in the study area is about 1340 mm. The driest month is January and the most precipitation falls in September. (climate-model, 2018).

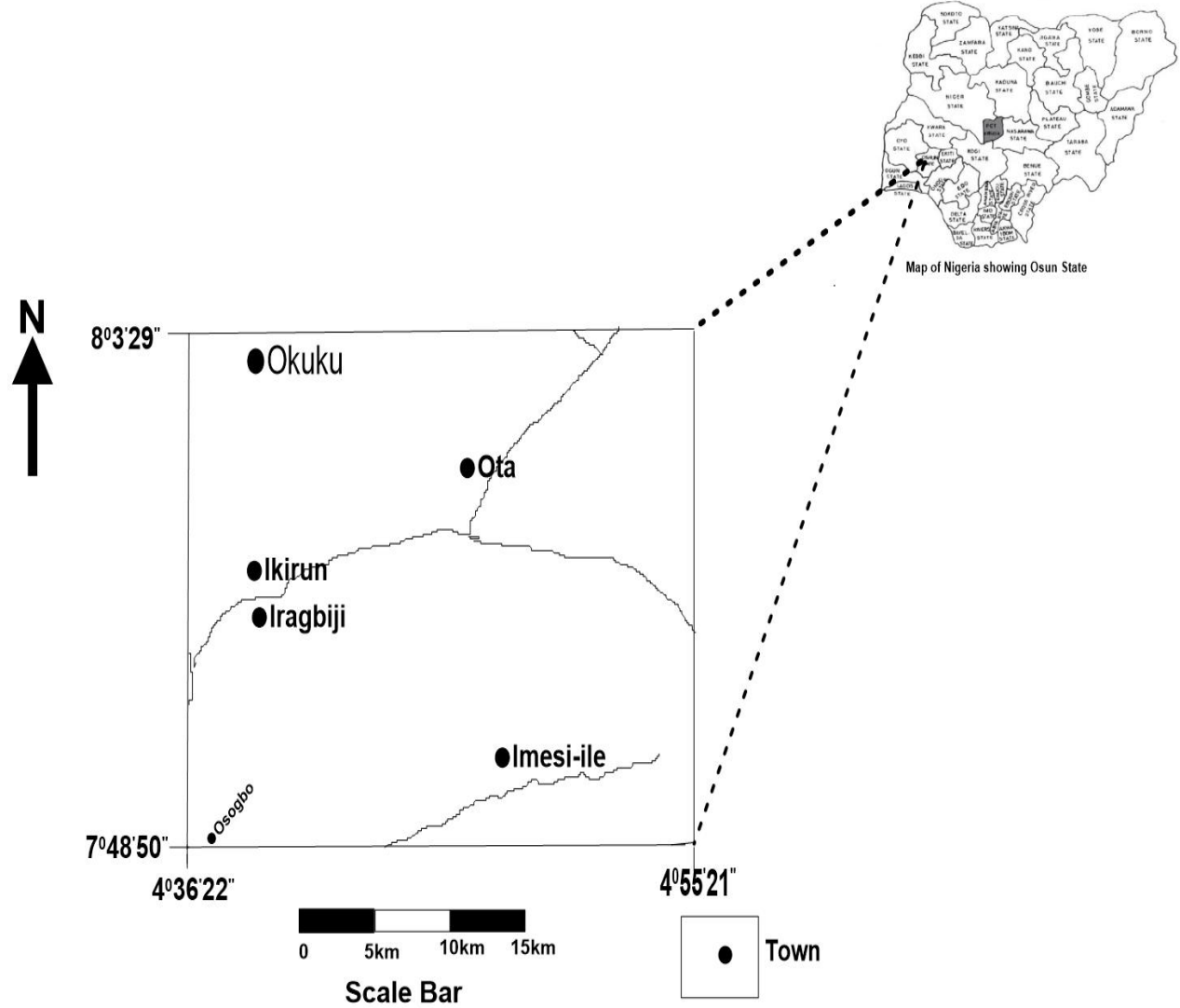


Figure 1.1: Map Showing Location of the Study Area (after NGSA, 2006)

1.4 AIM AND OBJECTIVES

The aim of the study is to investigate the relationship between groundwater yield and three geoelectric parameters of thickness, resistivity and coefficient of anisotropy in parts of the basement complex of Osun State using multivariate statistical analysis. The objectives of the study are to:

- a) acquire and interpret VES data for geoelectric parameters of thickness, resistivity and coefficient of anisotropy at the aquifer layer.
- b) estimate unsampled locations of the geoelectric parameters and borehole yield using geostatistics; and
- c) investigate the geostatistical relationships between yields and the estimated geoelectric parameters at different confidence intervals.

1.5 PREVIOUS WORK

There have been reasonable measures of interest in borehole yield prediction, VES data interpretation and the use of geostatistical method. The following authors whose works were reviewed is as follows:

Mogaji (2015), carried out a research on ‘Geoelectrical parameter-based multivariate regression borehole yield model for predicting aquifer yield in managing groundwater resource sustainability’. He successfully generated an equation for calculating yield using the R software from interpretation result of VES parameters (layer resistivity, thickness and electrical anisotropy).

Ezeh *et al.* (2013) carried out a research on ‘Using the relationships between geoelectrical and hydrogeological parameters to assess aquifer productivity in Udi LGA, Enugu State, Nigeria’. They concluded that the well yield parameter was strongly correlated with well yield conditioning factors. The efficiency of regression-based techniques in determining borehole yields from relevant borehole yield conditioning parameters obtained from different sources was also established.

Ungemach *et al.* (1969) carried out research on ‘Emphasis in determination of transmissivity coefficient and application in Nappe alluvial aquifer Rhine’. They concluded that The Electrical resistivity method can be widely used for the quantitative estimation of the water transmitting properties of aquifers, aquifer zone delineation and the evaluation of the geophysical properties of aquifer zones in several locations.

TaheriTizro *et al.* (2007) carried out a research on ‘Groundwater balance, safe yield and recharge feasibility in a semi-Arid environment: A case study from western part of Iran’. The authors concluded that the aquifer was overexploited.

1.6 Expected Contribution to knowledge

This study will improve the knowledge of the statistical correlation that exist between groundwater yield and geoelectric parameters in the study area.

CHAPTER TWO

GEOLOGY OF THE STUDY AREA

2.1 GENERAL INTRODUCTION

Nigeria lies south of the Sahara within the west Africa, with the Atlantic Ocean bordering the southern coastal region. The entire country lies within latitudes $4^{\circ}10'$ to $13^{\circ}48'N$ and longitudes $2^{\circ}50'$ to $14^{\circ}20' E$. Nigeria lies in the heart of the Pan-African mobile belt between the west African craton and Congo craton. The geology of Nigeria is made up of the crystalline rocks and the cretaceous-recent sedimentary rocks (Fig 2.1). The crystalline rocks are further subdivided into; Precambrian crystalline rocks which makes up 50% of the land surface of Nigeria (Rahaman, 1988), Mesozoic to Tertiary granites, Volcanic and Quaternary alluvial deposit (Kogbe 1989).

Several authors such as Oyawoye (1972), Okezie (1974), McCurry (1976), and Rahaman (1976) among others made the earliest review of the Nigerian Basement complex. Okezie (1974) geological map of Nigeria shows that the Basement complex can be distinctly divided into two zones (western and eastern zones).

Rahaman (1988) classified the basement complex rocks of SW into six major groups namely;

- Migmatite-Gniess-Quartzite Complex.
- Slightly Migmatized to Non-migmatized Metasedimentary and Metaigneous rocks (schist belts).
- Charnockitic, Gabbroic and Dioritic rocks
- Older Granites.
- Metamorphosed to Unmetamorphosed Alkaline Volcanic and Hyperbassal rocks

- Unmetamorphosed Dolerite dykes, Syenite dykes

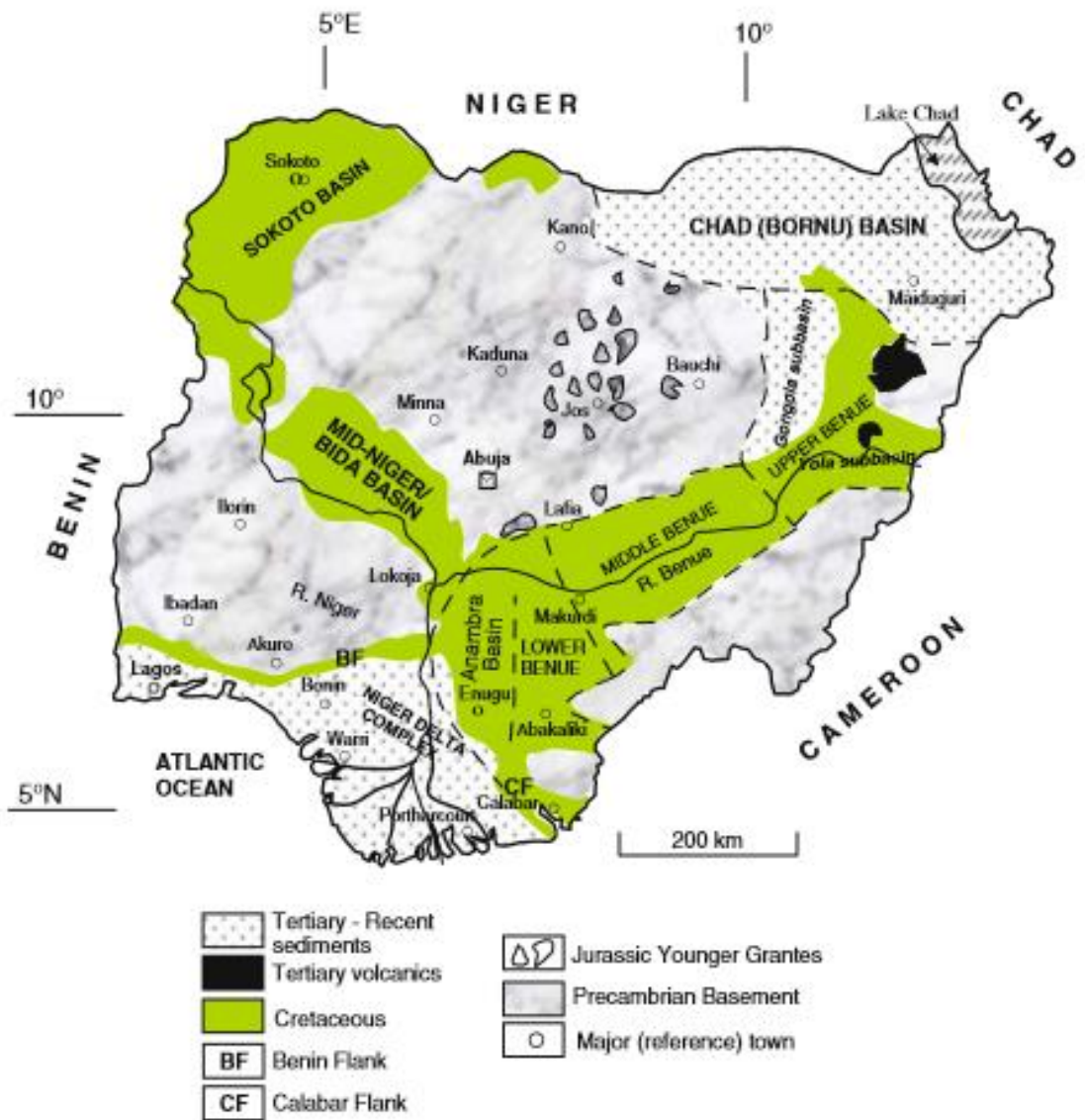


Figure 2.1: The Geological Map of Nigeria. (Obaje 2009)

2.1.1 The Migmatite-Gneiss-Quartzite Complex

This is the most abundant rock group. It comprises migmatitic and granitic gneisses; basic schists and gneisses. This group occupies about thirty percent of the total surface area of Nigeria. (McCurry, 1976). There are three main components of the Migmatite-gneiss-quartzite complex namely;

- Grey foliated biotite
- Biotite hornblende
- Early gneiss

2.1.2 Slightly Migmatized to Non-migmatized Metasedimentary and Metaigneous rocks

These rocks have been called different names from ‘Newer Sediments’ by Oyawoye (1964). ‘Schist Belts’ by Ajibade (1976) to ‘Younger Metasediments’ by McCurry (1976). The schist belts consist of supra-crustal sedimentary successions. Lithologically the schist belts are composed predominantly of metamorphosed pelitic-semi pelitic rocks, sandstones, calcareous rocks, acid to intermediate volcanic rocks and ultramafites. Upper Proterozoic age was suggested for the schist belts by McCurry (1976), Rahaman (1976), and Ajibade *et al* (1987). A total number of twelve schist belts have been mapped within Nigeria basement complex in which three fall within the southern part of Nigeria. They include the Ife-Ilesha schist Belt, the Igarra Schist Belt and the Iseyin-Oyan River Schist Belt.

2.1.3 Charnockitic, Gabbroic and Dioritic Rocks

Some authors consider these rocks to belong to the older granite suite (Ajibade *et al.*, 1987; Okezie, 1974). These rocks have three main modes of occurrence. First, it occurs as the core to

an aureole of granitic rocks. Second, they occur along the margins of older Granite bodies. Thirdly, they occur as discrete individual bodies within the Migmatite gneiss complex.

Rahaman (1976) reviewed the available evidence and suggested a Pan African age, and, geochronological studies by Tubosun (1984) confirmed a Pan African age for these charnockites.

2.1.4 Older Granite Suite

The older Granites include a wide range of rocks from the granodioritic to granite to Syenite. They account for 40-50% of the basement outcrop. They are the most obvious manifestations of the Pan-African Orogeny. They occur largely as distinct plutons often of batholithic dimensions.

2.1.5 Metamorphosed to Unmetamorphosed Alkaline Volcanic and Hyperbassal rocks

The most important of these are the tuffs, rhyolites, rhyodacites and dacite. Similar chemically to high K-calc-alkaline volcanic and Hyperbassal rocks presently occurring at the margins of the pacific Orogenic belts.

2.1.6 Unmetamorphosed Dolerite dykes, Syenite dykes

They are the youngest of all. Dolerite dykes are widespread in the basement complex. They occur as tabular unmetamorphosed bodies. They cross-cut pre-existing foliation in host rocks. The Syenites occur as dykes and as sills in the Igarre Kabba-Jakura Lokoja Schist belts.

2.2 GEOLOGY OF THE STUDY AREA

The study area is located within the crystalline basement complex terrain of southwestern Nigeria. The area is generally underlain by basement rocks categorized by Rahaman (1976) as banded gneiss, granite gneiss, schist undifferentiated, porphyritic granite and pegmatite. The area is dominated by metamorphic rocks which show evidence of several episodes of deformation and metamorphism. It is also covered by reddish brown laterite probably derived from weathering of the crystalline basement rocks. There are four major faults seen striking in the northeast direction. The general sequence of the subsurface layers of rock is often Topsoil to weathered layer to Fresh basement.

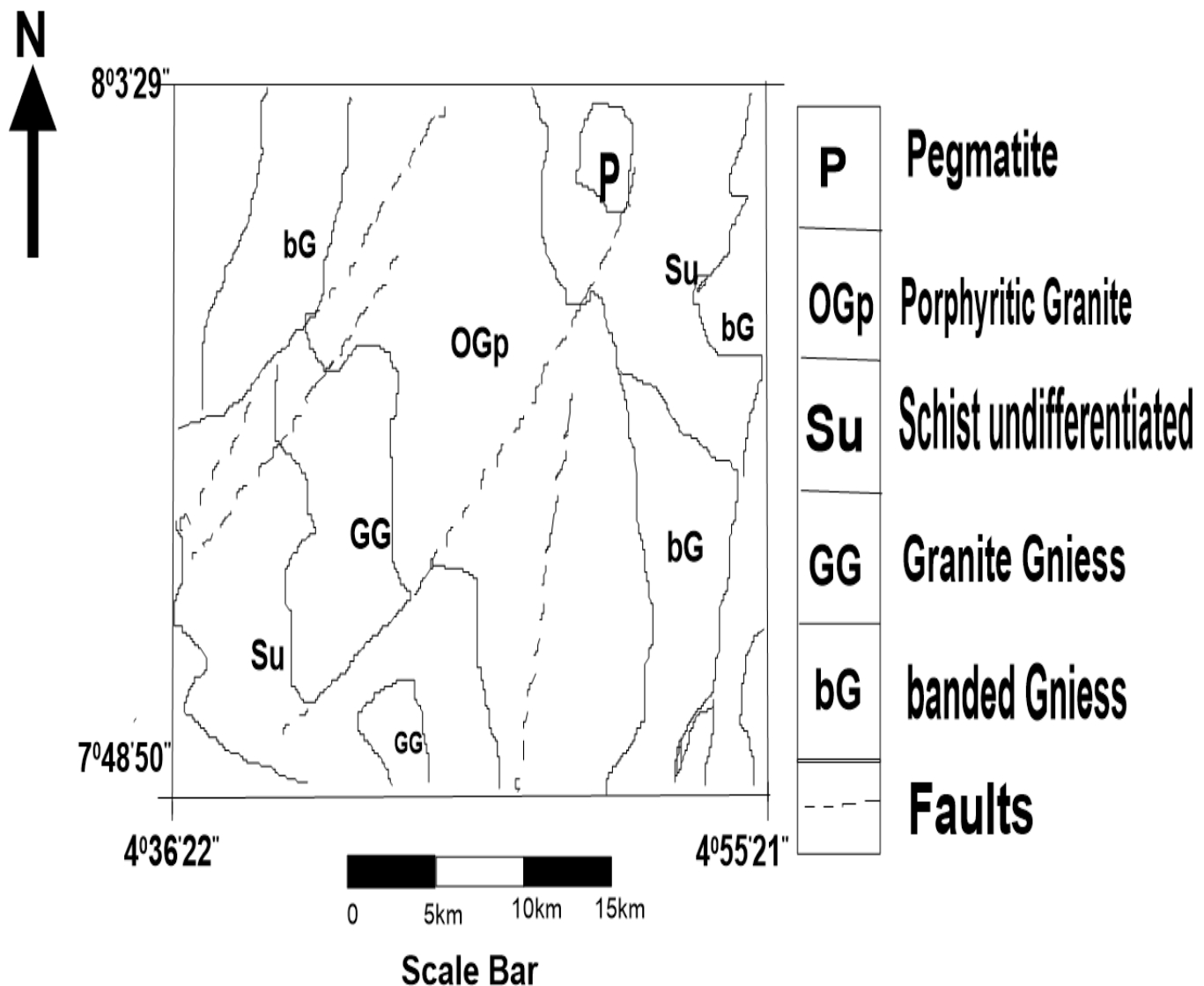


Figure 2.2: The Geology of the Study Area (after NGSA, 2006)

2.3 PRINCIPLES AND THEORIES OF GEOSTATISTICS

2.3.1 Definition of Geostatistics

As defined by Caers (2005), geostatistics is the branch of statistical sciences that studies spatial/temporal phenomena and capitalizes on spatial relationships to model possible values of variable(s) at unobserved, unsampled locations.

Also, Deutsch (2002) sees geostatistics as the study of phenomena that vary in space and/or time.

Olea (1999) also regarded it as a collection of numerical techniques that deal with the characterization of spatial attributes, employing primarily random models in a manner similar to the way in which time series analysis characterizes temporal data.

Lastly, Isaaks and Srivastava (1989) said geostatistics offers a way of describing the spatial continuity of natural phenomena and provides adaptations of classical regression techniques to take advantage of this continuity.

Generally, geostatistics is a tool used in doing the following to a data;

- Summarize a data
- estimate/populate unsampled points
- determine the uncertainty and reliability of an estimate
- Quantify the risk associated with an estimate

2.3.2 Geostatistics workflow

- a) Data Audit/Analysis: Here, data are being analysed in order to know the kind of data we are working on. There are three different classes of data that can work with geostatistical predictions (Bohling, 2007);
 - I. Continuous variables that usually represent physical properties (e.g. mineral grade, layer thickness)
 - II. Categorical variables (e.g. lithofacies, geological units, grade envelopes)
 - III. Objects that are defined by their location, shape and orientation (e.g. sedimentary channels, mineral grains).
- b) Spatial Analysis/Modelling: This involves the use of deterministic techniques in characterizing data. Here, a single map of all the estimated data are produced using the variogram and kriging techniques (Bohling, 2007).
- c) Mapping/Stochastic Simulation: In simulation, maps of the data at different probability level are produced which in turn could produce realizations (Vann et al, 2002).
- d) Uncertainty Analysis: Simulation would also help us here in testing the reliability of our estimates (Vann et al, 2002).

It should be noted that, Geostatistical methods are most accurate when data are

- normally distributed and

- stationary (mean and variance do not vary significantly in space)

2.3.3 Methods used in Geostatistics

a) **SEMI VARIOGRAM:** The variogram technique is a method that tests the degree of dissimilarity between two variables in space. (Bohling, 2007)

Similar to correlation and covariance computation, variogram is computed with the following formula;

$$\text{Semivariance: } Y(h) = \frac{1}{2N(h)} \sum_{\alpha=1}^{N(h)} (z(u_{\alpha} + h) - z(u_{\alpha}))^2 \quad (2.1)$$

Where,

u : vector of spatial coordinates

$z(u)$: variable under consideration as a function of spatial location

h : lag vector representing separation between two spatial locations

$z(u+h)$: lagged version of variable under consideration

$N(h)$: representing the number of pairs separated by lag h

The semivariogram obey the following relationships

$$y(\mathbf{h}) = C(0) - C(\mathbf{h}) \quad (2.2)$$

where $C(0)$ is known as the sill and $C(\mathbf{h})$ is the covariance.

Geostatisticians typically work with the semivariogram because the semivariogram often averages out the effect of spatially varying mean data.

Characteristics of a Variogram

As shown in Fig. 2.3,

Sill ($C(0)$): The sill is the maximum variance of usefulness.

Range(a): The range is the maximum lag distance of usefulness at which the semivariogram reaches the sill value. Data beyond the range distance are considered not useful for the correlation.

Nugget: this occurs when the variogram plot does not start from the origin.

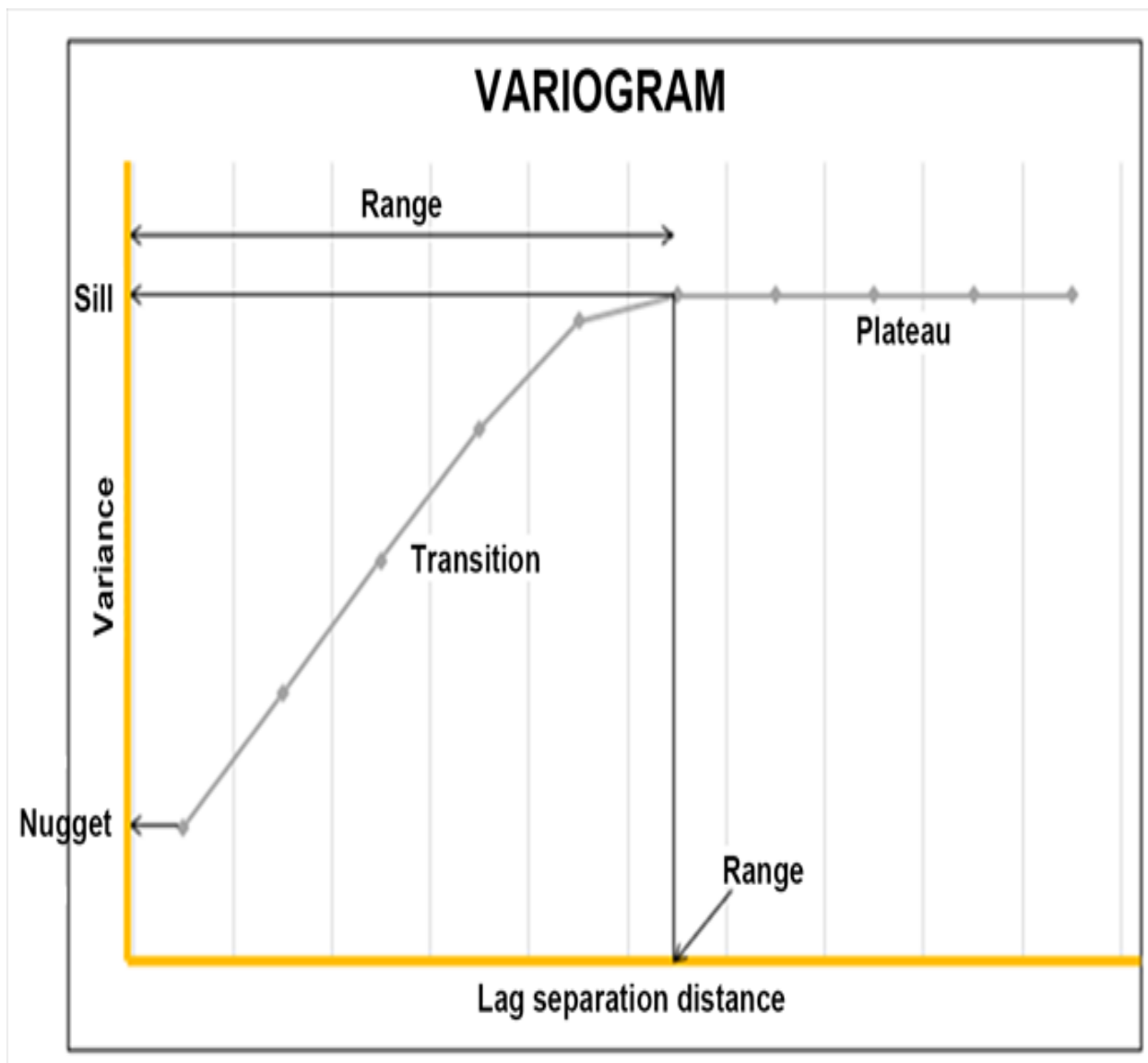


Figure 2.3: Parts of a Variogram (Bohling. 2007)

Modelling a (Semi)Variogram

For estimation to occur, a certain assumption must be made about the trend of the data. This assumption has a formular that helps it to compute what values are expected at a certain point. It is very important to model our data in other to carry out kriging.

Using h to represent lag distance, a to represent (practical) range, and c to represent sill, the five most frequently used models (Fig. 2.4) as said by (Bohling, 2007) are:

- Nugget: $g(h) = \begin{cases} 0 & \text{if } h=0 \\ c & \text{otherwise} \end{cases}$ (2.3)

The nugget model represents the discontinuity at the origin due to small-scale variation. On its own it would represent a purely random variable, with no spatial correlation.

- Spherical: $g(h)= \begin{cases} c \cdot \left(1.5\left(\frac{h}{a}\right) - 0.5\left(\frac{h}{a}\right)^3\right) & \text{if } h \leq a \\ c & \text{otherwise} \end{cases}$ (2.4)

The spherical model actually reaches the specified sill value, c , at the specified range, a .

- Exponential: $g(h)=c \cdot \left(1 - \exp\left(\frac{-3h}{a}\right)\right)$ (2.5)

- Guassian: $g(h)=c \cdot \left(1 - \exp\left(\frac{-3h^2}{a^2}\right)\right)$ (2.6)

The exponential and Gaussian approach the sill asymptotically, with a representing the practical range, the distance at which the semi variance reaches 95% of the sill value.

- Power: $g(h)=c \cdot h^\omega$ with $0 < \omega < 2$ (2.7)

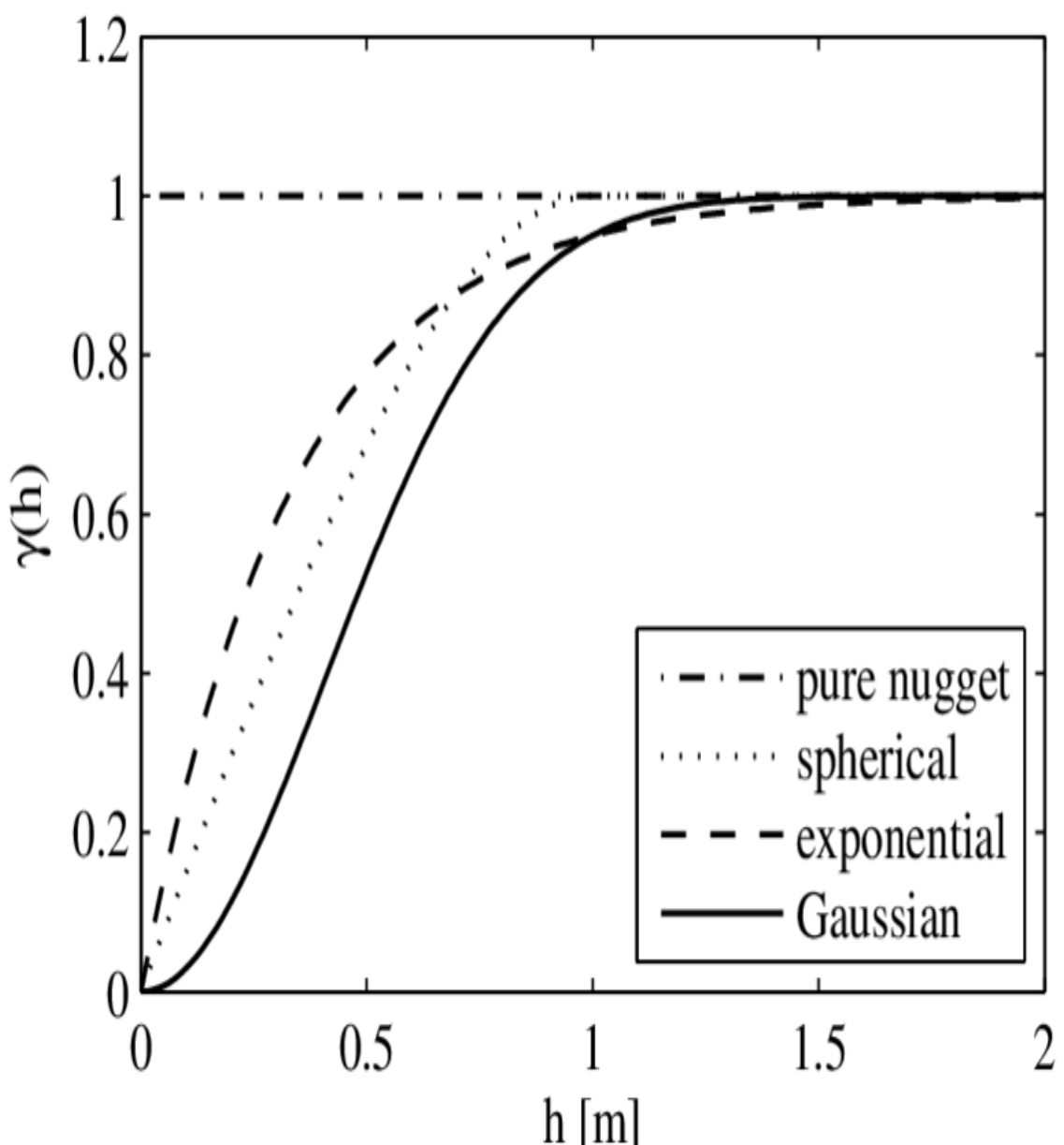


Figure 2.4: Types of Variogram Models. (Igel, 2007)

b) KRIGING: Optimal interpolation based on regression against observed z values of surrounding data points, weighted according to spatial covariance values (Bohling, 2007).

Kriging approach and terminology

The kriging estimator is also governed by an equation;

$$Z^*(u) - m(u) = \sum_{\alpha=1}^{n(u)} \lambda_\alpha [Z(u_\alpha) - m(u_\alpha)] \quad (2.8)$$

Where,

u, u_α : location vectors for estimation point and one of the neighboring data points, indexed by α

$n(u)$: number of data points in local neighborhood used for estimation of $Z^*(u)$

$m(u), m(u_\alpha)$ expected values (means) of $Z(u)$ and $Z(u_\alpha)$

$\lambda_\alpha (u)$: kriging weight assigned to datum $Z(u_\alpha)$ for estimation

The three main kriging types are, simple, ordinary, and kriging with a trend, they all differ in their treatments of the mean $m(u)$ (Bohling, 2007).

c) Simulation

Stochastic simulation is a probabilistic approach of treating our kriged data. It works by producing many equiprobable realizations of the data rather than just using our mean estimates. The realization produce helps us to quantify risk associated with the data at each probability level.

The two most commonly used forms of simulation are sequential Gaussian simulation for continuous variables like porosity and sequential indicator simulation for categorical variables like facies. Although this research does not involve simulation.

CHAPTER THREE

METHODOLOGY

3.1 VERTICAL ELECTRICAL SOUNDING TECHNIQUE

The VES technique measures the vertical variation in ground apparent resistivities with respect to a fixed center of array. The technique employs the collinear arrays designed to output a one-dimensional (1-D) vertical apparent resistivity versus depth model of the subsurface at a specific observation point. In this technique, a series of potential differences are acquired at successively larger electrode spacing while maintaining a fixed central reference point. The induced current passes through progressively deeper layers at greater electrode spacing. Apparent resistivity values are calculated from measured potential differences and can be interpreted in terms of overburden thickness, water table depth, etc.(Telford *et al* ; 1990).

3.1.1 ELECTRODE CONFIGURATION

Electrode configuration is determined by mode of arrangement of the current and potential electrodes. There are different types of electrode arrays that can be used in the vertical electrical resistivity technique. This include the Pole-Pole, Pole-Dipole, Dipole-Dipole, Wenner, Schlumberger, Lee partition, Square and others (Telford *et al* ; 1990).

In electrical resistivity survey, two current and two potential electrodes are used. An exception is the Lee partition electrode array which uses five electrodes. The Schlumberger electrode array was used for the purpose of this study.

- **SCHLUMBERGER ELECTRODE ARRAY**

The Schlumberger electrode array is collinear array of electrodes in which the potential electrode is located between the two current electrode (Fig 3.1). The electrode array is symmetrical because the station of measurement is at the center of the array.

For the VES data, the Schlumberger electrode configuration was used to acquire the data.

Typical configuration of other common electrode arrays are displayed in Figure 3.2.

3.1.2 DATA PRESENTATION

The apparent resistivity data obtained from the VES survey are presented as depth sounding curves by plotting the apparent resistivity along the ordinate axis (Y-axis) and the half current electrode spacing ($AB/2$) along the abscissa (X-axis). This plot was made on log-log paper. The resistivity depth sounding curves are classified based on layer resistivity combinations. There are four simplest type curves (Fig 3.3). The type curves generally found in the study area are H, HA, KH, and QH.

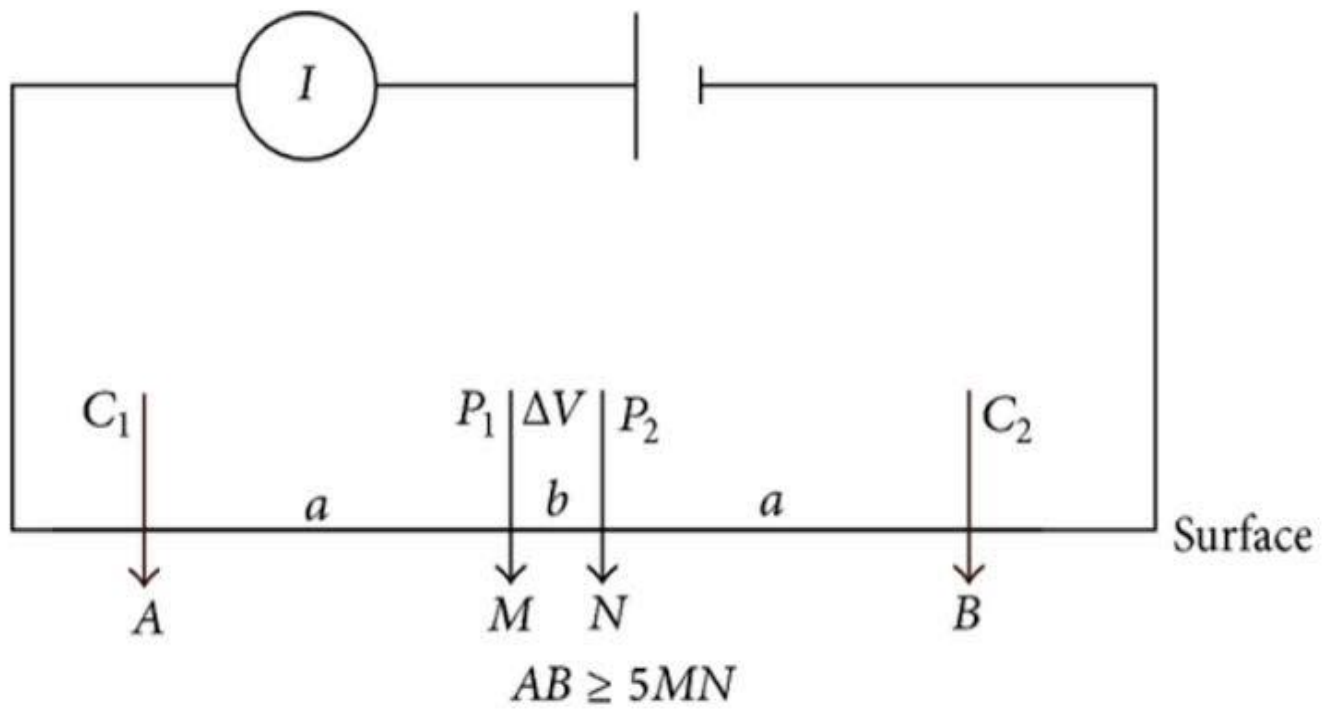


Figure 3.1: Schlumberger Electrode Configuration (Telford *et al*, 1990)

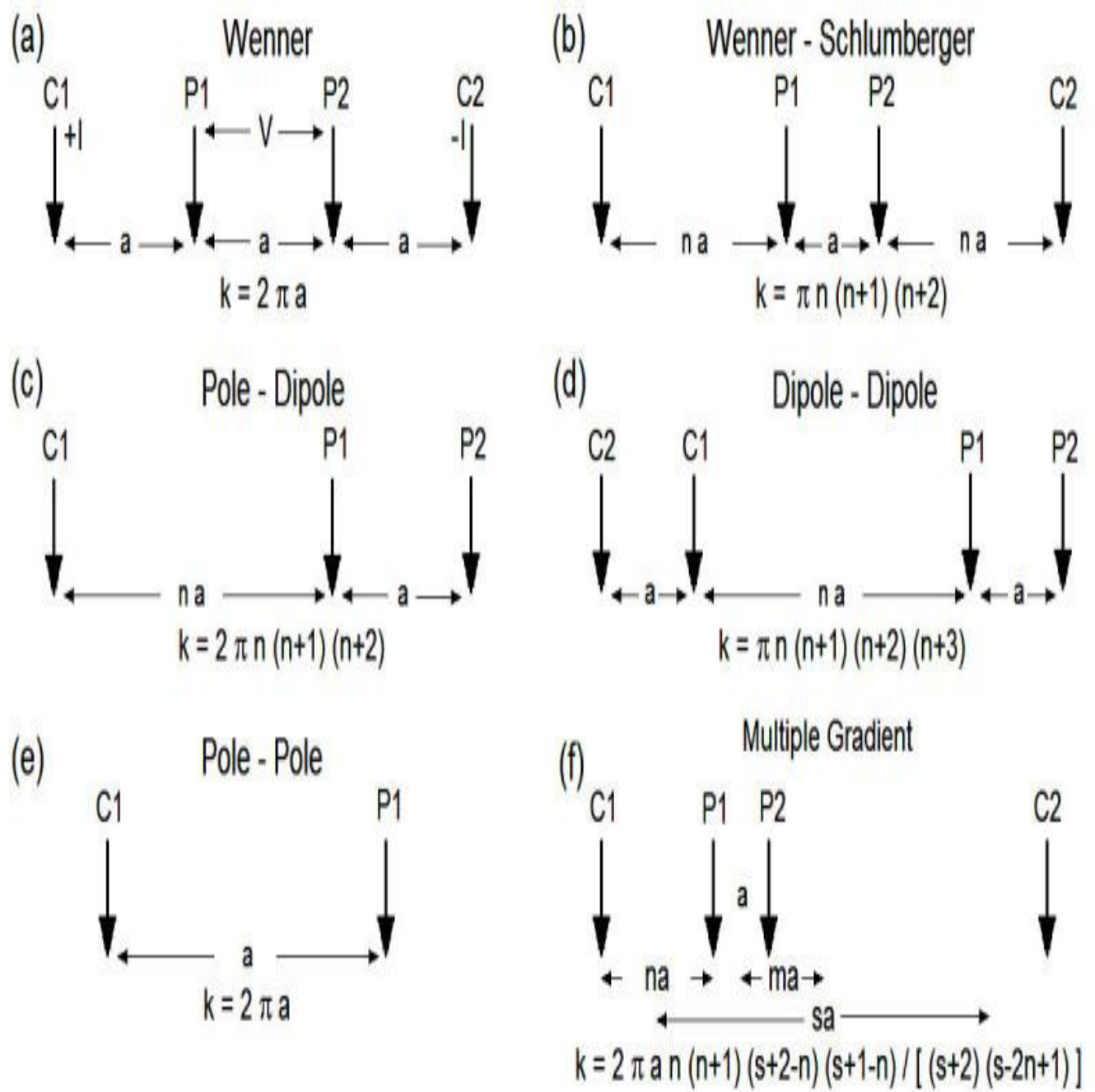


Figure 3.2: Other common Electrode Arrays. (Aizebeokhai, 2011)

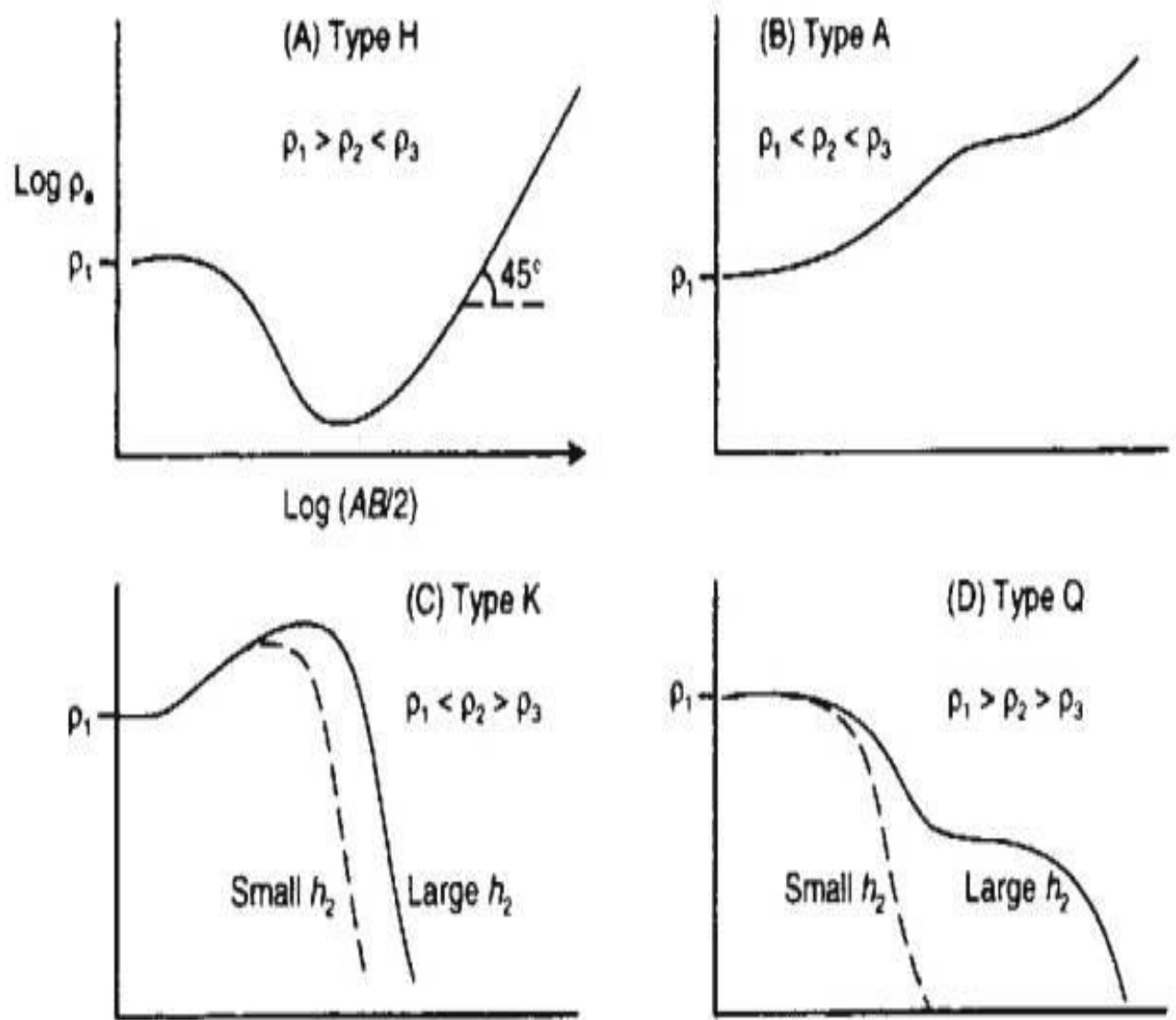


Figure 3.3: Four typical three layer curves (Telford *et al*; 1990)

3.1.3 DATA INTERPRETATION

The depth sounding curves are interpreted quantitatively by adopting the partial curve matching techniques (Bhattacharya and Patra, 1968). In order to this, the VES data is plotted log-log (Fig 3.5) paper overlain by a transparent overlay (tracing paper).

The partial curve matching technique involves the use of a standard two-layer curve (fig 3.4, 3.6 and 3.7) and four auxiliary type curves (H, K, A and Q) (Fig 3.3). This technique involves segment-by-segment curve matching of field multilayered curves starting from small electrode spacing and progressing towards large electrode spacing.

The field curve which has been plotted on the transparent overlay is superimposed on the master curve and it is moved until a match is obtained while keeping the axis parallel. When a match is obtained, the intersection of the heavy axis of the master curve is marked with a cross-point on the superimposed field curve and labelled accordingly while the reflection coefficient (K_1) is read. This cross-point is then placed at the origin of the appropriate auxiliary curve while the auxiliary curve corresponding to the reflection coefficient value (K_1) is traced out with broken lines. The coordinates of the first cross point give the resistivity (ρ_1) and thickness (h_1) of the first layer.

The field curve is then placed on the master curve in other to curve match the next segment of the curve which is done by allowing the previously marked Broken lines to pass through the origin of the master curve with the axes parallel. Again, when a match is obtained, the origin of the master curve is marked on the field curve with a cross-point while its reflection coefficient (K_2) is recorded. This second cross-point is then placed on the origin of the appropriate auxiliary

curve while the auxiliary curve corresponding to the reflection coefficient value (K_2) is traced out with broken lines on the field curves. The coordinate of (K_2) gives the replacement resistivity (ρ_{2r}) and replacement thickness (h_{2r}) of a layer combining both the first and second layer. In order to curve match the other segments of the field curve, the approach outlined above can be followed until all segments of the field curve are matched. The coordinate of the subsequent cross-point gives the replacement resistivities (ρ_{3r} , ρ_{4r} , etc.) and replacement thicknesses (h_{2r} , h_{3r} etc.) respectively.

To determine the thickness of the second layer, the depth ratio $(\partial n / \partial r)_1$ has to be determined by replacing the cross-point at the origin of the auxiliary curve while the depth ratio $(\partial n / \partial r)_1$ is read at the second cross-point. The resistivity and the thickness of the second layer can be calculated using the expression below.

$$\rho_2 = K_1 \times \rho_1 \quad \& \quad h_2 = (\partial n / \partial r)_1 \times h_1 \quad (3.1)$$

For subsequent layers, the resistivities and thicknesses can be obtained using equation (3.2)

$$\rho_{n+1} = K_n \times \rho_{nr} \quad \& \quad h_{n+1} = (\partial n / \partial r)_n \times h_{nr}; \text{ for } n \geq 2, n \text{ is an integer} \quad (3.2)$$

The result of the partial curve matching technique were then used to constrain the interpretation by computer assisted forward modelling software, known as interpretVES. The computer software carries out a 1-D forward modelling of the results obtained through the partial curve matching. This invariably reduces over-estimation of depth. It also gives use the geoelectric section of the layers.

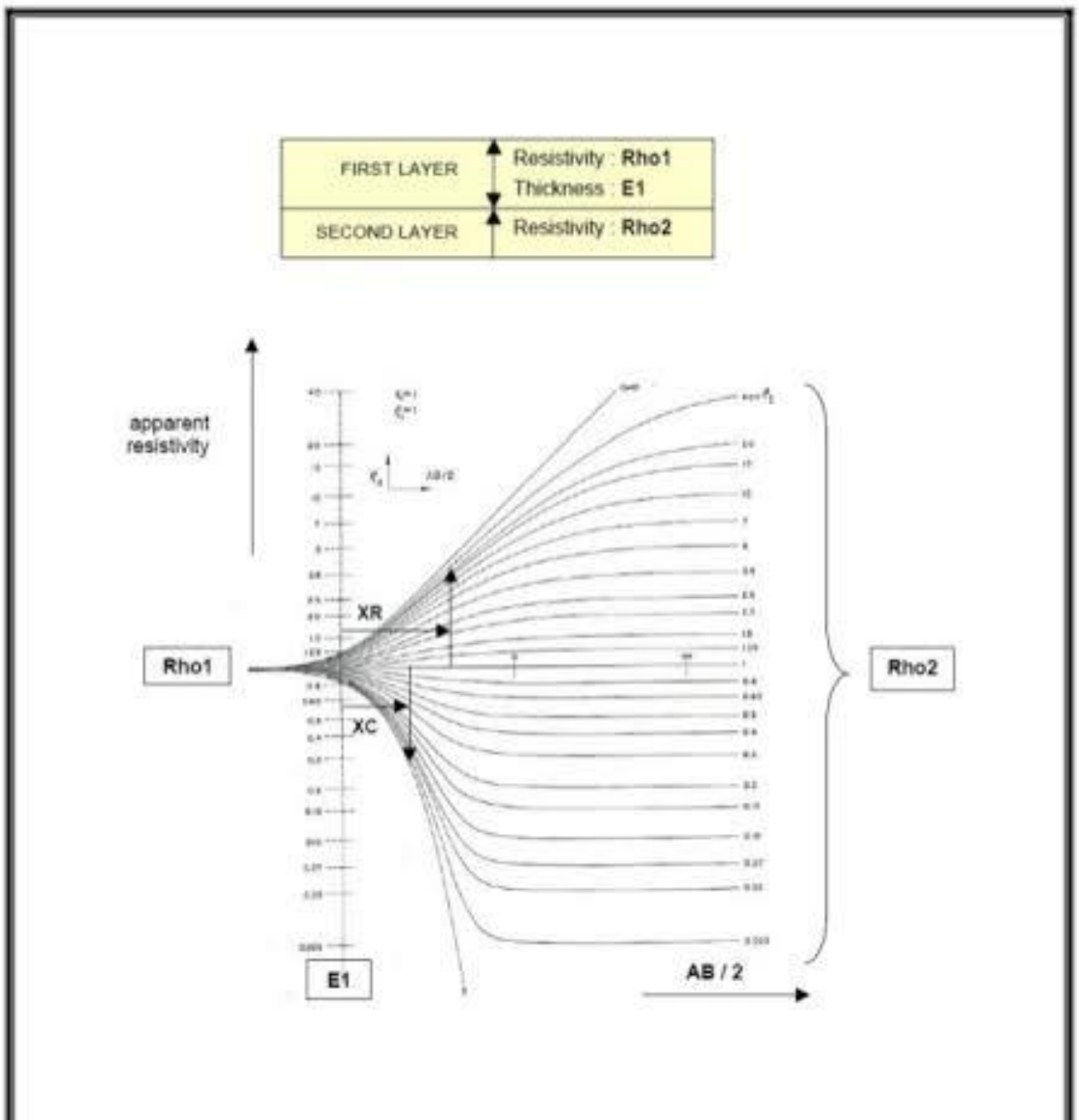


Figure 3.4: Two layers Master curves (After Orellana and Mooney, 1966)

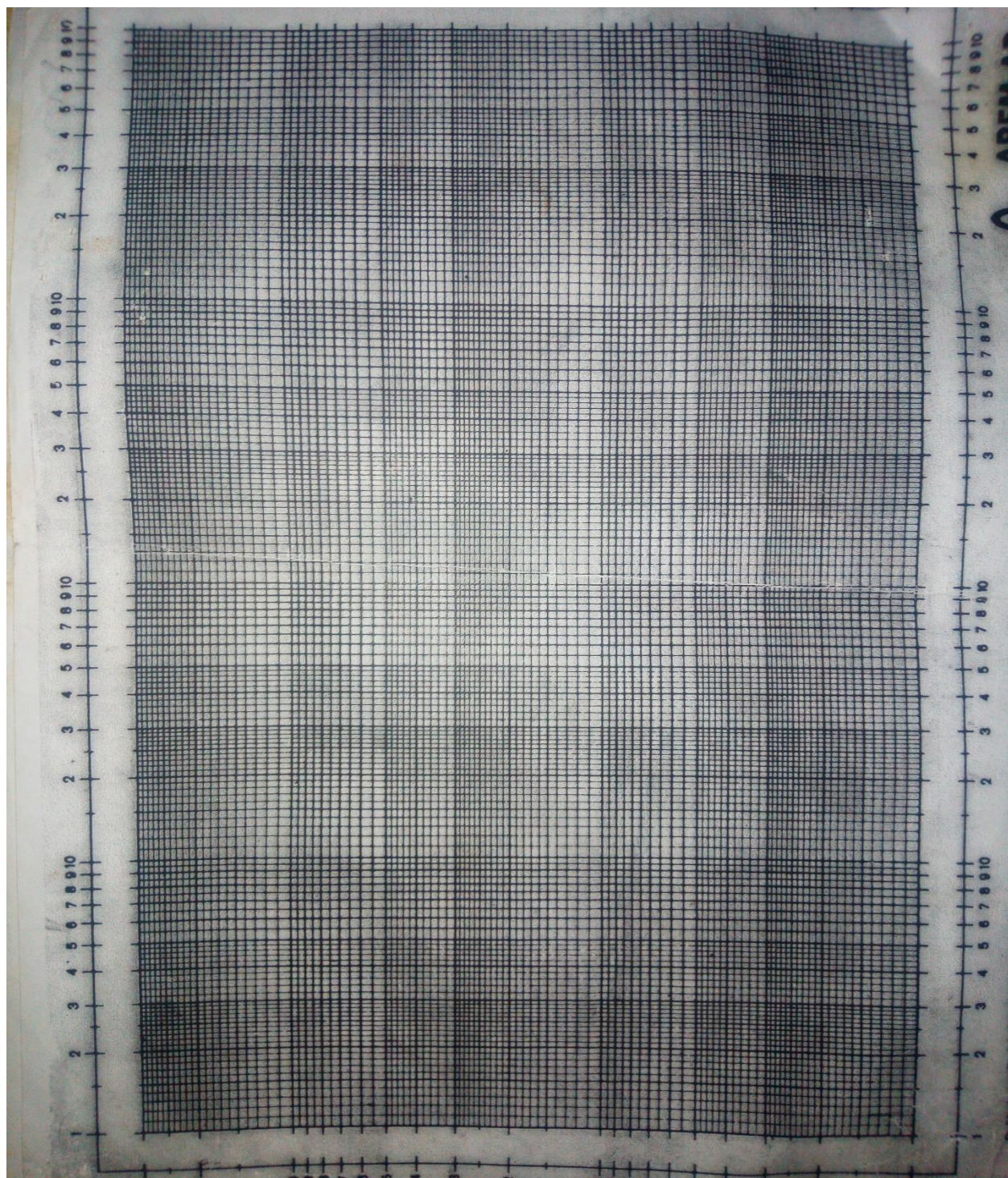


Figure 3.5: The Log-Log paper

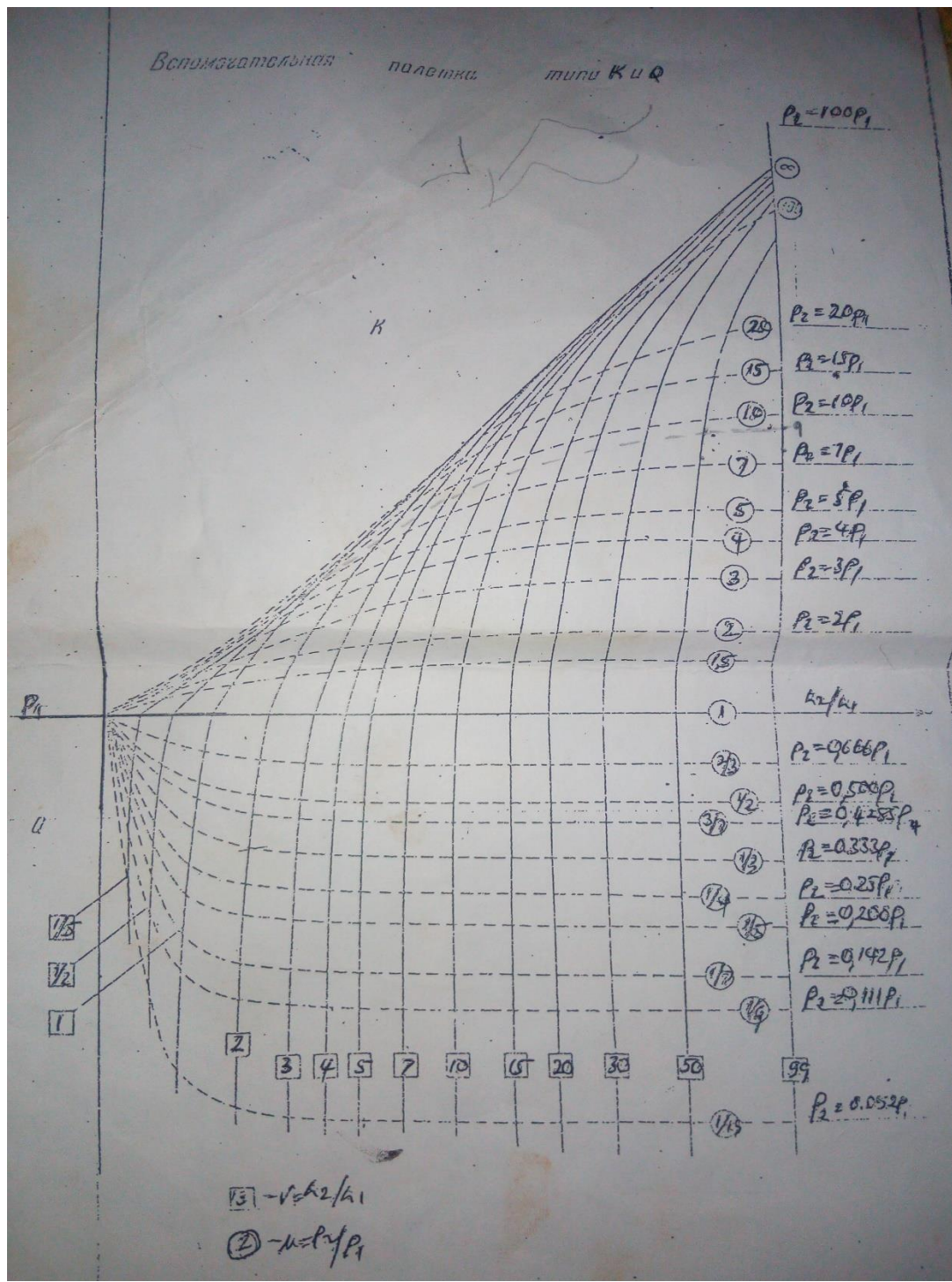


Figure 3.6: K and Q type Auxiliary Curve

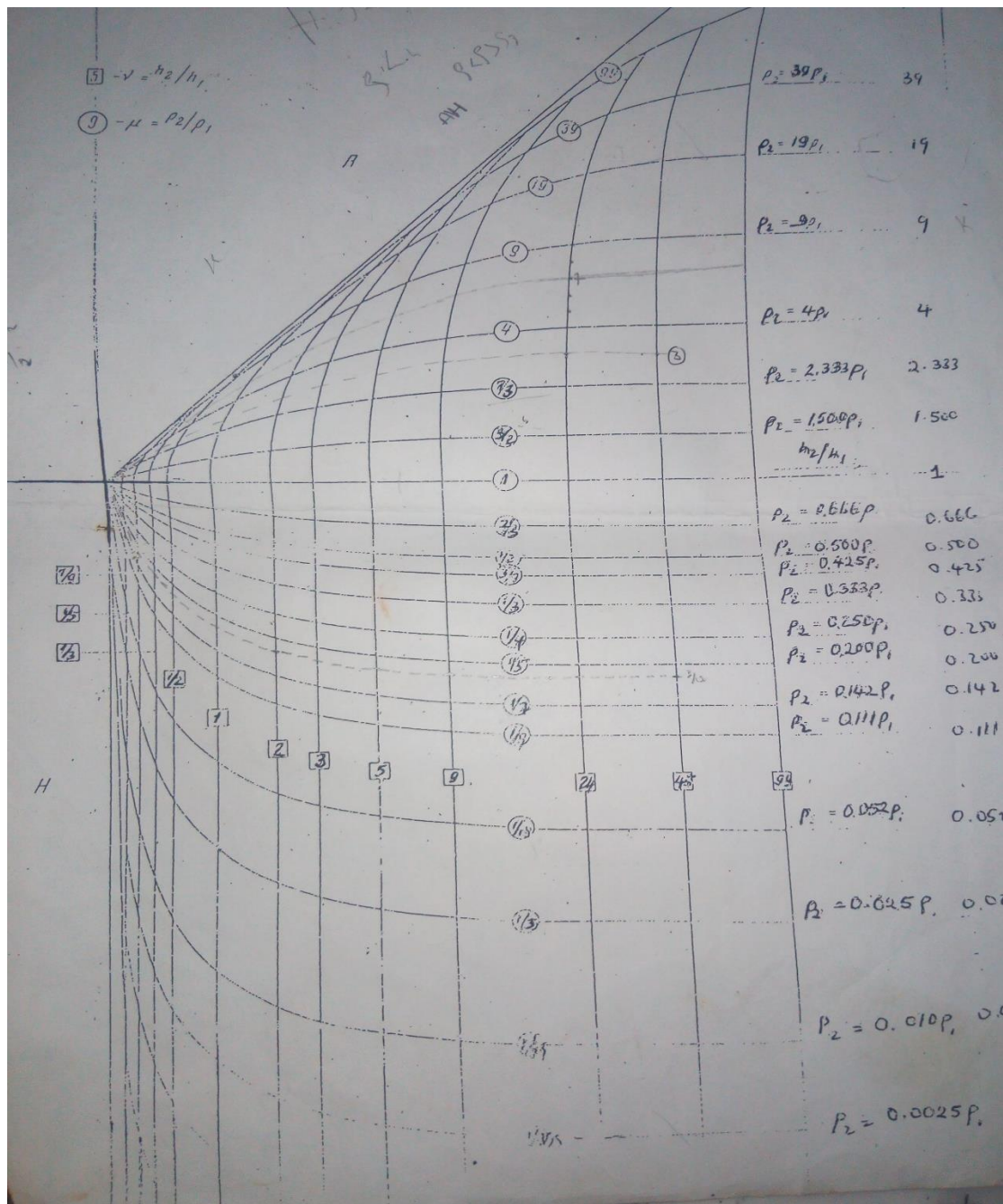


Figure 3.7: The A and H Type Auxiliary Curve

3.2 DETERMINATION OF THE COEFFICIENT OF ANISOTROPY

The coefficient of anisotropy has been studied by many authors like Keller and Frischknecht, 1966. The i th layer in a geoelectric unit can be characterized by two fundamental parameters; its resistivity ρ_i and thickness h_i . From these two parameters, other secondary parameter used to describe such a layer may also be determined such as the coefficient of anisotropy.

$$a) \text{ Longitudinal unit Conductance } S = \sum_{i=1}^n \frac{h_i}{\rho_i} \quad (3.3)$$

$$b) \text{ Transverse unit Resistance } T = \sum_{i=1}^n h_i \rho_i \quad (3.4)$$

$$c) \text{ Longitudinal Resistance } = \rho_l = \frac{h_i}{S_i} \quad (3.5)$$

$$d) \text{ Transverse Resistivity } = \rho_t = \frac{T_i}{h_i} \quad (3.6)$$

Where i , is the summation limits varying from 1 to $n-1$ and the n th layer represent the infinitely resistive bedrock. The parameters above are usually found in rock with total thickness H , cut from a geoelectric unit of infinite lateral extent. The longitudinal conductance S and the transverse resistance T constitute the Dar- Zarrouk parameter and can be found direct by some software during interpretation. They are expressed in “mhos” and ohms-m² respectively. The electrical coefficient of anisotropy λ is then given by

$$\text{Electrical Coefficient of Anisotropy } \lambda = \sqrt{\frac{\rho_t}{\rho_l}} = \sqrt{\frac{\sum h_i n_i \sum \frac{h_i}{\rho_i}}{(\sum h_i)^2}} = \sqrt{\frac{ST}{H}} \quad (3.7)$$

3.3 GEOSTATISTICAL METHOD

3.3.1 Techniques used for Geostatistics Method

a) SEMI VARIOGRAM: The variogram technique tests the degree of dissimilarity between two variables in space. (Bohling, 2007)

variogram is often computed with the following formular;

$$\text{Semivariance: } Y(h) = \frac{1}{2N(h)} \sum_{\alpha=1}^{N(h)} (z(u_\alpha + h) - z(u_\alpha))^2 \quad (3.1)$$

The technique was easily computed for this study using the SURFER™ version 11 software. Each of our four parameters (resistivity, thickness, coefficient of anisotropy and groundwater yield) 39 data points were loaded one after the other on the computer software to compute the variogram. In the process of computing the variogram, a trial and error process was done to find a perfect model for each parameters. The best model that fit for each was seen to be the exponential model.

The variogram model for each parameter provided us with a sill and range value which was adapted during the kriging estimate.

b) KRIGING: The kriging estimator is also governed by an equation;

$$Z^*(u) - m(u) = \sum_{\alpha=1}^{n(u)} \lambda_\alpha [Z(u_\alpha) - m(u_\alpha)] \quad (3.2)$$

Kriging was also carried out using SURFER™ version 11, the kriging estimator adapted sill and range values from the variogram plot. This estimated points beyond the original 39 data points. Kriging also estimated both the mean (m) and standard deviation (σ) values for each parameter.

The geostatistics steps are listed in Fig 3.8.

3.4 DATA PROCESSING

3.4.1 Conversion of Krigged mean (m) and standard deviation (σ) values to three confidence intervals

The result from kriging our data using geostatistics provided us with the mean(m) and standard deviation(σ) values. These values are then assessed at different confidence intervals guided by the following normal distribution confidence interval equations.

$$\bullet \quad m \pm 3\sigma = 99.73\% \quad (3.16)$$

$$\bullet \quad m \pm 2\sigma = 95.55\% \quad (3.17)$$

$$\bullet \quad m \pm \sigma = 68.27\% \quad (3.18)$$

Where.

m ; mean

σ ; standard deviation

3.4.2 Multivariate Regression Analysis of yield and geoelectric parameters.

This R software helps to performs a multivariate regression analysis on our data. It has helped us in this project to compute linear yield equations at the mean level and at the three confidence intervals using the geoelectric parameters (resistivity, anisotropy and thickness). It also tells us the degree of correlation of the geoelectric parameters to the yield at each confidence interval.

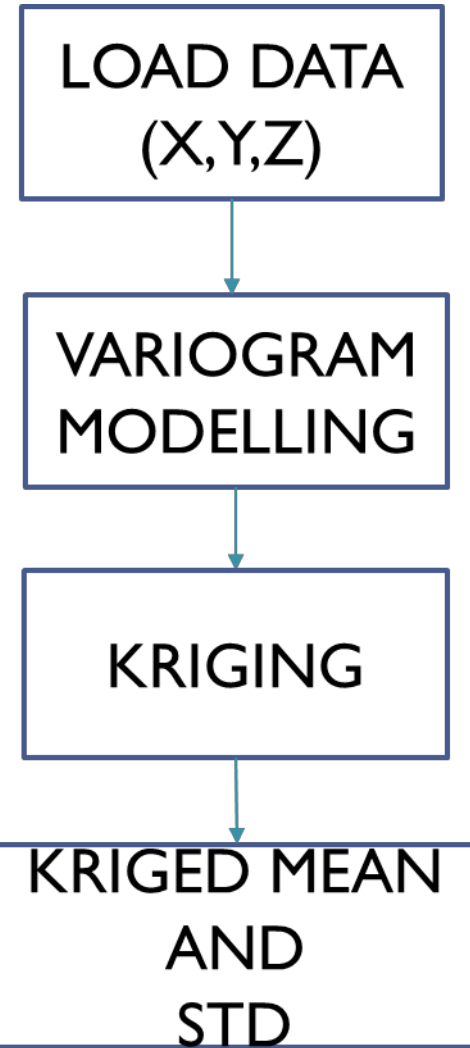


Figure 3.8: Flow Chat of Steps in Performing a Geostatistical Estimation.

3.4.3 Find the Best Fit Yield Equation from the Confident Intervals.

A newly estimated yield value was obtained and computed by inputting the original 39 VES data into the regression equations obtained in 3.4.2 above for each confidence interval.

The best fit yield equation was gotten by comparing this newly estimated 39 yield values to the original 39 yield data.

Steps;

1. Input the equation gotten at each confidence interval and slot in the 39 VES data to get the new yield.
2. Find the average in the new yield between the upper and lower limit.
3. Plot the original yield against the estimated yield gotten in step 2.
4. Then use excel to find the multiple regression and correlation between the two yield data.
5. The confidence interval with the highest correlation value gives us our best predicting equations.

CHAPTER FOUR

RESULTS AND DISCUSSION

4.1 VES RESULTS

4.1.1 The VES Map.

In Fig 4.1, the 39 VES stations are seen distributed round the study area. More stations are on the porphyritic granite rock (OGp) and the undifferentiated schist (Su). We have about two stations on the banded gneiss(bG), five stations on the granite gneiss (GG) and one station on the pegmatite at the northeastern part of the study area..

4.1.2 The VES Type Curves

There are five different type of curves interpreted. These are the H, HA, KH, AKH and HKH curves. The representative curves with their geoelectric section are seen the Figures 4.2 and 4.3.

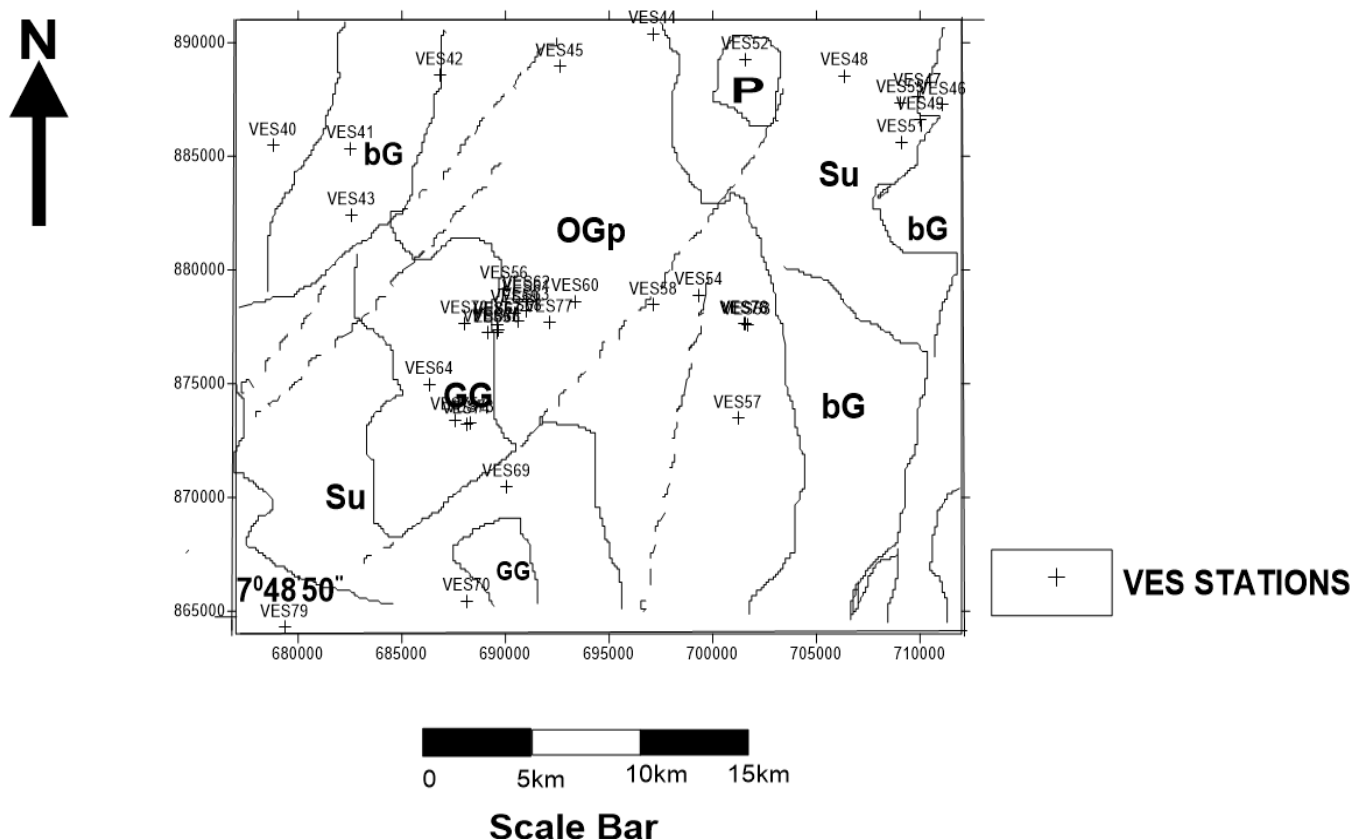


Figure4.1: Map Showing the 39 VES Positions.

a) HKH curve

This curve has subsurface layers of five. The representative curve below shows a topsoil having the medium resistivity value and the lowest thickness, followed by the laterite clay layer which has the lowest resistivity, then the laterite layer which has a very high resistivity value, followed by the weathered layer which can be taken as the aquifer zone. It has thickness ranging from 5 m to 7 m and then the fresh basement which has the highest resistivity value and an infinite thickness.

b) H curve

The curve is a three-layered curve with the topsoil having a higher resistivity but lower thickness than the weathered layer. The third layer is the fresh basement which has the highest resistivity and an infinite thickness. The aquifer here is in the weathered basement.

c) HA curve

The curve is a four-layered curve with the topsoil, followed by weathered layer, then the fractured basement and lastly the fresh basement. The weathered basement has the lowest resistivity which can be taken to be the aquifer in this curve type. The fresh basement has the highest resistivity value.

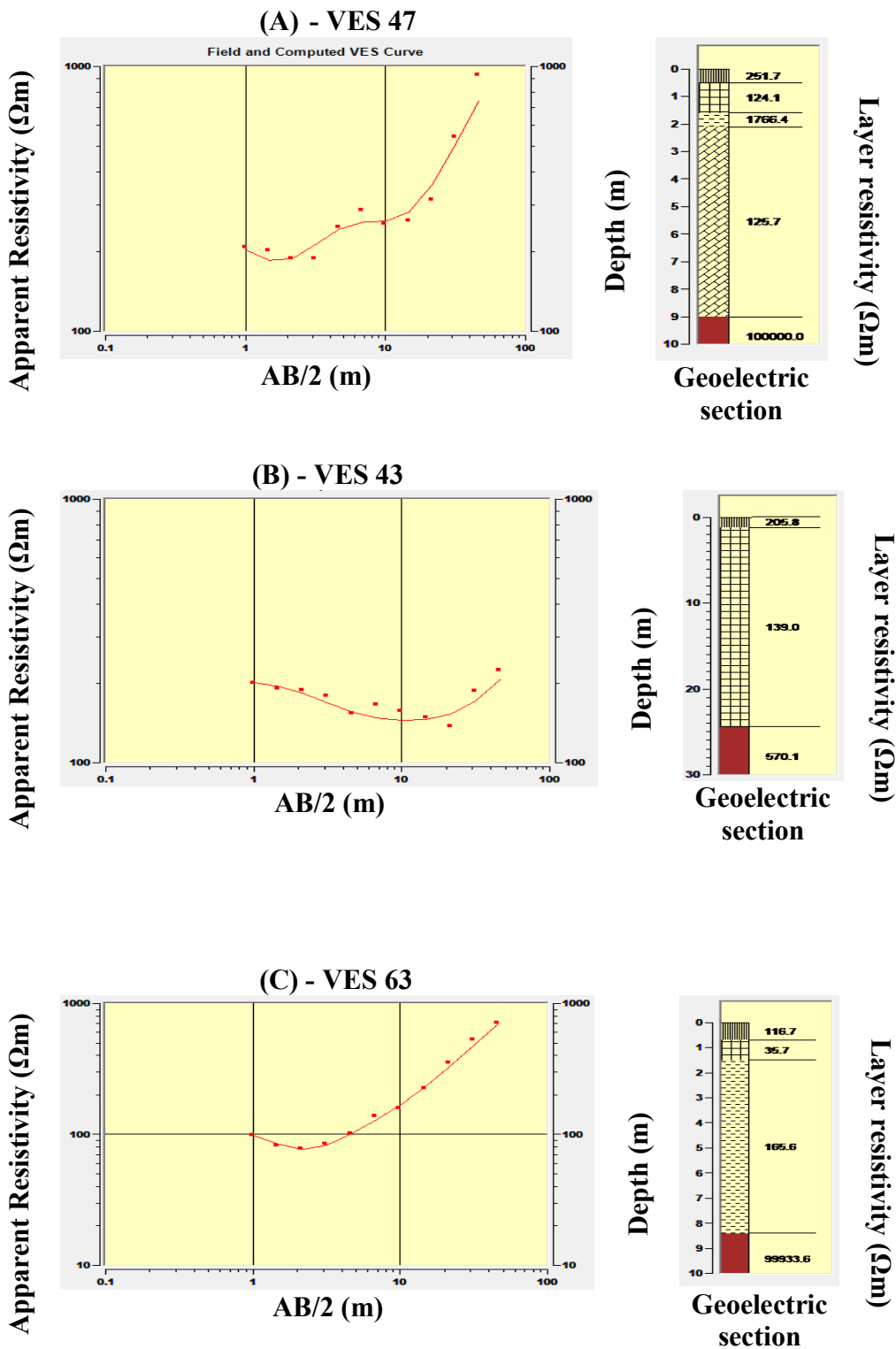


Figure 4.2: The Curve Types (A) HKH Curve, (B) H Curve and (C) HA Curves

d) AKH curve

The curve is a five-layered curve ranging from topsoil to weathered layer to fresh basement to fractured basement and lastly fresh basement. The fractured basement is seen to have the lowest resistivity value which can be taken to be the aquifer in this curve type. The fresh basements have the highest resistivity values.

e) KH curve

This curve is a four-layered curve ranging from topsoil, a thin layer of lateritic soil, a weather layer and finally the fresh basement. The weathered layer has the lowest resistivity here which is taken as the aquifer zone here. The lateritic zone in this case has the highest resistivity value.

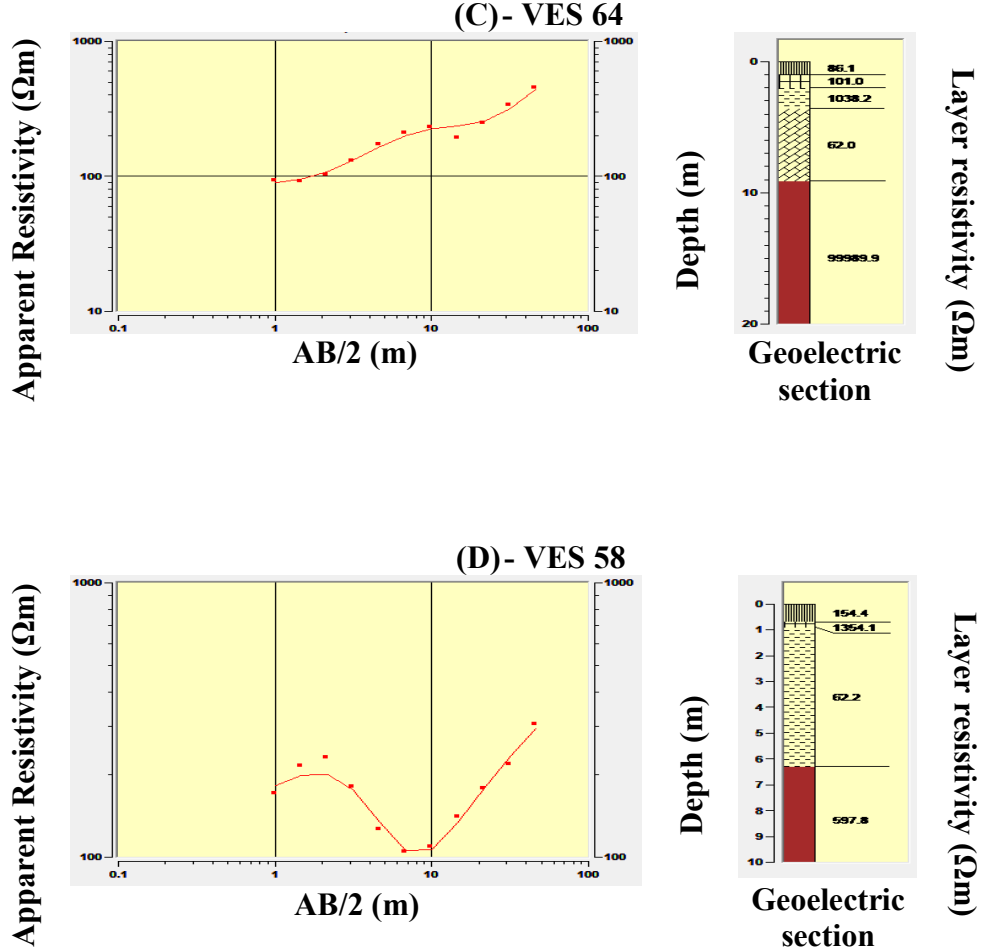


Figure 4.3: The Curve Types (D) AKH Curve AND (E) KH Curve

4.1.3 The VES General Interpretation

Table 4.1, presents the result of the 39 VES curves interpreted. The inversion of the VES data resulted in three to five layer models. The stations can be seen to have a topsoil, a weathered layered and a fresh basement. Other layers found in some stations are the lateritic and fractured layer. The Aquifer zone can be said to be mostly in the weathered layer and fractured because of the extremely low resistivity of the layer. The type curves are mainly H-type , KH-type, HA-type, AKH-type and HKH-type. The weathered layers' thickness ranged from 0.1m to 37.2m

TABLE 4.1 A Summary of the VES Interpretation Results

VES	Longitude(x)	Latitude(y)	Elevation	Resistivity		Thickness(h)	Depth	Curve	Geology		Inferred Lithology
No.	(°)	(°)	(m)	(Ω-m)		(m)	(m)	Type			
40	4.62237	8.00811	373	P1	83		1.2	1.2	H	Granite Gneiss	Topsoil
					h1						Weathered layer
					P2	30	h2	11.5	12.7		Fresh basement
41	4.65623	8.00683	393	p1	33	h1	0.3	0.3	KH	Banded Gneiss	Topsoil
					p2	496	h2	11.5	11.8		Laterite
					p3	88	h3	37.2	49		Weathered layer
					p4	10000					Fresh basement
42	4.69532	8.03577	393	p1	58	h1	0.9	0.9	HA	Banded Gneiss	Topsoil
					p2	38	h2	3.4	4.3		Weathered layer
					p3	121	h3	13.6	17.9		Weathered layer
					p4	4212					Fresh basement
43	4.65652	7.98029	370	p1	206	h1	1.2	1.2	H	Banded Gneiss	Topsoil
					p2	139	h2	23.2	24.4		Weathered layer
					p3	570					Fresh basement
44	4.78859	8.0519	437	p1	91	h1	0.7	0.7	H	Porphyritic Granite	Topsoil
					p2	18	h2	0.9	1.6		Weathered layer
					p3	241					Fresh basement
45	4.7479	8.03903	453	p1	56	h1	0.5	0.5	H	Porphyritic Granite	Topsoil
					p2	4	h2	0.5	1		Weathered layer
					p3	96076					Fresh basement
46	4.91518	8.0231	488	p1	304	h1	0.5	0.5	HKH	Banded Gneiss	Topsoil
					p2	93	h2	1.2	1.7		Weathered layer
					p3	3780	h3	0.1	1.8		Fresh basement
					p4	255	h4	22	23.8		Fracture basement
					p5	1815					Fresh basement
47	4.90442	8.02651	484	p1	252	h1	0.5	0.5	HKH	Schist Undifferentiated	Topsoil
					p2	124	h2	1.1	1.6		Lateritic clay
					p3	1766	h3	0.5	2.1		Laterite
					p4	126	h4	6.9	9		Weathered layer
					p5	10000					Fresh basement
48	4.87251	8.03487	486	p1	79	h1	1	1	KH	Schist Undifferentiated	Topsoil
					p2	159	h2	2.2	3.2		Lateritic clay
					p3	40	h3	5.3	8.5		Weathered layer
					p4	10000					Fresh basement
49	4.90558	8.01715	488	p1	27	h1	1	1	HKH	Schist Undifferentiate	Topsoil
					p2	16	h2	6.2	7.2		Weathered layer

				p3	126	h3	4	11.2				Fresh basement
				p4	22	h4	23.9	35.1				Fracture basement
				p5	10000							Fresh basement
51	4.89703	8.00816	475	p1	105	h1	0.7	0.7	KH	Schist Undifferentiate	Topsoil	
				p2	1402	h2	0.7	1.4				Laterite
				p3	92	h3	10.8	12.2				Weathered layer
				p4	99917							Fresh basement
52	4.82907	8.04148	442	p1	341	h1	0.5	0.5	HKH	Schist Undifferentiate	Topsoil	
				p2	54	h2	0.4	0.9				Clay
				p3	1416	h3	1.7	2.6				Laterite
				p4	201	h4	26	28.6				Weathered layer
				p5	5232							Fresh basement
53	4.82934	7.93595	488	p1	848	h1	0.7	0.7	H	Porphyritic Granite	Topsoil	
				p2	291	h2	11.2	11.9				Weathered layer
				p3	674							Fresh basement
54	4.80828	7.94788	554	p1	248	h1	1	1	KH	Porphyritic Granite	Topsoil	
				p2	968	h2	7.9	8.9				Laterite
				p3	130	h3	41.8	50.7				Weathered layer
				p4	99916							Fresh basement
55	4.89683	8.02386	510	p1	234	h1	0.7	0.7	HKH	Schist Undifferentiate	Topsoil	
				p2	52	h2	1.1	1.8				Weathered layer
				p3	448	h3	0.9	2.7				Fresh basement
				p4	42	h4	5.9	8.6				Fracture basement
				p5	10000							Fresh basement
56	4.72324	7.95064	401	p1	157	h1	0.7	0.7	H	Porphyritic Granite	Topsoil	
				p2	31	h2	0.5	1.2				Weathered layer
				p3	10000							Fresh basement
57	4.82515	7.89877	603	p1	457	h1	0.7	0.7	KH	Porphyritic Granite	Topsoil	
				p2	807	h2	1.4	2.1				Laterite
				p3	224	h3	2.2	4.3				Weathered layer
				p4	484							Fresh basement
58	4.7884	7.94407	488	p1	154	h1	0.7	0.7	KH	Porphyritic Granite	Topsoil	
				p2	1354	h2	0.2	0.9				Laterite
				p3	62	h3	5.4	6.3				Weathered layer
				p4	598							Fresh basement
59	4.72789	7.94121	434	p1	44	h1	1	1	HA	Granite Gneiss	Topsoil	
				p2	34	h2	1.4	2.4				Weathered layer
				p3	68	h3	11.3	13.7				Partly weathered/
				p4	7386							Fracture basement
												Fresh basement

60	4.75438	7.94554	562	p1	154	h1	1	1	H	Porphyritic Granite		Topsoil	
				p2	74	h2	2.5	3.5				Weathered layer	
				p3	10000							Fresh basement	
61	4.73287	7.94534	473	p1	106	h1	1	1	HA	Porphyritic Granite		Topsoil	
				p2	69	h2	1.1	2.1				Weathered layer	
												Partly weathered/	
				p3	327	h3	6.7	8.8				Fracture basement	
				p4	3080							Fresh basement	
62	4.73295	7.94677	456	p1	72	h1	0.8	0.8	HA	Porphyritic Granite		Topsoil	
				p2	25	h2	0.7	1.5				Weathered layer	
												Partly weathered/	
				p3	88	h3	13.1	14.6				Fracture basement	
				p4	1757							Fresh basement	
63	4.73267	7.94205	470	p1	117	h1	0.7	0.7	HA	Porphyritic Granite		Topsoil	
				p2	36	h2	0.8	1.5				Weathered layer	
												Partly weathered/	
				p3	166	h3	6.9	8.4				Fracture basement	
				p4	99934							Fresh basement	
64	4.69026	7.91296	407	p1	86	h1	1	1	AKH	Granite Gneiss		Topsoil	
				p2	101	h2	1	2				Weathered layer	
				p3	1038	h3	1.6	3.6				Fresh basement	
				p4	62	h4	5.5	9.1				Fracture basement	
				p5	99990							Fresh basement	
65	4.71567	7.93334	429	p1	216	h1	2.2	2.2	H	Granite Gneiss		Topsoil	
				p2	134	h2	13.4	15.6				Weathered layer	
				p3	2906							Fresh basement	
66	4.71985	7.93335	436	p1	51	h1	1	1	H	Granite Gneiss		Topsoil	
				p2	24	h2	1.3	2.3				Weathered layer	
				p3	2080							Fresh basement	
67	4.72022	7.93636	431	p1	120	h1	0.7	0.7	KH	Granite Gneiss		Topsoil	
				p2	200	h2	1.1	1.8				Lateritic clay	
				p3	38	h3	2.7	4.5				Weathered layer	
				p4	99911							Fresh basement	
68	4.72925	7.93786	439	p1	121	h1	1	1	H	Porphyritic Granite		Topsoil	
				p2	27	h2	3.5	4.5				Weathered layer	
				p3	511							Fresh basement	
69	4.72392	7.87198	403	p1	102	h1	1.1	1.1	H	Porphyritic Granite		Topsoil/Weathered layer	
				p2	806							Fresh basement	
70	4.70634	7.82665	370	p1	168	h1	1	1	H	Schist Undifferentiate		Topsoil	
				p2	67	h2	2.9	3.9				Weathered layer	

				p3	1754							Fresh basement
71	4.72031	7.93435	431	p1	163	h1	0.8	0.8	KH	Granite Gneiss	Topsoil	
				p2	1096	h2	0.2	1			Laterite	
				p3	116	h3	6.9	7.9			Weathered layer	
				p4	1206						Fresh basement	
72	4.7058	7.93694	421	p1	1149	h1	0.6	0.6	HKH	Granite Gneiss	Topsoil	
				p2	128	h2	1.1	1.7			Weathered layer	
				p3	382	h3	5.5	7.2			Fresh basement	
				p4	192	h4	14.4	21.6			Fracture basement	
				p5	4935						Fresh basement	
73	4.70825	7.89755	425	p1	29	h1	1	1	KH	Granite Gneiss	Topsoil/Weathered layer	
				p2	83	h2	1.9	2.9			Fresh basement	
				p3	29	h3	5.9	8.8			Fracture basement	
				p4	472						Fresh basement	
74	4.70634	7.89696	420	p1	542	h1	0.5	0.5	HKH	Granite Gneiss	Topsoil	
				p2	148	h2	1.2	1.7			Lateritic clay	
				p3	872	h3	0.6	2.3			Laterite	
				p4	75	h4	5.1	7.4			Weathered layer	
				p5	10000						Fresh basement	
75	4.70128	7.89855	412	p1	214	h1	0.9	0.9	H	Granite Gneiss	Topsoil	
				p2	163	h2	0.9	1.8			Weathered layer	
				p3	32	h3	2.4	4.2			Weathered layer	
				p4	96182						Fresh basement	
76	4.82798	7.93631	485	p1	119	h1	0.7	0.7	KH	Porphyritic Granite	Topsoil	
				p2	867	h2	0.4	1.1			Laterite	
				p3	55	h3	4.4	5.5			Weathered layer	
				p4	10000						Fresh basement	
77	4.74287	7.93731	525	p1	395	h1	0.7	0.7	H	Porphyritic Granite	Topsoil	
				p2	3	h2	0.5	1.2			Weathered layer	
				p3	53	h3					Fresh basement	
78	4.82838	7.93642	486	p1	443	h1	0.5	0.5	HKH	Porphyritic Granite	Topsoil	
				p2	41	h2	0.4	0.9			Weathered layer	
				p3	285	h3	2.1	3			Weathered layer	
				p4	67	h4	6.8	9.8			Weathered layer	
				p5	10000						Fresh basement	
79	4.6266	7.81652	367	p1	96	h1	0.4	0.4	HKH	Banded Gneiss	Topsoil	
				p2	35	h2	2.6	3			Weathered layer	
				p3	1184	h3	0.3	3.3			Fresh basement	
				p4	33	h4	13.7	17			Fracture basement	
				p5	10000						Fresh basement	

4.1.4 Results from the Aquifer zone

The aquifer zone is mostly found at the weathered and fractured zone of each type curve. The resistivity of the area ranged from 4 ohm to 201 ohm which is relatively low compared to other layers in the subsurface. The coefficient of anisotropy values of the layers is also greater than 1 (Table 4.2) which shows the contributing factors in the layer is inhomogeneous.

4.2 GEOSTATISTICS RESULTS

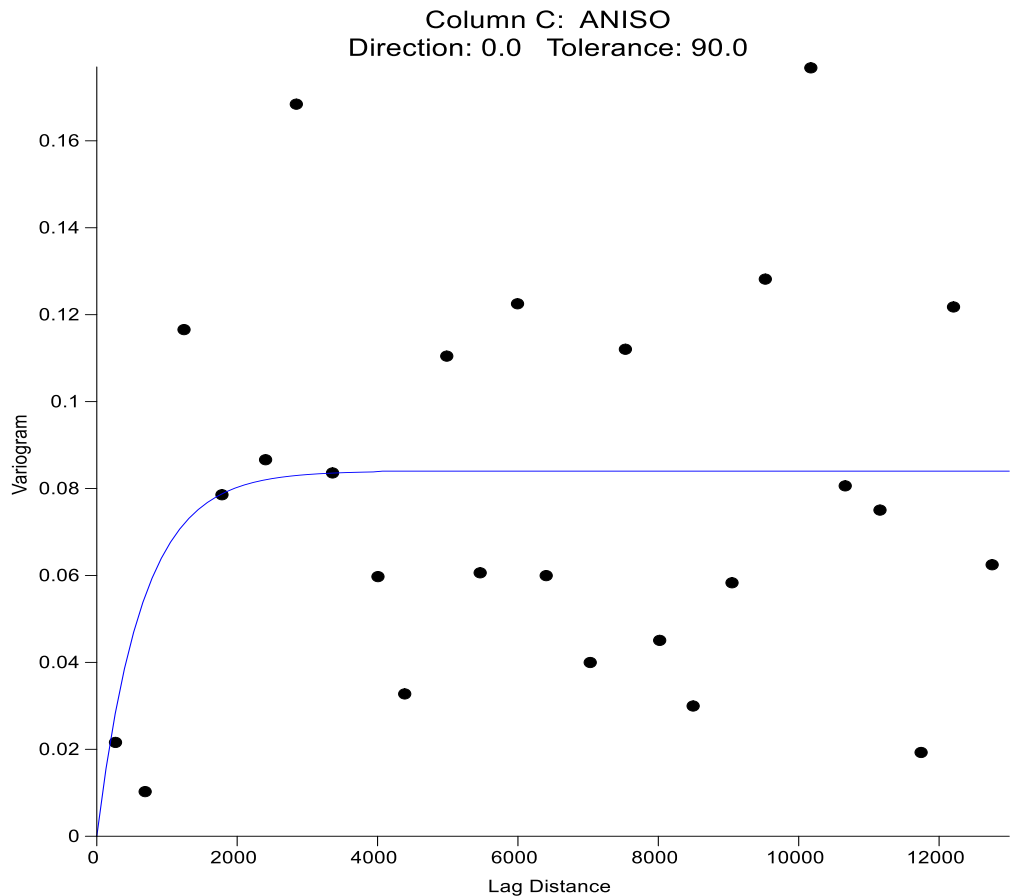
4.2.1 Variogram Plots

Figures 4.4 – 4.7 show the variogram plot for each selected geoelectric parameters and yield data for the 39 data points. An exponential model was seen to fit for each of the plots.

TABLE 4.2: The VES Results and Coefficient of Anisotropy at the Aquifer Zone.

Easting	Northing	VES Point	Curve Types	GROUNDWATER YIELD (Li/Sec)	RESISTIVITY(Ω)	THICKNESS(m)	COEFFICIENT OF ANISOTROPY
678806.8	885466.4	VES40	HKH	1.03	30.3	11.5	1.0
682540.2	885339.8	VES41	KH	1.42	87.7	37.2	1.3
686836.4	888557.7	VES42	HA	1.32	37.5	3.4	1.0
682583.9	882404.9	VES43	H	1.20	139.0	23.2	1.0
697110.8	890385.3	VES44	H	1.13	18.0	0.9	1.3
692631.3	888942.6	VES45	H	1.30	3.9	0.5	2.0
711081.4	887263.2	VES46	HKH	1.20	93.2	1.2	1.2
709893.3	887634.8	VES47	HKH	1.50	125.7	6.9	1.3
706370.9	888543.3	VES48	KH	1.30	40.3	5.3	1.2
710026	886600.2	VES49	HKH	1.48	15.9	6.2	1.0
709087.9	885601.6	VES51	KH	1.40	91.5	10.8	1.3
701578.5	889252.7	VES52	HKH	1.17	201.2	26.0	1.2
701660.1	877581.6	VES53	HKH	1.21	291.0	11.2	1.0
699332	878890.8	VES54	KH	1.24	129.6	41.8	1.3
709057.8	887337.9	VES55	HKH	1.20	42.1	5.9	1.4
689953.7	879156.1	VES56	HKH	1.20	31.1	0.5	1.3
701216.1	873467.6	VES57	KH	1.35	224.0	2.2	1.0
697141.7	878459.9	VES58	KH	1.50	62.2	5.4	1.3
690470.8	878115.3	VES59	HA	1.23	34.2	1.4	1.0
693389.7	878606.5	VES60	H	1.35	73.7	2.5	1.1
691018	878574.4	VES61	HA	1.30	69.0	1.1	1.0
691026.1	878732.5	VES62	HA	1.20	25.1	0.7	1.1
690997.4	878210.4	VES63	HA	1.22	35.7	0.8	1.2
686334.2	874974.1	VES64	AKH	1.50	62.0	5.5	1.7
689126.9	877239.4	VES65	H	1.24	133.5	13.4	1.0
689587.8	877242.4	VES66	H	1.50	23.9	1.3	1.1
689391.3	877578.9	VES67	KH	1.30	37.6	2.7	1.3
690622.3	877745.5	VES68	H	1.44	27.1	3.5	1.2
690064.7	870457.4	VES69	AKH	1.03	101.9	1.1	1.0
688146.3	865436.5	VES70	H	1.20	66.7	2.9	1.1
689638.1	877353.2	VES71	KH	1.50	116.4	6.9	1.1
688037	877633	VES72	HKH	1.36	127.6	1.1	1.6
688325	873278	VES73	KH	1.26	28.6	5.9	1.1
688114.6	873211.9	VES74	HKH	1.38	75.2	5.1	1.4
687555.9	873385.5	VES75	QH	1.11	31.8	2.4	1.4
701509.9	877620.7	VES76	KH	1.20	55.1	4.4	1.4
692124.4	877690.9	VES77	H	1.30	3.2	0.5	2.1
701554	877633.1	VES78	HKH	1.43	66.7	6.8	1.3
679355.9	864281.4	VES79	HKH	1.27	35.3	2.6	1.1

Coefficient of Anisotropy



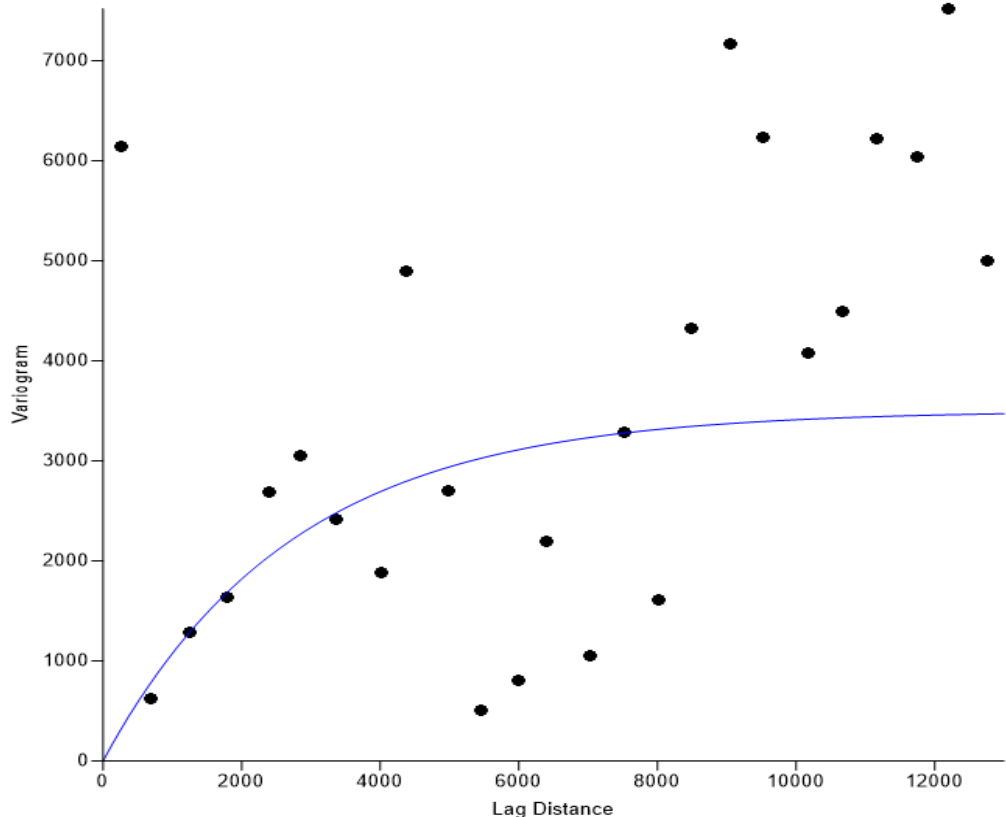
Exponential Model

SILL	0.084
RANGE	1176
Anisotropy Ratio	2
Anisotropy angle	62.46

Figure 4.4: Variogram Plot for Coefficient of Anisotropy

RESISTIVITY

Column C: RESIS
Direction: 0.0 Tolerance: 90.0



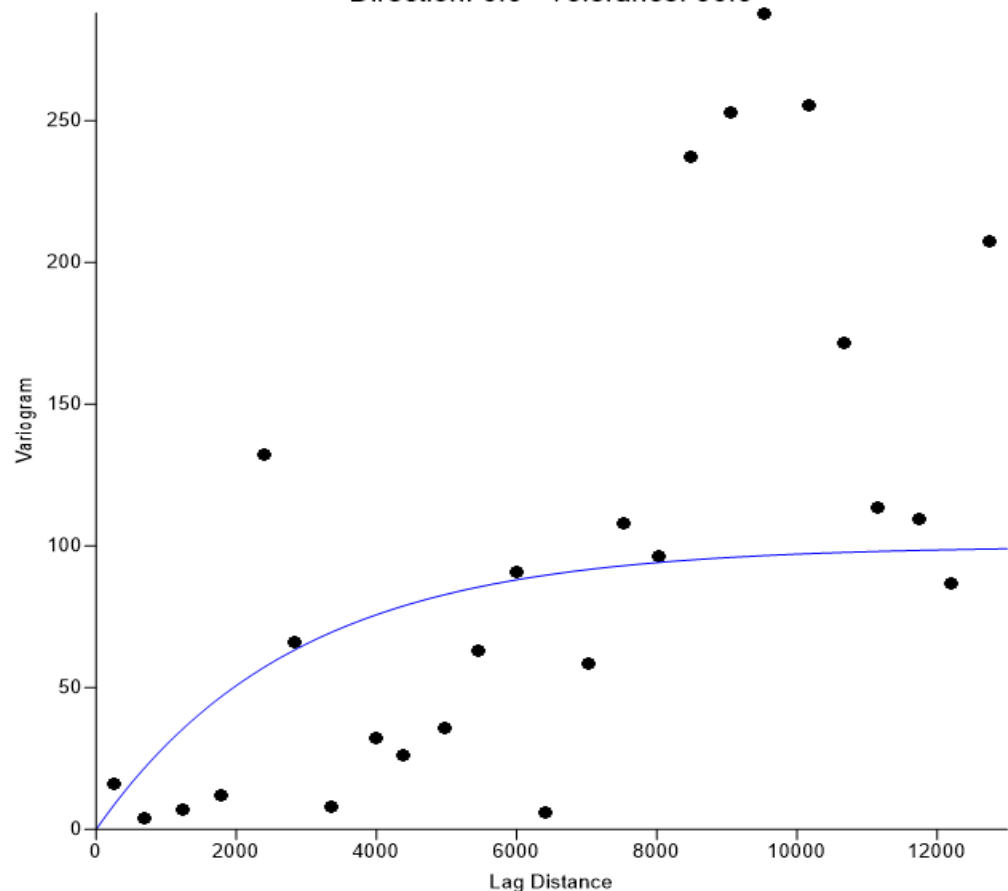
Exponential Model

SILL	3500
RANGE	4660
Anisotropy Ratio	2
Anisotropy angle	53

Figure 4.5: Variogram Plot for Resistivity

THICKNESS

Column C: THICK
Direction: 0.0 Tolerance: 90.0



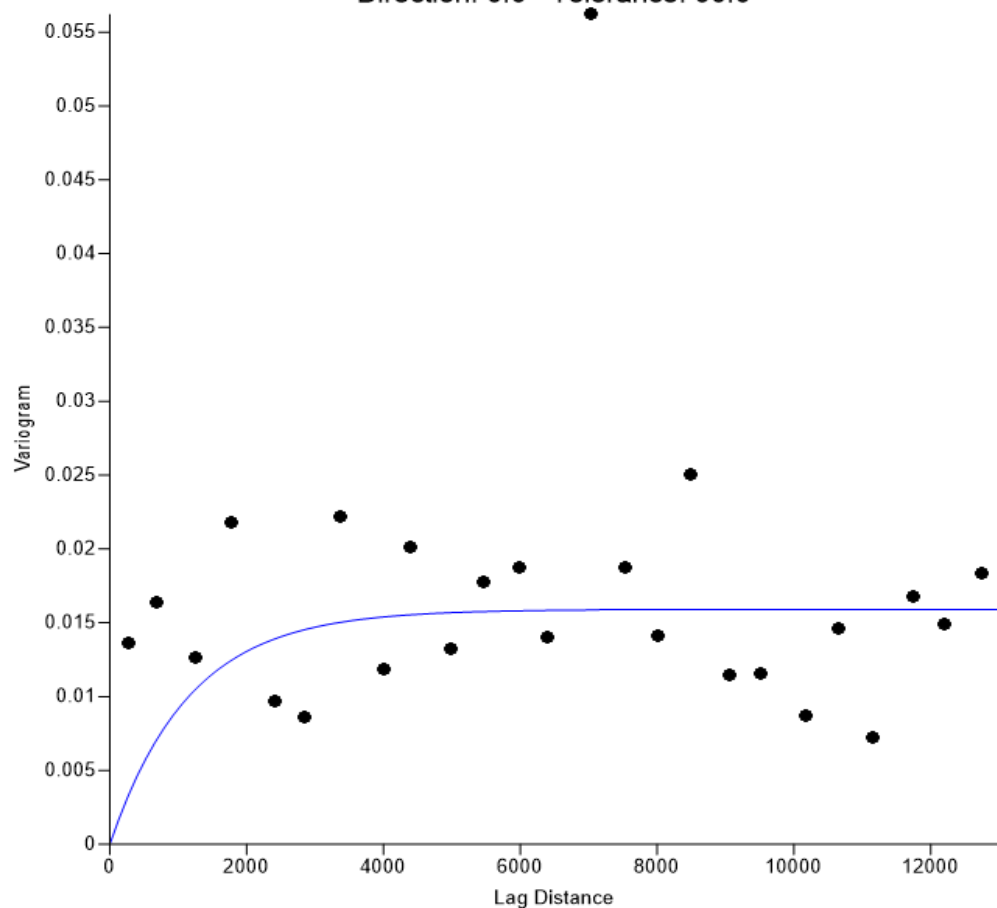
Exponential Model

SILL	140
RANGE	5430
Anisotropy Ratio	2
Anisotropy angle	71.33

Figure 4.6: Variogram Plot for Thickness

YIELD

Column C: YIELD
Direction: 0.0 Tolerance: 90.0



Exponential Model

SILL	0.0159
RANGE	1170
Anisotropy Ratio	1.999
Anisotropy angle	175.8

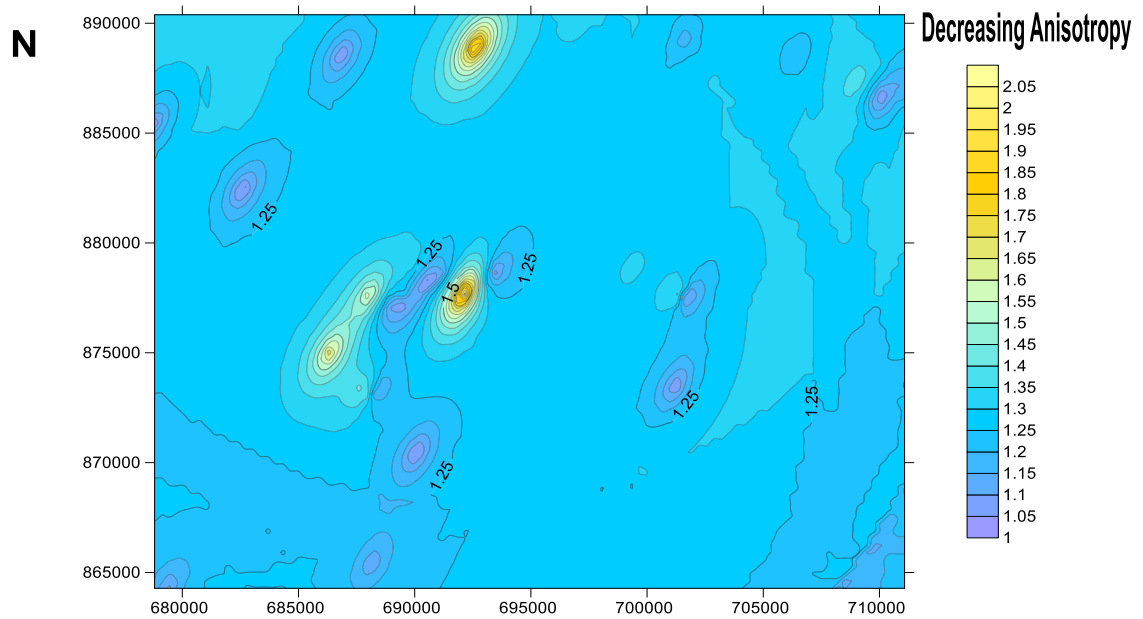
Figure 4.7: Variogram Plot for Yield

4.2.2 KRIGING

Figures 4.8 – 4.11 show the Mean(m) and Standard Deviation(σ) values obtained from kriging the 39 geoelectric parameters and yield data. The standard deviation values tend to be lower than the mean for each parameter, which means the data points are clustered closely around the mean value.

- a. In Fig 4.12 A, the coefficient of anisotropy seems to have higher values around areas lying on the porphyritic granite while the lowest values came from the points lying on the banded gneisses on the mean map.
- b. In Fig 4.12 B, the points lying on the undifferentiated schist is more resistive than the rest of the points on the resistivity mean map.
- c. In Fig 4.12 C, the points lying on the fault of the porphyritic granite shows higher aquifer thickness than the rest of the area.
- d. In Fig 4.12 D the highest yield rate is found at the center of the mean map which is underlain by faulted porphyritic granite rock.

KRIGING MEAN



KRIGING STANDARD DEVIATION

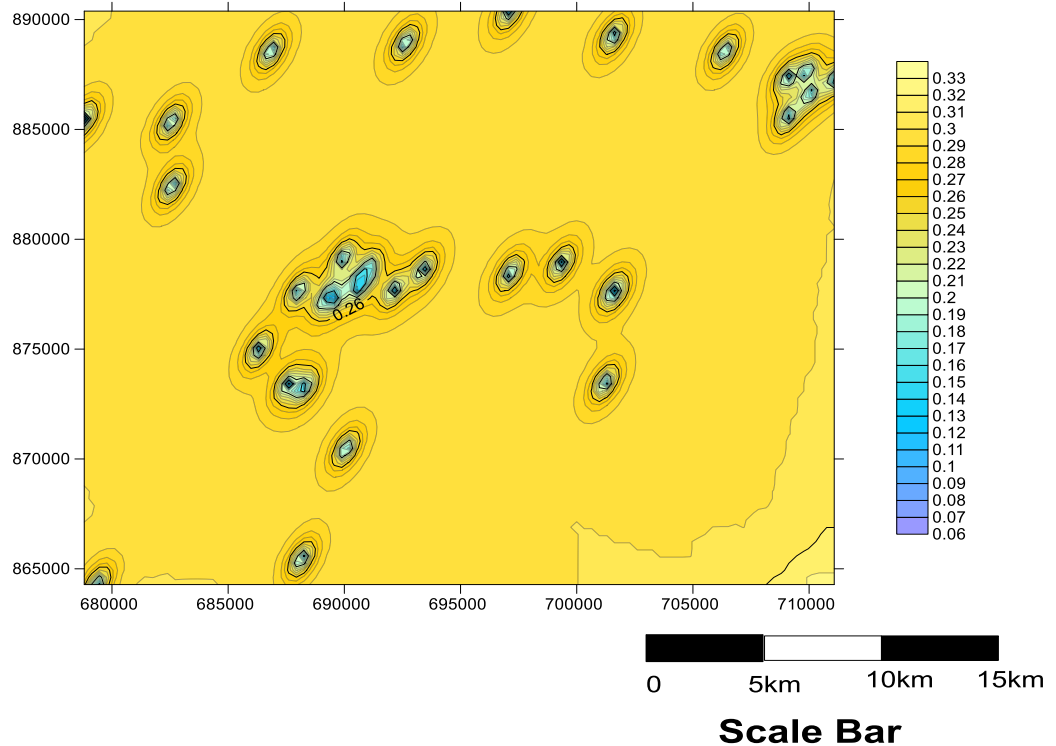
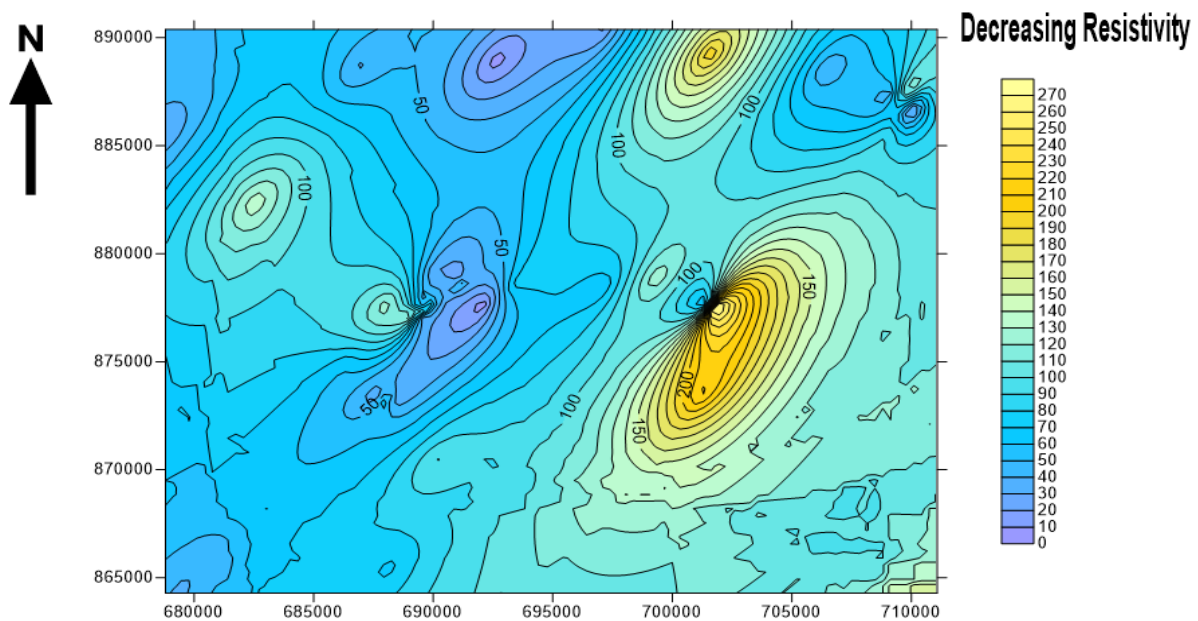


Figure 4.8: Kriged Contoured Coefficient of Anisotropy Map

KRIGING MEAN



KRIGING STANDARD DEVIATION

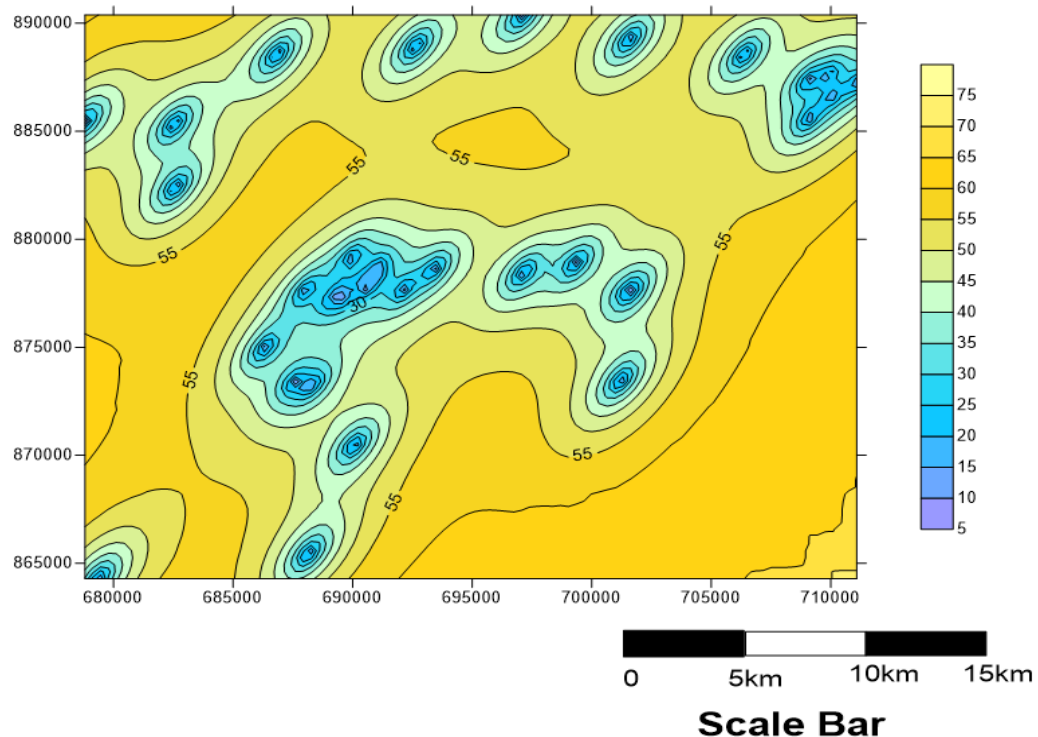
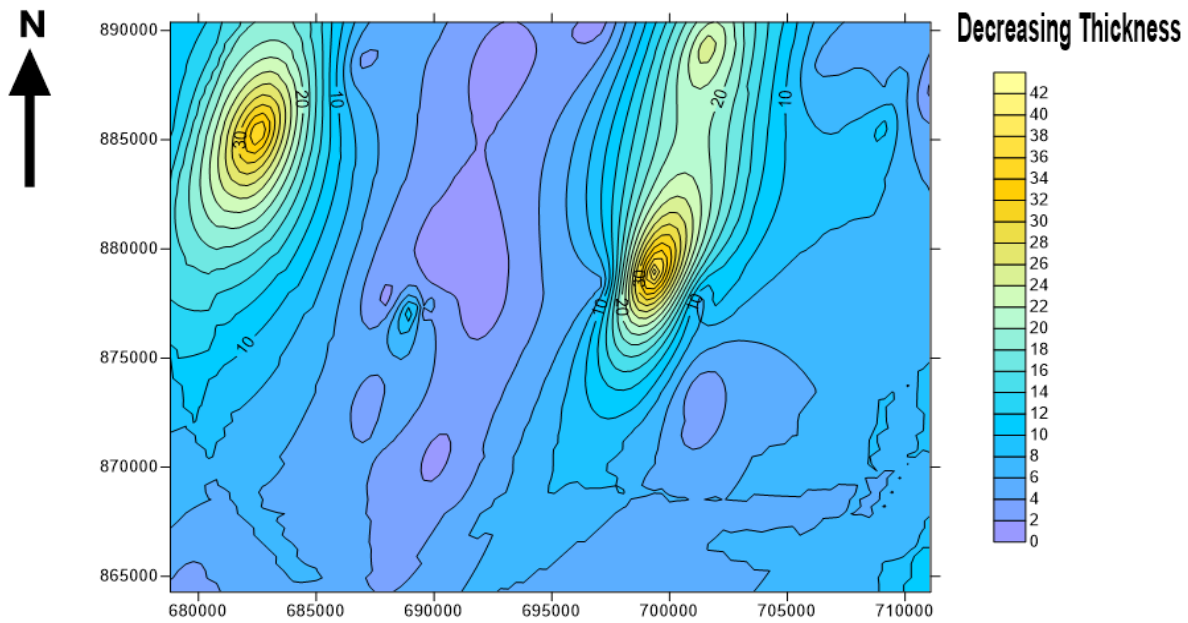


Figure 4.9: Kriged Contoured Resistivity Map

KRIGING MEAN



KRIGING STANDARD DEVIATION

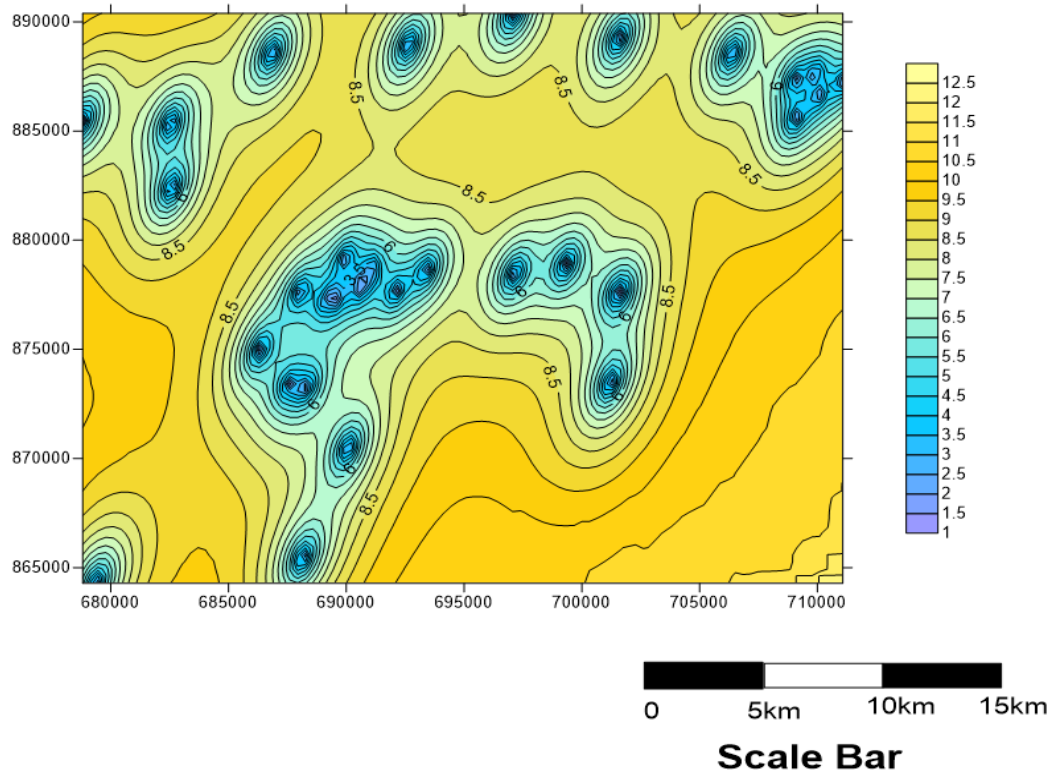
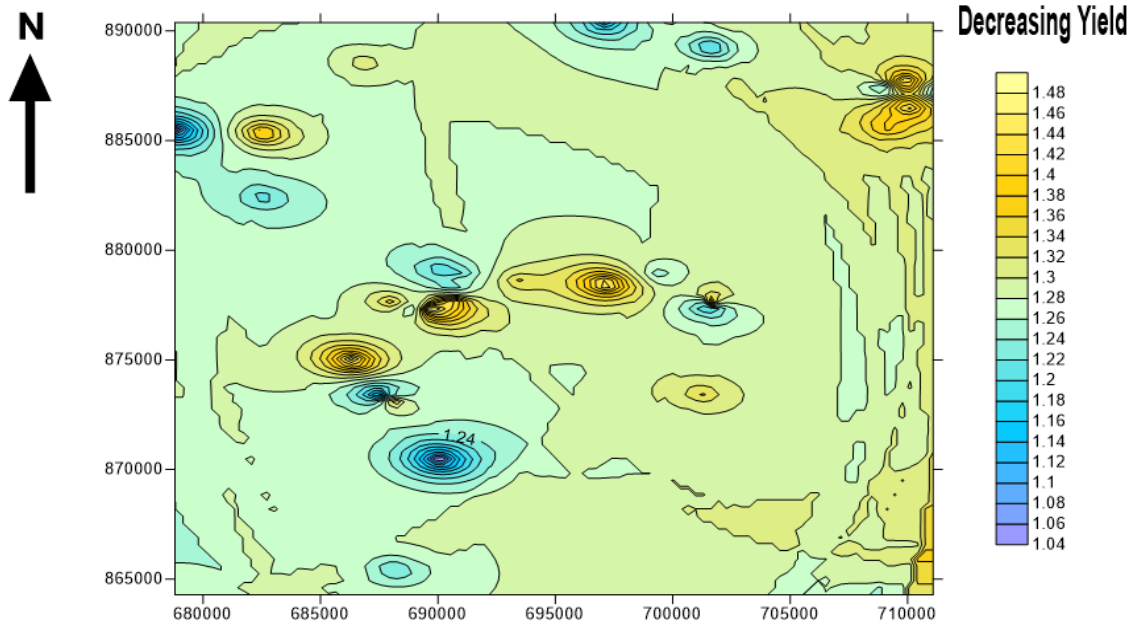


Figure 4.10: Kriged Contoured Thickness Data

KRIGING MEAN



KRIGING STANDARD DEVIATION

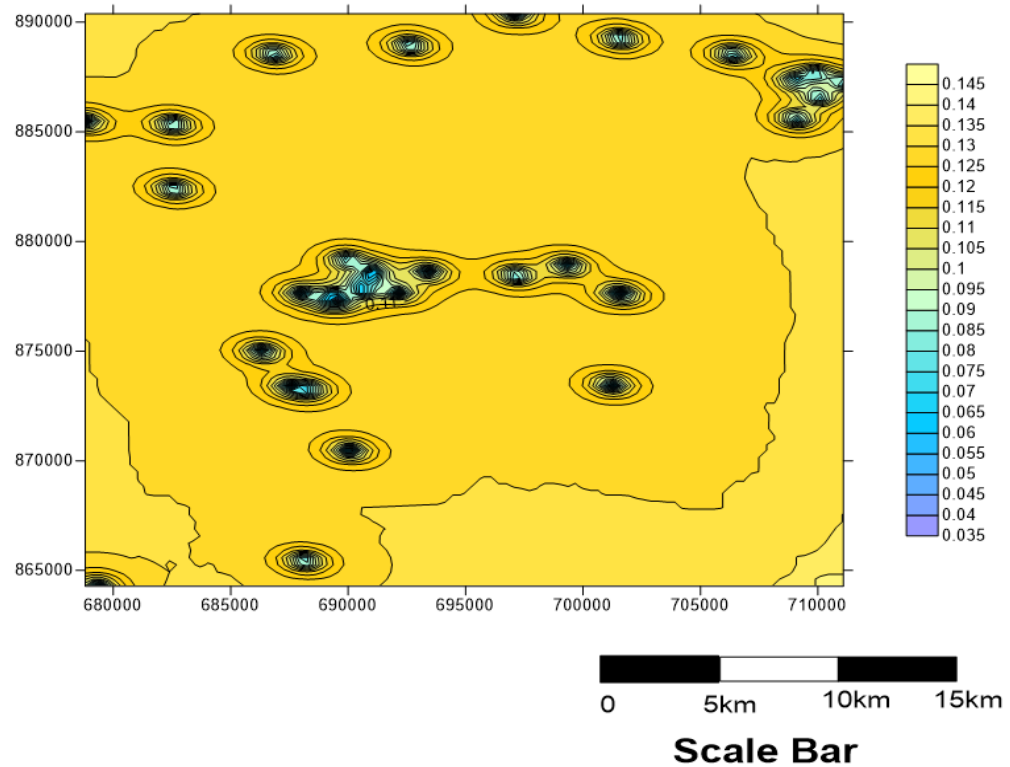


Figure 4.11: Kriged Contoured Yield Data

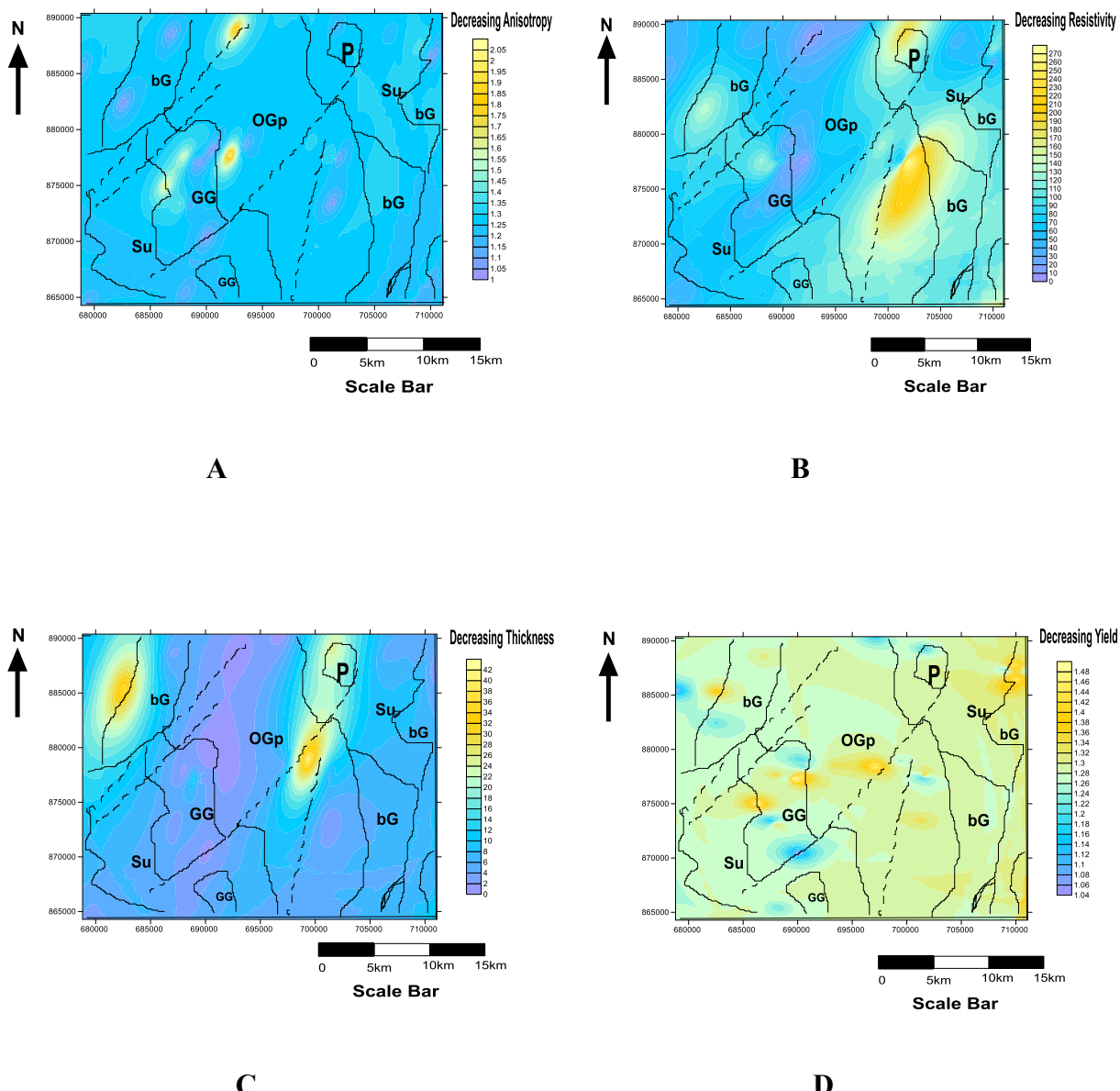


Figure 4.12: Superimposed Map of the Geologic Map and Kriged Mean Maps (A) Coefficient of Anisotropy, (B) Resistivity, (c) Thickness, (D) Yield.

4.3 The Multivariate Regression Analysis.

4.3.1 The Governing Regression Models at Each Distribution Levels.

Given that,

Y = Yield; A = coefficient of Anisotropy; R = Resistivity and T = Thickness

Yield is related to the VES parameters at different conditions by the following equations

A. At the mean level, yield equation is as follows;

$$Y = 1.229 + A * (0.03232) + R * (0.0001346) - T * (0.00002928) \quad (4.1)$$

The correlation coefficient(R) between Yield and VES parameters is 24%

B. At 99.73% Confidence Interval = ($m \pm 3(\sigma)$)

The correlation coefficient(R) between Yield and VES parameter are:

- At upper limit (99.73%), $R=59\%$
- At lower limit (0.27%), $R=60\%$

Yield Equation at the upper (99.73%) and lower limits (0.27%);

$$Y_{99.73\%} = R * (0.0001542) + T * (0.0003285) + A * (0.0484777) + (1.4659919) \quad (4.2)$$

$$Y_{0.27\%} = R * (0.0002138) - T * (0.0002317) + A * (0.0582666) + (0.939821) \quad (4.3)$$

C. At 95.45% Confidence interval= ($m \pm 2(\sigma)$)

The correlation coefficient(R) between Yield and VES parameter are:

- At upper limit (95.45%), $R=48\%$

- At lower limit (4.55%), R=49%

Yield Equation at the upper (95.45%) and lower limits (4.55%);

$$Y_{95.45\%} = R*(0.0001594) + T*(0.0002502) + A*(0.0437027) + (1.391341) \quad (4.4)$$

$$Y_{4.55\%} = R*(0.000195) - T*(0.0000729) + A*(0.0530104) + (1.0249312) \quad (4.5)$$

D. At 68.27% Confidence interval=(m±σ)

The correlation coefficient(R) between Yield and VES parameter are:

- At upper limit (68.27%), R=33%
- At lower limit (31.73%), R=34%

Yield Equation at the upper (68.27%) and lower limits (31.73%);

$$Y_{68.27\%} = T*(0.00009555) + R*(0.0001509) + A*(0.03625) + 1.319 \quad (4.6)$$

$$Y_{31.73\%} = T*(0.0000004566) + R*(0.0001631) + A*(0.04399) + 1.119 \quad (4.7)$$

4.3.2 Relationship Between Estimated and Original Yield Values.

I. Table 4.3 shows the relationship between the original yield and new yield gotten from the average of upper limit and lower limit yield values at the 99.73% CFI. The new yield values can be seen to be slightly different from the original yield values in most stations except in station 79. From Figure (4.13), the highest correlation between them gives 7% when the relationship between them is linear.

Table 4.3: Relationship Between the Original and Estimated Yield Values at 99.73% (CI).

Easting	Northing	VES Point	Original Yield	Original VES			99.75% CONFIDENCE INTERVAL		Estimated Average Yield	
				yield	ANISO	RESIS	THICK	UL(99.75%)		
678806.8	885466.4	VES40	1.03	1.0	30.3	11.5		1.53	1.00	1.26
682540.2	885339.8	VES41	1.42	1.3	87.7	37.2		1.56	1.03	1.29
686836.4	888557.7	VES42	1.32	1.0	37.5	3.4		1.52	1.01	1.26
682583.9	882404.9	VES43	1.20	1.0	139	23.2		1.54	1.02	1.28
697110.8	890385.3	VES44	1.13	1.3	18	0.9		1.53	1.02	1.28
692631.3	888942.6	VES45	1.30	2.0	3.9	0.5		1.57	1.06	1.31
711081.4	887263.2	VES46	1.20	1.2	93.2	1.2		1.54	1.03	1.28
709893.3	887634.8	VES47	1.50	1.3	125.7	6.9		1.55	1.04	1.29
706370.9	888543.3	VES48	1.30	1.2	40.3	5.3		1.53	1.02	1.27
710026	886600.2	VES49	1.48	1.0	15.9	6.2		1.52	1.00	1.26
709087.9	885601.6	VES51	1.40	1.3	91.5	10.8		1.55	1.03	1.29
701578.5	889252.7	VES52	1.17	1.2	201.2	26		1.56	1.04	1.30
701660.1	877581.6	VES53	1.21	1.0	291	11.2		1.56	1.06	1.31
699332	878890.8	VES54	1.24	1.3	129.6	41.8		1.56	1.03	1.30
709057.8	887337.9	VES55	1.20	1.4	42.1	5.9		1.54	1.03	1.29
689953.7	879156.1	VES56	1.20	1.3	31.1	0.5		1.54	1.02	1.28
701216.1	873467.6	VES57	1.35	1.0	224	2.2		1.55	1.05	1.30
697141.7	878459.9	VES58	1.50	1.3	62.2	5.4		1.54	1.03	1.28
690470.8	878115.3	VES59	1.23	1.0	34.2	1.4		1.52	1.01	1.26
693389.7	878606.5	VES60	1.35	1.1	73.7	2.5		1.53	1.02	1.27
691018	878574.4	VES61	1.30	1.0	69	1.1		1.53	1.01	1.27
691026.1	878732.5	VES62	1.20	1.1	25.1	0.7		1.53	1.01	1.27
690997.4	878210.4	VES63	1.22	1.2	35.7	0.8		1.53	1.02	1.27
686334.2	874974.1	VES64	1.50	1.7	62	5.5		1.56	1.05	1.31
689126.9	877239.4	VES65	1.24	1.0	133.5	13.4		1.54	1.02	1.28
689587.8	877242.4	VES66	1.50	1.1	23.9	1.3		1.52	1.01	1.26
689391.3	877578.9	VES67	1.30	1.3	37.6	2.7		1.54	1.02	1.28
690622.3	877745.5	VES68	1.44	1.2	27.1	3.5		1.53	1.02	1.27
690064.7	870457.4	VES69	1.03	1.0	101.9	1.1		1.53	1.02	1.28
688146.3	865436.5	VES70	1.20	1.1	66.7	2.9		1.53	1.02	1.27
689638.1	877353.2	VES71	1.50	1.1	116.4	6.9		1.54	1.03	1.28
688037	877633	VES72	1.36	1.6	127.6	1.1		1.56	1.06	1.31
688325	873278	VES73	1.26	1.1	28.6	5.9		1.53	1.01	1.27
688114.6	873211.9	VES74	1.38	1.4	75.2	5.1		1.55	1.04	1.29
687555.9	873385.5	VES75	1.11	1.4	31.8	2.4		1.54	1.03	1.28
701509.9	877620.7	VES76	1.20	1.4	55.1	4.4		1.54	1.03	1.29
692124.4	877690.9	VES77	1.30	4.2	3.2	0.1		1.67	1.19	1.43
701554	877633.1	VES78	1.43	1.3	66.7	6.8		1.54	1.03	1.28
679355.9	864281.4	VES79	1.27	1.1	35.3	2.6		1.52	1.01	1.27

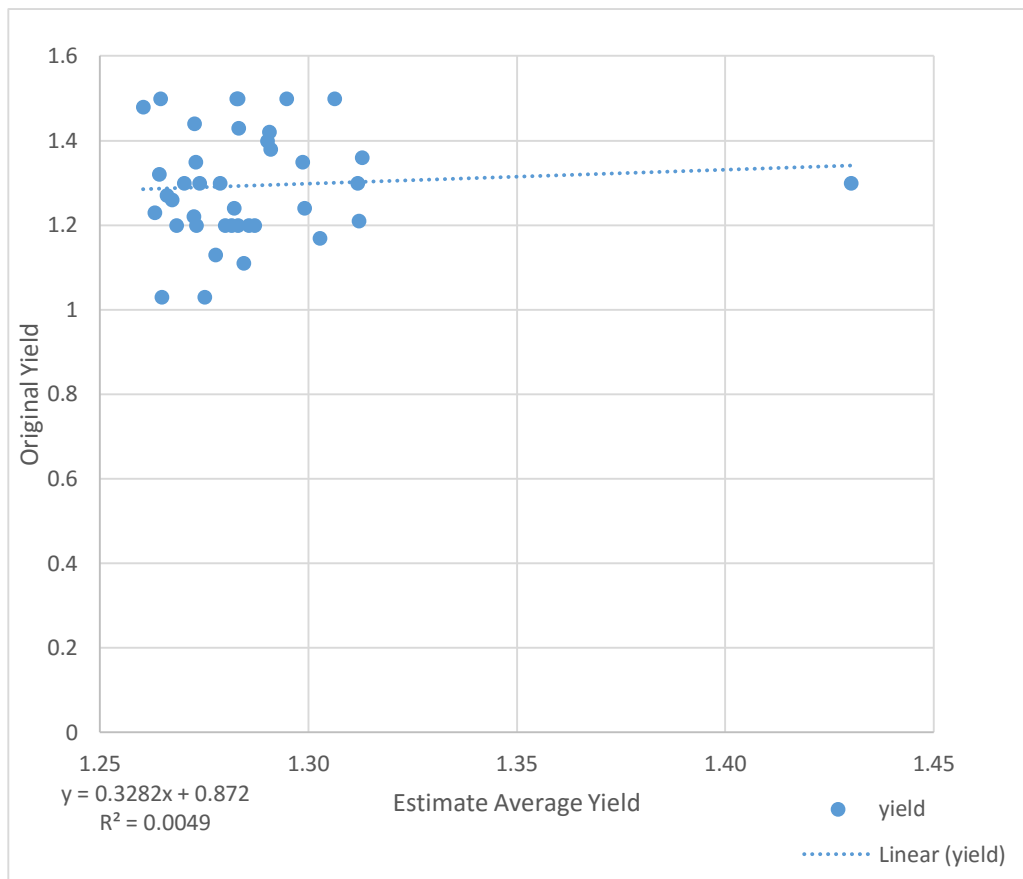


Figure 4.13: Relationship Between Original Yield and Estimated Yield at 99.73%

II. Table 4.4 shows the relationship between the original yield and new yield gotten from the average of upper limit and lower limit yield values at the 95.45% CFI. The new yield values can be seen to be also slightly different from the original yield values in most stations except in station 79. From Figure (4.14), the highest correlation between them gives 6.93% when the relationship between is linear.

III. Table 4.5 shows the relationship between the original yield and new yield gotten from the average of upper limit and lower limit yield values at the 68.27% CFI. The new yield values can be seen to be also slightly different from the original yield values in most stations except in stations 45 and 79. From Figure (4.15), the highest correlation between them gives 6.86% when the relationship between is linear.

4.3.3 Best fit Yield Prediction Equation.

The best fit yield prediction equation for the upper and lower limit is at the 99.73% confidence interval because from the results above, this confidence interval gave us the highest correlation between the original and estimated yield values.

Table 4.4: Relationship Between the Original and Estimated Yield Values at 95.45%

Easting	Northing	VES Point	Original Yield	Original VES			95.45% CONFIDENCE INTERVAL		Estimated average yield
				yield	ANISO	RESIS	THICK	UL(95.45%)	
678806.8	885466.4	VES40	1.03	1.0	30.3	11.5	1.44	1.09	1.27
682540.2	885339.8	VES41	1.42	1.3	87.7	37.2	1.47	1.11	1.29
686836.4	888557.7	VES42	1.32	1.0	37.5	3.4	1.44	1.09	1.26
682583.9	882404.9	VES43	1.20	1.0	139	23.2	1.46	1.10	1.28
697110.8	890385.3	VES44	1.13	1.3	18	0.9	1.45	1.10	1.28
692631.3	888942.6	VES45	1.30	2.0	3.9	0.5	1.48	1.13	1.31
711081.4	887263.2	VES46	1.20	1.2	93.2	1.2	1.46	1.10	1.28
709893.3	887634.8	VES47	1.50	1.3	125.7	6.9	1.47	1.12	1.29
706370.9	888543.3	VES48	1.30	1.2	40.3	5.3	1.45	1.10	1.27
710026	886600.2	VES49	1.48	1.0	15.9	6.2	1.44	1.08	1.26
709087.9	885601.6	VES51	1.40	1.3	91.5	10.8	1.47	1.11	1.29
701578.5	889252.7	VES52	1.17	1.2	201.2	26	1.48	1.12	1.30
701660.1	877581.6	VES53	1.21	1.0	291	11.2	1.49	1.14	1.31
699332	878890.8	VES54	1.24	1.3	129.6	41.8	1.48	1.12	1.30
709057.8	887337.9	VES55	1.20	1.4	42.1	5.9	1.46	1.11	1.28
689953.7	879156.1	VES56	1.20	1.3	31.1	0.5	1.45	1.10	1.28
701216.1	873467.6	VES57	1.35	1.0	224	2.2	1.47	1.12	1.30
697141.7	878459.9	VES58	1.50	1.3	62.2	5.4	1.46	1.10	1.28
690470.8	878115.3	VES59	1.23	1.0	34.2	1.4	1.44	1.08	1.26
693389.7	878606.5	VES60	1.35	1.1	73.7	2.5	1.45	1.10	1.27
691018	878574.4	VES61	1.30	1.0	69	1.1	1.45	1.09	1.27
691026.1	878732.5	VES62	1.20	1.1	25.1	0.7	1.45	1.09	1.27
690997.4	878210.4	VES63	1.22	1.2	35.7	0.8	1.45	1.09	1.27
686334.2	874974.1	VES64	1.50	1.7	62	5.5	1.48	1.13	1.30
689126.9	877239.4	VES65	1.24	1.0	133.5	13.4	1.46	1.10	1.28
689587.8	877242.4	VES66	1.50	1.1	23.9	1.3	1.44	1.09	1.26
689391.3	877578.9	VES67	1.30	1.3	37.6	2.7	1.45	1.10	1.28
690622.3	877745.5	VES68	1.44	1.2	27.1	3.5	1.45	1.09	1.27
690064.7	870457.4	VES69	1.03	1.0	101.9	1.1	1.45	1.10	1.27
688146.3	865436.5	VES70	1.20	1.1	66.7	2.9	1.45	1.10	1.27
689638.1	877353.2	VES71	1.50	1.1	116.4	6.9	1.46	1.10	1.28
688037	877633	VES72	1.36	1.6	127.6	1.1	1.48	1.14	1.31
688325	873278	VES73	1.26	1.1	28.6	5.9	1.45	1.09	1.27
688114.6	873211.9	VES74	1.38	1.4	75.2	5.1	1.47	1.11	1.29
687555.9	873385.5	VES75	1.11	1.4	31.8	2.4	1.46	1.11	1.28
701509.9	877620.7	VES76	1.20	1.4	55.1	4.4	1.46	1.11	1.29
692124.4	877690.9	VES77	1.30	4.2	3.2	0.1	1.58	1.25	1.41
701554	877633.1	VES78	1.43	1.3	66.7	6.8	1.46	1.10	1.28
679355.9	864281.4	VES79	1.27	1.1	35.3	2.6	1.44	1.09	1.27

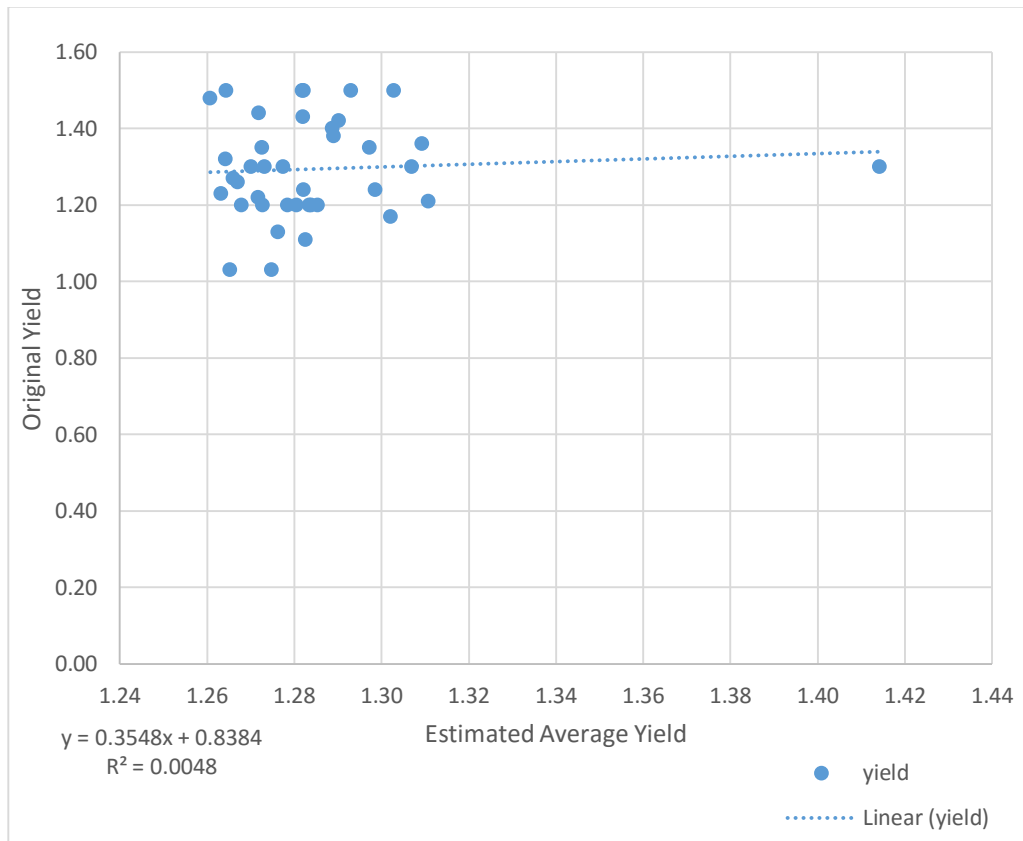


Figure 4.14: Relationship Between Original Yield and Estimated Yield at 95.45%

Table 4.5: Relationship Between the Original and Estimated Yield Values at 68.27%

Easting	Northing	VES Point	Original Yield	Original VES			68.27% CONFIDENCE INTERVAL		Estimated average yield	
				yield	ANISO	RESIS	THICK	UL(68.27%)		
678806.8	885466.4	VES40	1.03	1.0	30.3	11.5		1.36	1.17	1.27
682540.2	885339.8	VES41	1.42	1.3	87.7	37.2		1.38	1.19	1.29
686836.4	888557.7	VES42	1.32	1.0	37.5	3.4		1.36	1.17	1.27
682583.9	882404.9	VES43	1.20	1.0	139	23.2		1.38	1.19	1.28
697110.8	890385.3	VES44	1.13	1.3	18	0.9		1.37	1.18	1.28
692631.3	888942.6	VES45	1.30	2.0	3.9	0.5		1.39	1.21	1.30
711081.4	887263.2	VES46	1.20	1.2	93.2	1.2		1.37	1.18	1.28
709893.3	887634.8	VES47	1.50	1.3	125.7	6.9		1.39	1.20	1.29
706370.9	888543.3	VES48	1.30	1.2	40.3	5.3		1.37	1.18	1.27
710026	886600.2	VES49	1.48	1.0	15.9	6.2		1.36	1.17	1.26
709087.9	885601.6	VES51	1.40	1.3	91.5	10.8		1.38	1.19	1.29
701578.5	889252.7	VES52	1.17	1.2	201.2	26		1.39	1.20	1.30
701660.1	877581.6	VES53	1.21	1.0	291	11.2		1.40	1.21	1.31
699332	878890.8	VES54	1.24	1.3	129.6	41.8		1.39	1.20	1.29
709057.8	887337.9	VES55	1.20	1.4	42.1	5.9		1.38	1.19	1.28
689953.7	879156.1	VES56	1.20	1.3	31.1	0.5		1.37	1.18	1.28
701216.1	873467.6	VES57	1.35	1.0	224	2.2		1.39	1.20	1.30
697141.7	878459.9	VES58	1.50	1.3	62.2	5.4		1.38	1.19	1.28
690470.8	878115.3	VES59	1.23	1.0	34.2	1.4		1.36	1.17	1.26
693389.7	878606.5	VES60	1.35	1.1	73.7	2.5		1.37	1.18	1.27
691018	878574.4	VES61	1.30	1.0	69	1.1		1.37	1.18	1.27
691026.1	878732.5	VES62	1.20	1.1	25.1	0.7		1.36	1.17	1.27
690997.4	878210.4	VES63	1.22	1.2	35.7	0.8		1.37	1.18	1.27
686334.2	874974.1	VES64	1.50	1.7	62	5.5		1.39	1.20	1.30
689126.9	877239.4	VES65	1.24	1.0	133.5	13.4		1.38	1.19	1.28
689587.8	877242.4	VES66	1.50	1.1	23.9	1.3		1.36	1.17	1.27
689391.3	877578.9	VES67	1.30	1.3	37.6	2.7		1.37	1.18	1.28
690622.3	877745.5	VES68	1.44	1.2	27.1	3.5		1.37	1.18	1.27
690064.7	870457.4	VES69	1.03	1.0	101.9	1.1		1.37	1.18	1.28
688146.3	865436.5	VES70	1.20	1.1	66.7	2.9		1.37	1.18	1.27
689638.1	877353.2	VES71	1.50	1.1	116.4	6.9		1.38	1.19	1.28
688037	877633	VES72	1.36	1.6	127.6	1.1		1.40	1.21	1.30
688325	873278	VES73	1.26	1.1	28.6	5.9		1.36	1.17	1.27
688114.6	873211.9	VES74	1.38	1.4	75.2	5.1		1.38	1.19	1.29
687555.9	873385.5	VES75	1.11	1.4	31.8	2.4		1.38	1.19	1.28
701509.9	877620.7	VES76	1.20	1.4	55.1	4.4		1.38	1.19	1.28
692124.4	877690.9	VES77	1.30	4.2	3.2	0.1		1.47	1.31	1.39
701554	877633.1	VES78	1.43	1.3	66.7	6.8		1.38	1.19	1.28
679355.9	864281.4	VES79	1.27	1.1	35.3	2.6		1.36	1.17	1.27

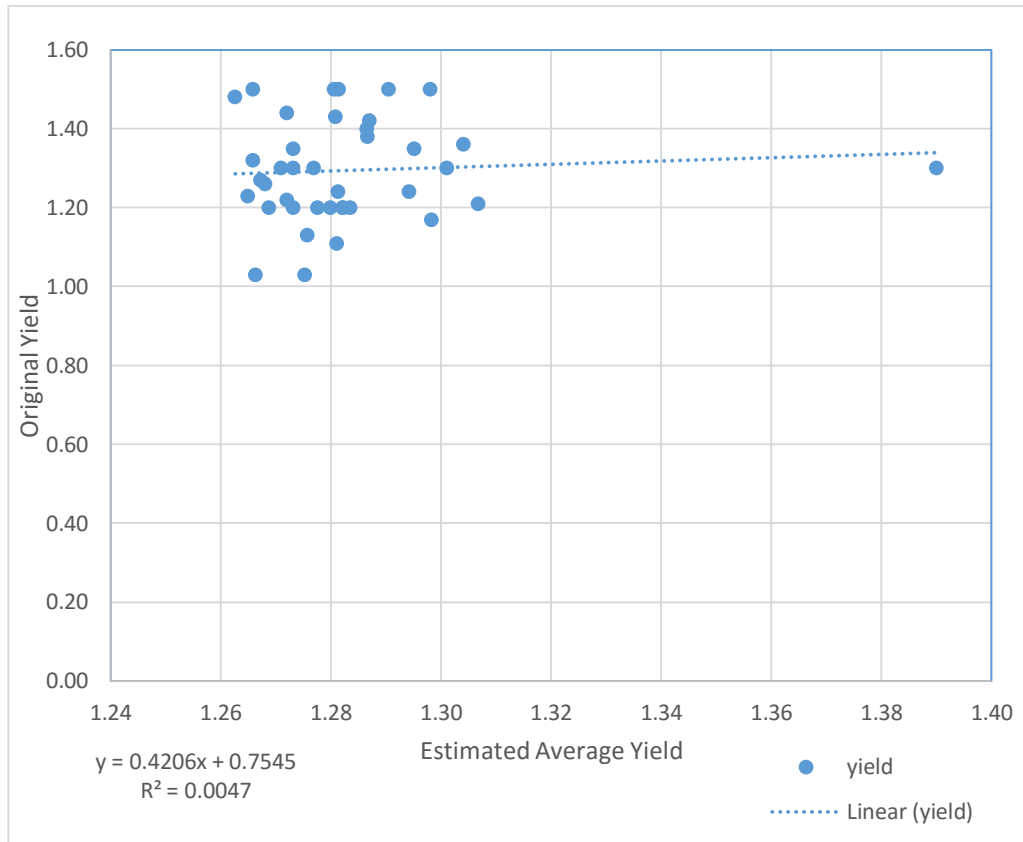


Figure 4.15: Relationship Between Original Yield and Estimated Yield at 68.27%

CHAPTER FIVE

CONCLUSION AND RECOMMENDATION

5.1 CONCLUSION

The study appraised the relationships between groundwater yields and three selected geoelectric parameters of thickness, resistivity and coefficient of anisotropy at different confidence intervals in part of the basement complex of northeastern Osun State. The relationships were determined by using geostatistical kriging of the original 39 data and a multivariate regression analysis on the data.

The methodology used include acquisition of a 39 VES and yield data as secondary data from the northeastern part of Osun State. The VES was interpreted using the partial curve matching method for; resistivity and thickness. The coefficient of anisotropy was then obtained from the resistivity and thickness by applying Dar-Zarrouk's method. Geostatistics was used to estimate beyond the 39 data locations by performing variogram and kriging. The variogram modelled the data while the kriging estimated point by using information from variogram. The mean and standard deviation data estimated from kriging each data was used to assess the data at confidence intervals 99.73%, 95.45% and 68.27% respectively. The best fit yield equation was then determined by comparing the estimated yield values to the original yield values at different confidence intervals.

The results from the analysis showed six major curve types with H curve type dominating the whole area. The data also showed an exponential trend during variogram while the kriging mean estimate were generally greater than their standard deviation for each of the parameters. The

99.73% confidence interval gave the best linear correlation, equation and relationship between groundwater yield and geoelectric parameters in the study area.

The study concluded that there is a positive linear relationship between yield and the geoelectric parameters, although the correlations may be low, maybe because some other parameters need to be considered.

5.2 RECOMMENDATION

It can be recommended that even though the geoelectric parameters are related to the yield at different levels around the study area, other aquifer parameters should also be considered in order to find a better relationship between yield and aquifer parameters. More original data points should also be considered from the beginning.

REFERENCES

- Ajibade A.C. (1976).** Provisional classification and correlation of the schist belts of northwestern Nigeria. In *C.A Kogbe (Editor) Geology of Nigeria, Elizabethan Publishing Company, Lagos, pp. 85-90.*
- Ajibade A.C, Woakes M., Rahaman M.A. (1987).** Proterozoic Crustal Development in the Pan-African Regime of Nigeria: *America Geophysics Union, 259-271.*
- Ahzegbobor Philips Aizebeokhai (2011)** 2D and 3D geoelectrical resistivity imaging: Theory and field design, *scientific research and essays, vol 23 pp. 3592-3605.*
- Bhattacharya, A.P.K and Patra H.P (1968)** Direct current geo-electric sounding: principles and interpretations: *Methods of geochemistry and geophysics, Vol.9, pp.133.*
- Bohling G. (2007).** Introduction to Geostatistics
- Caers J. (2005).** Petroleum Geostatistics, Society of Petroleum Engineers, 88 pages.
- Climate model (2018).** The climate of Osun State
- Deutsch C.V (2002)** Geostatistical Reservoir Modeling, Oxford University Press, 376 pages.
- Excel** Version 16.0, 2016
- Ezeh C.C., Ugwu G.Z., Okonkwo A., Okamkpa J. (2013)** Using the relationships between geoelectrical and hydrogeological parameters to assess aquifer productivity in Udi LGA, Enugu State, Nigeria. International Research Journal of Geology and Mining Vol 3(1), pages 9-18.
- Igel J. (2007)** On the small-scale variability of electrical soil properties and its influence on geophysical measurements.

Isaaks, H.E, Srivastava R.M (1989) An introduction to applied Geostatistics. Oxford University press, New York, 561 p.,ISBN 0-19-505012-6.

Kogbe, C.A (1989). *Geology of the Nigeria*. Elizabethan Publishing Company, Lagos, pp. 530.

Keller, G.V, Frischknecht, F.C (1966) Electrical Methods in Geophysical prospecting, pp.519

Mogaji K.A (2015) Geoelectrical parameter-based multivariate regression borehole yield model for predicting aquifer yield in managing groundwater resource sustainability. *Journal of Taibah University for science*, Vol10, pages 584-600.

McCurry (1976) The Geology of the Precambrian to Lower Paleozoic rocks of Northern Nigeria- A review. In *C.A Kogbe (Editor)Geology of the Nigeria*. Elizabethan Publishing Company, Lagos, pp. 15-40

Nigeria Geological Survey Agency (2006). Geological Map of Nigeria.

Okesie C. N (1974). Geological Map of Nigeria, Geological Survey of Nigeria.

Oyawoye M.O. (1964). The geology of the Nigeria basement complex. *Journal of Nigeria mining, geological and metallurgical society*, vol. 1 pp.87-102.

Orellam E. and Mooney, H.M. (1966) Master tables and curves for Vertical Electrical Sounding over Layered Structures. Interciencia, Madrid.

Oyawoye M.O. (1972) The Basement Complex of Nigeria. University of Ibadan Press, Ibadan 67-99

Olea, R. A. (1999). Step by step mathematical development of key concepts, with clearly documented numerical examples. *Geostatistics for Engineers and Earth Scientists*, Kluwer Academic Publishers, 303 pages.

Ungemach, P., Moslaghini, F. and A. Duprat (1969). Emphasising determination of transmissivity coefficient and application in nappe alluvial aquifer Rhine. Bull. Inst. Assoc. Sci., Hydrol., vol 413 (3), pages 169-190.

Rahaman M. A. (1976). Review of the basement geology of southwestern Nigeria. *Geology of Nigeria*, pp. 41-58.

R version 3.5.1 (2018-07-02). Copyright (C) 2018. The R foundation for Statistical Computation.

Rahaman M. A. (1988). Recent advances in the study of the basement complex of Nigeria. In *Precambrian Geology of Nigeria G.S.N* pp. 11-41.

TaheriTizro, A., Voudouri K. S. and Eini M. (2007). Groundwater balance, safe yield and recharge feasibility in a semi-Arid environment: A case study from western part of Iran. Journal of Applied Sciences Vol7, pages 2967-2976.

SurferTM Version 11 Surface Mapping System 1993-2012, Golden Software, Inc.

Telford W.M, Geldart L.P. and Sheriff R.E (1990) Applied Geophysics Second Edition.

Tubosun I.A, Lancelot J.R, Rahaman M.A. and Ocan O. (1984) U-Pb Pan African ages of two Charnockitic-Granite Association from SW Nigeria. *Contrib. Mineral. Petrol. Pp. 88, 188-195.*

InterpretVES Version 1.0 Developed for 32-bit Applications by Jerry F. Ayers, 2000.

Liu C., White M., Graeme N. (2017) Detecting outliers in species distribution data. Journal of Biogeography, vol 45, issue 1.

APPENDIX

APPENDIX - VES DATA

AB /2	4.622 370	4.656 230	4.695 320	4.656 520	4.747 900	4.747 900	4.915 180	4.904 420	4.872 510	4.905 580	4.897 030	4.829 070
(m)	6.008 110	8.006 830	8.035 770	7.980 290	8.051 900	8.039 030	8.023 100	8.026 510	8.026 870	8.017 150	8.008 160	8.041 448
	VES 40	VES 41	VES42	VES43	VES44	VES 45	VES 46	VES 47	VES 48	VES 49	VES 51	VES 52
	MSCV ES32	MSCV ES31	MSCV ES30	MSCV ES35	MSCV ES36	MSCV ES37	MSCV ES38	MSCV ES39	MSCV ES40	MSCV ES43	MSCV ES42	MSCV ES44
	Resistivity		Resistivity	Resistivity								
	(Ωm)											
1	74	85	55	200	74	30	207	207	88	25	141	229
2	72	164	50	187	45	18	155	191	92	23	217	172
3	53	227	49	183	43	26	137	185	102	21	260	288
5	41	307	51	154	62	39	186	250	117	18	295	395
6	39	308	57	164	66	46	194	275	115	18	270	397
6	39	306	56	152	63	51	253	280	110	18	275	385
8	38	301	57	160	89	65	259	284	99	19	231	408
10	37	332	60	156	117	82	281	253	98	21	195	406
10	37	313	68	174	107	84	245	250	95	22	200	360
12	40	346	74	159	126	103	243	245	95	24	180	357
15	45	377	83	146	137	128	253	265	98	27	183	329
20	56	361	100	133	185	167	247	310	124	32	190	310
25	69	320	126	156	167	207	278	340	156	33	225	280
30	84	318	147	181	187	230	269	487	200	34	255	300
40	111	231	207	206	167	281	360	740	305	36	357	320
40	102	242	175	199	226	278	379	732	300	37	346	326
50	128	192	226	233	213	320	419	900	384	44	440	360
60		193					467	1000	500	58	590	400
70		220								65		

AB/2	4.82 9340	4.80 8280	4.89 6830	4.72 3240		4.82 5150	4.78 8400		4.72 AB/2	4.75 7890	4.73 4380	4.73 2870	4.73 2950
(m)	7.93 5950	7.94 7880	8.02 3860	7.95 0640	(m)	7.89 8770	7.94 4070		7.94 (m)	7.94 1210	7.94 5540	7.94 5340	7.94 6770
	VES 53	VES 54	VES 55	VES 56		VES 57	VES 58		VES 59	VES 60	VES 61	VES 62	
	MSC VES4 6	MSC VES4 7	MSC VES4 5		MSCVES53	MSC VES5 0		MSCVES51	MSC VES5 5	MSC VES5 6	MSC VES5 7	MSC VES5 8	
	Resistivity (Ωm)	Resistivity (Ωm)	Resistivity (Ωm)	Resistivity (Ωm)	Resistivity Resistivity	Resistivity (Ωm)	Resistivity (Ωm)	Resistivity Resistivity	Resistivity (Ωm)	Resistivity (Ωm)	Resistivity (Ωm)	Resistivity (Ωm)	
1	690	296	184	140	1	509	170	1	45	147	108	65	
2	463	360	117	107	2	592	233	2	42	131	98	51	
3	404	417	100	165	3	650	190	3	44	122	115	55	
5	330	558	104	270	4	695	140	5	48	130	151	63	
6	310	605	112	320	6	652	112	6	53	150	175	63	
6	315	610	116	325	6	516	115	6	54	150	170	67	
8	289	650	130	410	8	502	99	8	59	187	201	75	
10	300	700	111	502	12	580	123	10	63	242	232	79	
10	305	705	122	492	15	627	143	10	65	246	229	81	
12	308	700	102		15	629	147	15	75	359	308	96	
15	325	650	110	753	20	799	171	20	95	494	382	116	
20	353	525	116	1005	25	679	190	30	141	805	515	141	
25	380	440	150		32	558	221	40	180	1140	703	184	
30	409	360	177	1503	40	516	271	40	175	1145	709	188	
40	455	265	260	2106	40	454	269	50	221	1700	890	256	
40	465	269	265	2113	50	329	316						
50	521	230	341	2707									
60	600	212	405										
70		226											
80		251											
100		312											
120													
150		442											

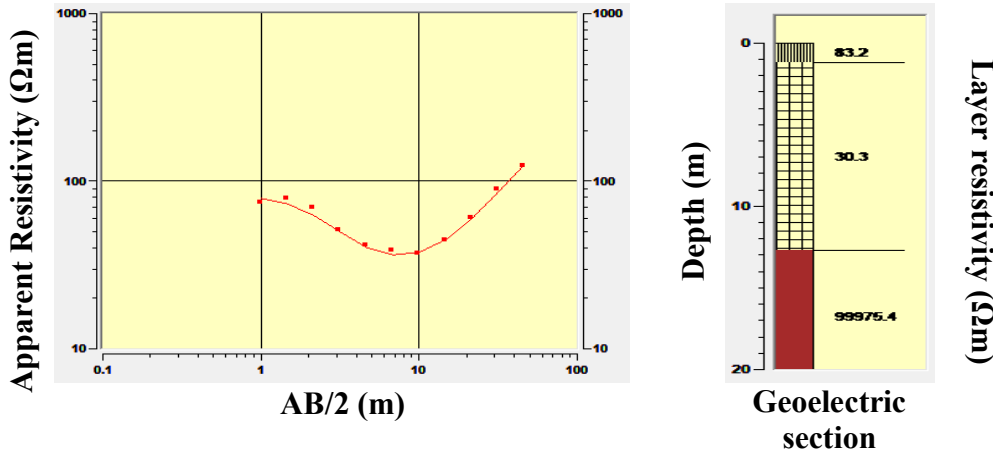
AB/2	4.732 67		4.690 26	AB/2	4.715 670	4.719 850	4.720 220	4.729 250	4.723 920	4.706 340	4.720 310
(m)	7.942 05	(m)	7.912 96	(m)	7.933 340	7.933 350	7.936 360	7.937 860	7.871 980	7.871 980	7.934 350
	VES 63		VES 64		VES 65	VES 66	VES 67	VES 68	VES 69	VES 70	VES 71
	MSCVES59		MSC VES1 5		MSC VES1 7	MSC VES1 8	MSC VES2 1	MSC VES2 5	MSC VES1 9	MSC VES2 2	MSC VES2 3
	Resistivity		Resis tivity		Resis tivity						
	(Ωm)		(Ωm)		(Ωm)						
1	98	1	92	1	216	51	129	110	109	157	177
2	77	2	99	2	215	42	136	75	171	127	221
3	83	3	125	3	210	50	146	50	220	109	206
5	104	5	173	5	171	72	111	43	321	113	168
6	133	6	194	6	174	83	97	47	362	132	154
6	117	6	195	6	183	88	110	45	358	138	149
8	135	8	226	8	178	104	111	56	418	146	149
10	157	10	231	10	168	131	134	66	468	182	167
10	163	10	228	10	152	135	136	64	505	179	159
15	224	12	209	12	151	151	153	81	551	211	186
20	320	15	191	15	161	179	201	99	577	264	218
30	500	20	231	20	189	229	302	122	619	335	272
40	647	25	280	25	239	265	354	141	650	389	303
40	650	30	321	30	261	323	432	157	681	422	342
50	731	40	405	40	334	418	539	188	703	522	400
		40	399	40	310	404	497	193	698	528	409
		50	480	50	410	538	602	223	753	652	470
		60	594	60	544	649	816		753	742	530
				70					780		

AB/2	4.707 580	4.708 250	4.706 340	4.701 280	AB/2	4.827 980	4.742 870	AB/2	4.828 380	4.626 600
(m)	7.936 940	7.897 550	7.896 960	7.898 550	(m)	7.936 310	7.937 310	(m)	7.936 420	7.816 520
	VES 72	VES 73	VES 74	VES 75		VES 76	VES 77		VES 78	VES 79
	MSCV ES24	MSCV ES20	MSCV ES26	MSCVES29		MSCV ES52	MSCVES49		MSCV ES48	MSCV ES27
	Resist ivity	Resist ivity	Resist ivity	Resistivity		Resist ivity	Resistivity		Resist ivity	Resist ivity
	(Ωm)	(Ωm)	(Ωm)	(Ωm)		(Ωm)	(Ωm)		(Ωm)	(Ωm)
1	738	31	359	197	1	146	171	1	243	61
2	316	39	228	177	2	191	95	2	135	46
3	227	47	185	142	3	195	120	3	148	44
5	245	53	221	92	4	170	160	5	170	43
6	269	47	224	91	6	133	220	6	174	51
6	255	50	205	86	6	130	215	6	168	49
8	310	53	200	102	8	125	240	8	155	63
10	325	48	182	133	12	140	225	10	141	77
10	315	49	178	137	15	175	210	10	136	73
12	309	52	166	155	15	171		12	132	70
15	299	58	191	201	20	225	145	15	135	64
20	288	69	247	251	25	321	105	20	165	61
25	293	88	309	309	32	438	60	25	180	56
30	320	90	386	375	40	525	36	30	205	66
40	385	111	555	471	40	530	37	35		
40	378	115	547	466	50	800	18	40	352	88
50	465	142	717	552				40	355	88
60	530	180	809	607				50	503	109
								60	598	129

APPENDIX - VES INTERPRETED CURVES

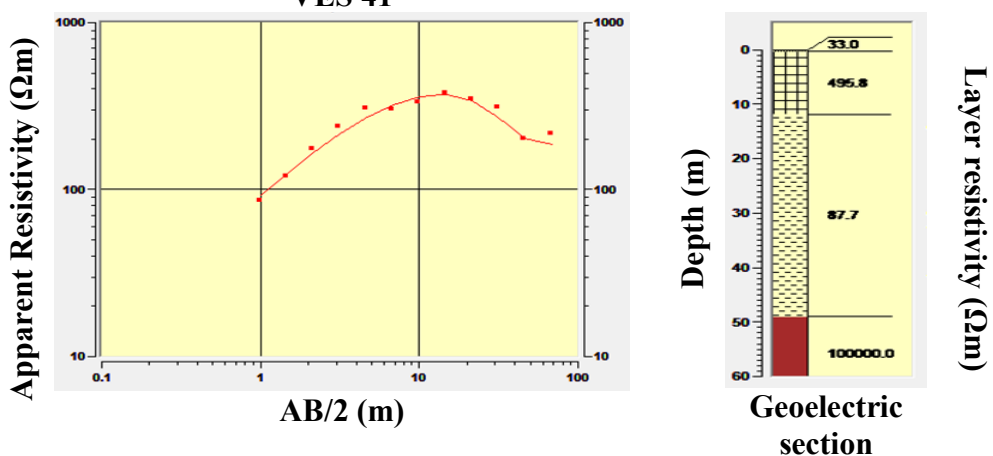
Thickness	Resistivity	Long. Conductance	Trans. Resist.
1.2	83.2	0.01442	99.9
11.5	30.3	0.37948	348.5
Infinite	99975.4		

VES 40



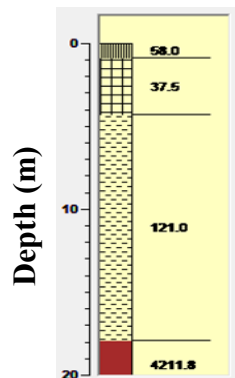
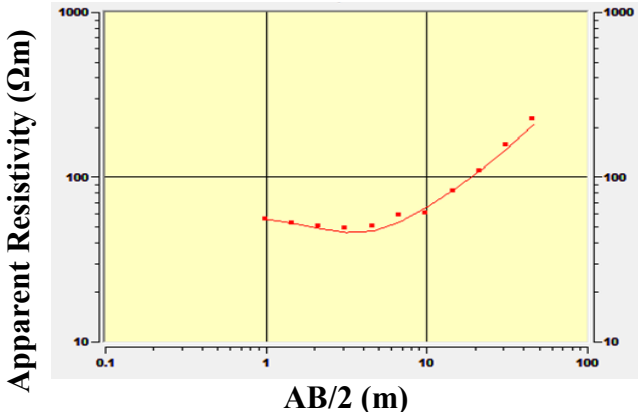
Thickness	Resistivity	Long. Conductance	Trans. Resist.
0.3	33.0	0.00909	9.9
11.5	495.8	0.0232	5701.4
37.2	87.7	0.42433	3261.3
Infinite	100000.		

VES 41



Thickness	Resistivity	Long. Conductance	Trans. Resist.
0.9	58.0	0.01551	52.2
3.4	37.5	0.0906	127.6
13.6	121.0	0.1124	1645.6
Infinite	4211.8		

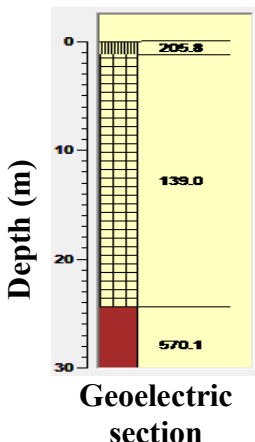
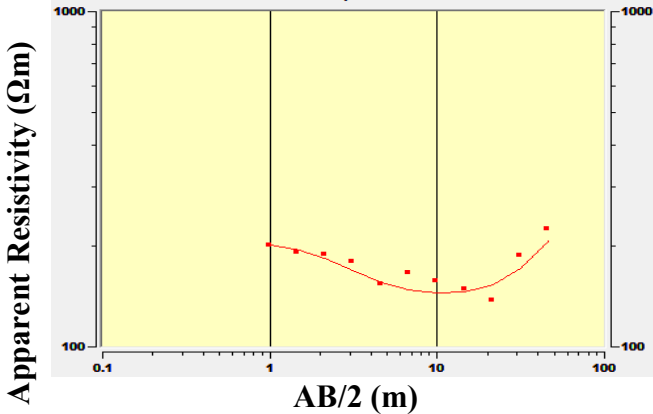
VES 42



Layer resistivity (Ωm)

Thickness	Resistivity	Long. Conductance	Trans. Resist.
1.2	205.8	0.00583	247.0
23.2	139.0	0.16696	3223.7
Infinite	570.1		

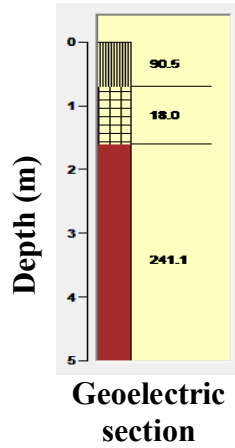
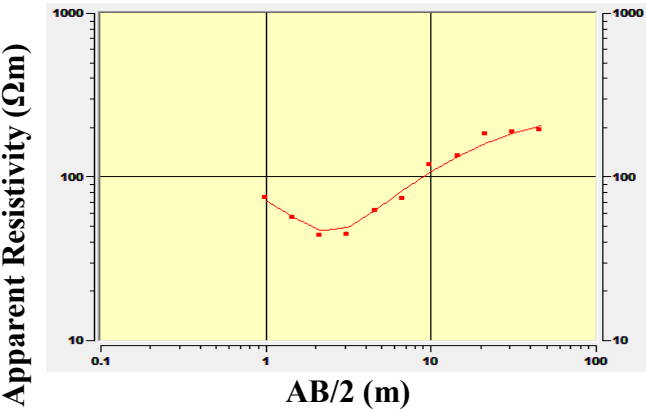
VES 43



Layer resistivity (Ωm)

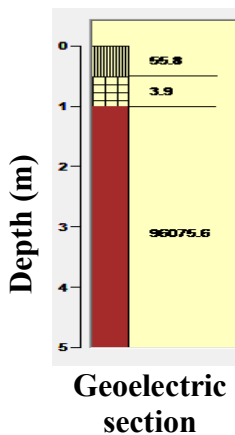
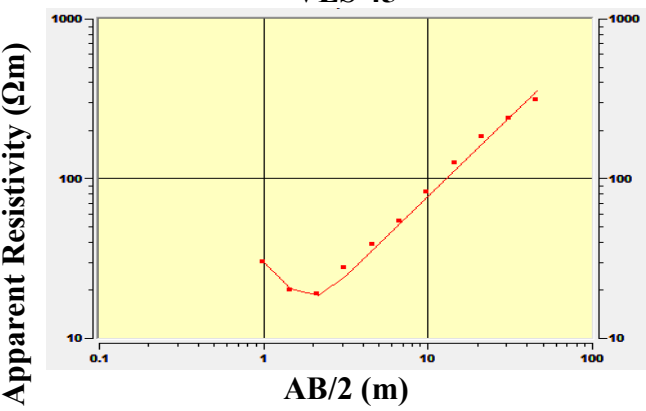
Thickness	Resistivity	Long. Conductance	Trans. Resist.
0.7	90.5	0.00774	63.3
0.9	18.0	0.05007	16.2
Infinite	241.1		

VES 44



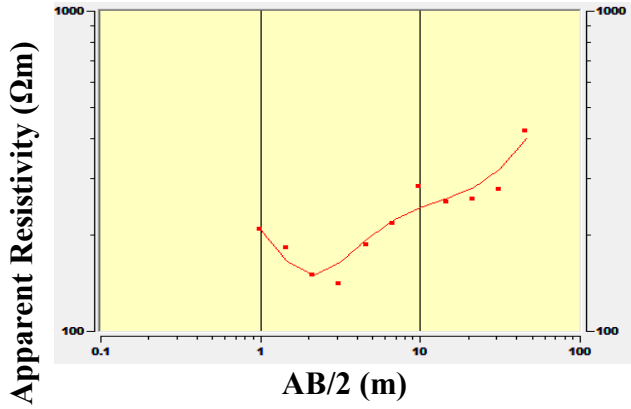
Thickness	Resistivity	Long. Conductance	Trans. Resist.
0.5	55.8	0.00896	27.9
0.5	3.9	0.12891	1.9
Infinite	96075.6		

VES 45

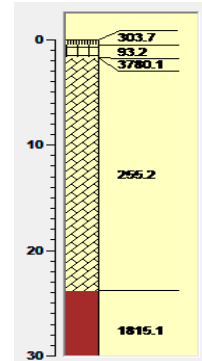


Thickness	Resistivity	Long. Conductance	Trans. Resist.
0.5	303.7	0.00165	151.8
1.2	93.2	0.01288	111.8
0.1	3780.1	0.00003	378.0
22.0	255.2	0.0862	5615.1
Infinite	1815.1		

VES 46



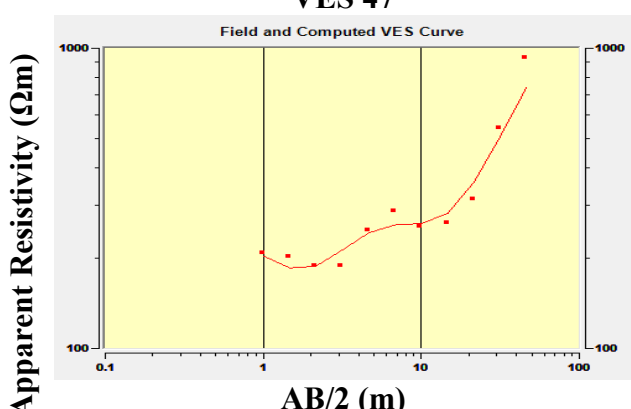
Depth (m)



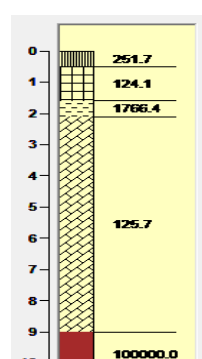
Layer resistivity (Ωm)

Thickness	Resistivity	Long. Conductance	Trans. Resist.
0.5	251.7	0.00199	125.8
1.1	124.1	0.00886	136.5
0.5	1766.4	0.00028	883.2
6.9	125.7	0.05491	867.1
Infinite	100000.		

VES 47



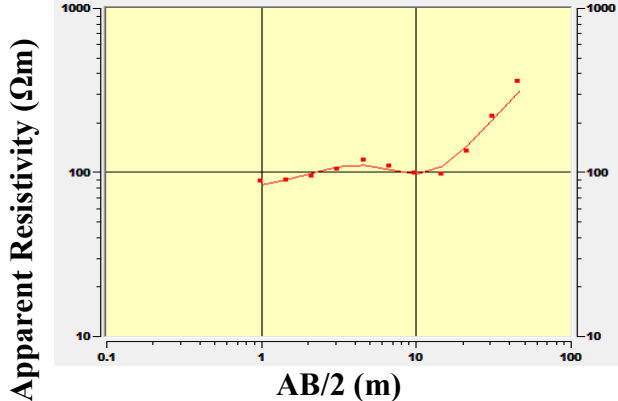
Depth (m)



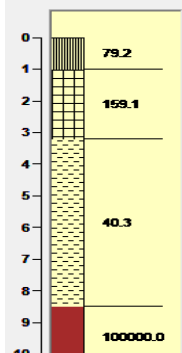
Layer resistivity (Ωm)

Thickness	Resistivity	Long. Conductance	Trans. Resist.
1.0	79.2	0.01263	79.2
2.2	159.1	0.01383	350.0
5.3	40.3	0.13137	213.8
Infinite	100000.		

VES 48



Depth (m)

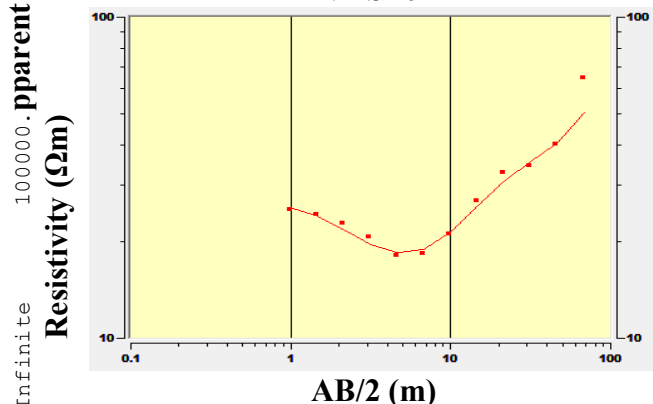


Layer resistivity (Ωm)

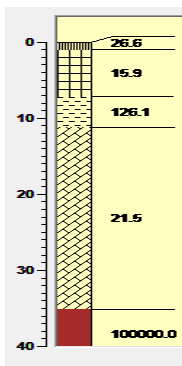
Geoelectric section

Thickness	Resistivity	Long. Conductance	Trans. Resist.
1.0	26.6	0.03762	26.6
6.2	15.9	0.39042	98.5
4.0	126.1	0.03172	504.3
23.9	21.5	1.10947	514.8

VES 49



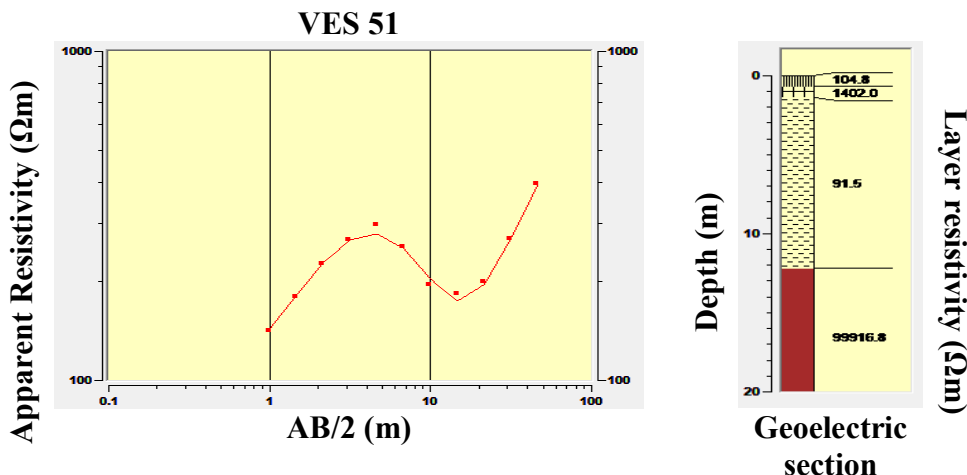
Depth (m)



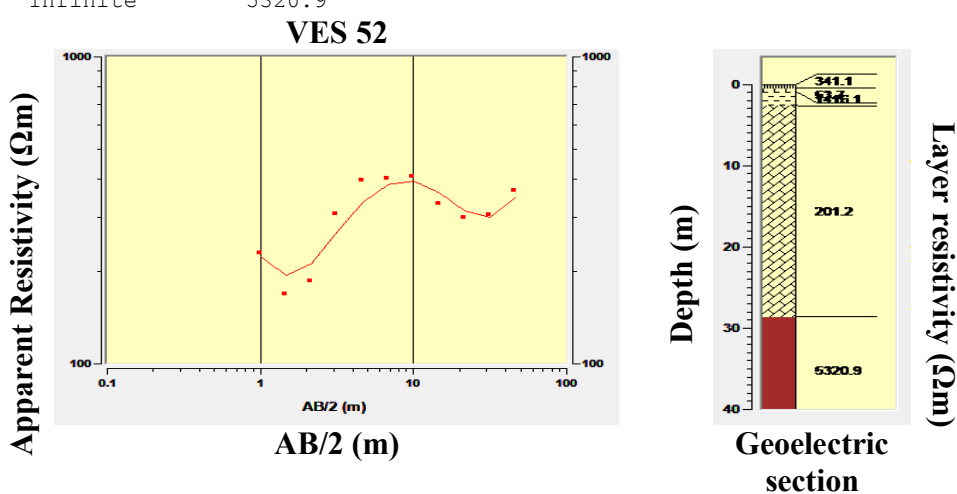
Layer resistivity (Ωm)

Geoelectric section

Thickness	Resistivity	Long. Conductance	Trans. Resist.
0.7	104.8	0.00668	73.3
0.7	1402.0	0.0005	981.4
10.8	91.5	0.11797	988.7
Infinite	99916.8		

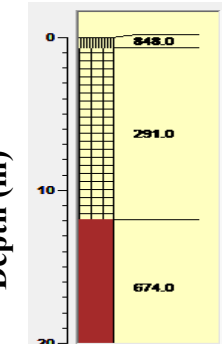
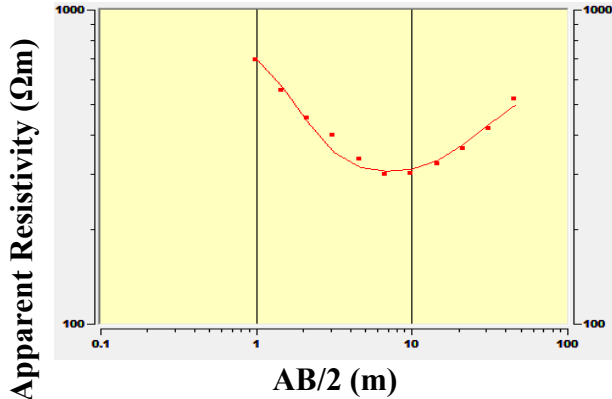


Thickness	Resistivity	Long. Conductance	Trans. Resist.
0.5	341.1	0.00147	170.5
0.4	53.7	0.00745	21.5
1.7	1416.1	0.0012	2407.4
26.0	201.2	0.1292	5232.2
Infinite	5320.9		



Thickness	Resistivity	Long. Conductance	Trans. Resist.
0.7	848.0	0.00083	593.6
11.2	291.0	0.03849	3259.2
Infinite	674.0		

VES 53

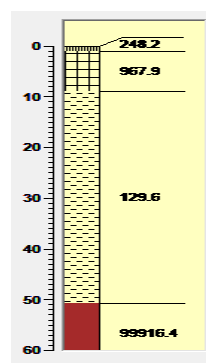
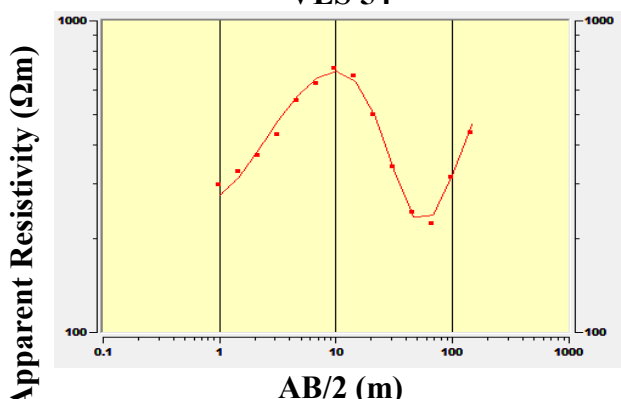


Layer resistivity (Ωm)

Geoelectric section

Thickness	Resistivity	Long. Conductance	Trans. Resist.
1.0	248.2	0.00403	248.2
7.9	967.9	0.00816	7646.2
41.8	129.6	0.32251	5417.6
Infinite	99916.4		

VES 54

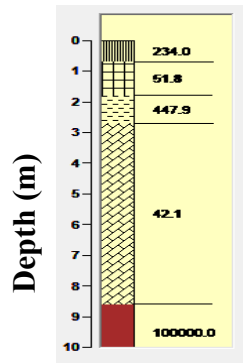
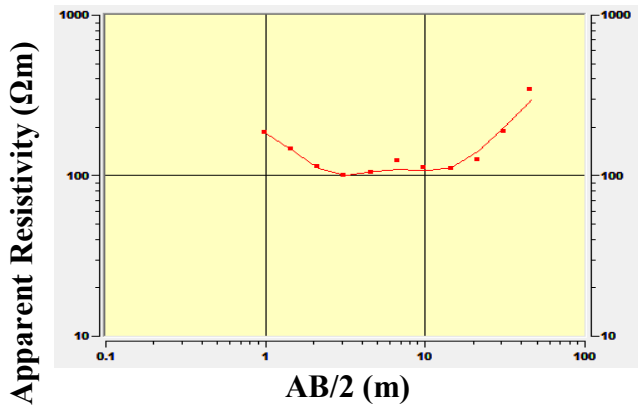


Layer resistivity (Ωm)

Geoelectric section

Thickness	Resistivity	Long. Conductance	Trans. Resist.
<hr/>			
0.7	234.0	0.00299	163.8
1.1	51.8	0.02124	57.0
0.9	447.9	0.00201	403.1
5.9	42.1	0.1403	248.1
Infinite	100000.		

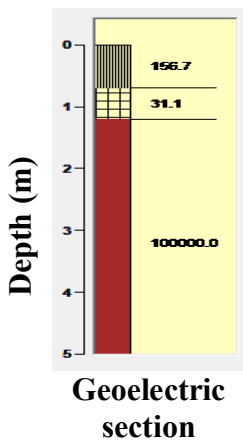
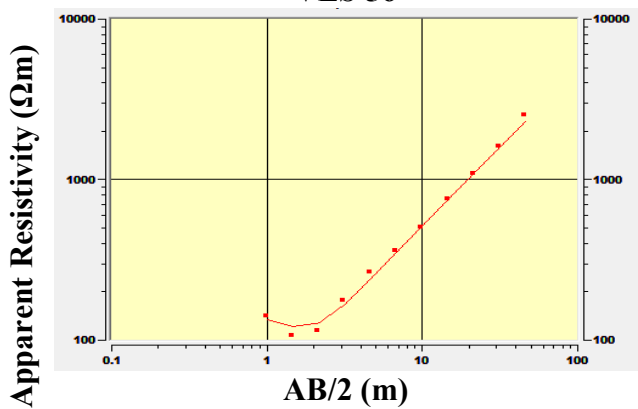
VES 55



Layer resistivity (Ωm)
Geoelectric section

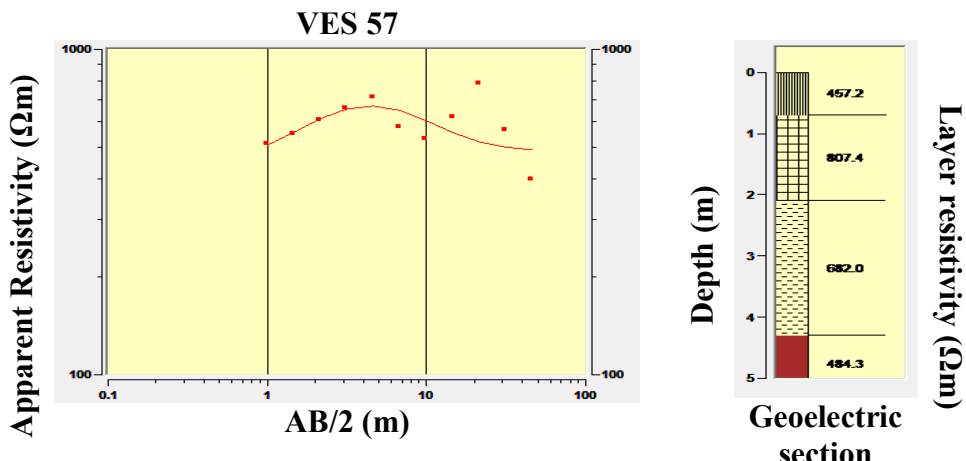
Thickness	Resistivity	Long. Conductance	Trans. Resist.
<hr/>			
0.7	156.7	0.00447	109.7
0.5	31.1	0.01608	15.5
Infinite	100000.		

VES 56

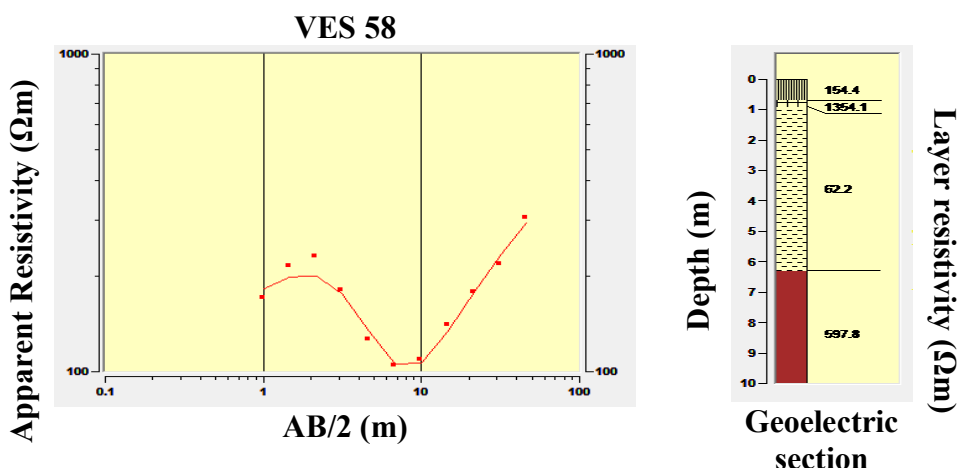


Layer resistivity (Ωm)
Geoelectric section

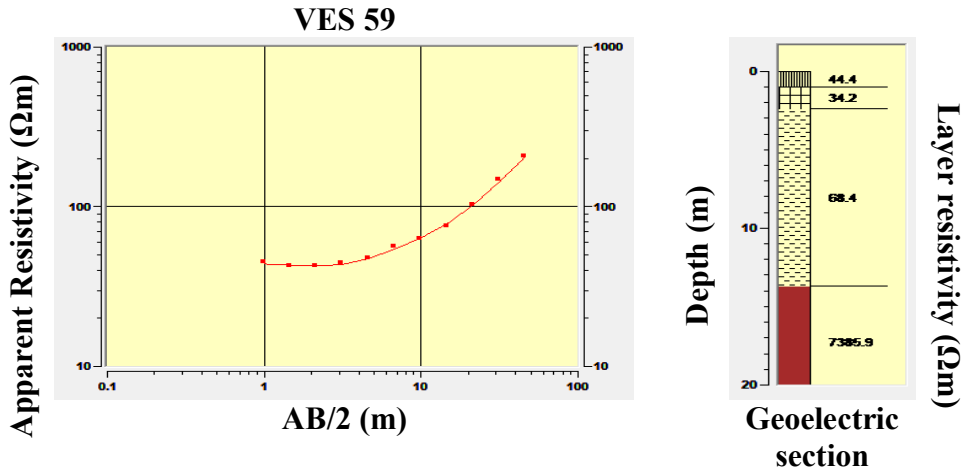
Thickness	Resistivity	Long. Conductance	Trans. Resist.
<hr/>			
0.7	457.2	0.00153	320.1
1.4	807.4	0.00173	1130.3
2.2	682.0	0.00323	1500.4
Infinite	484.3		



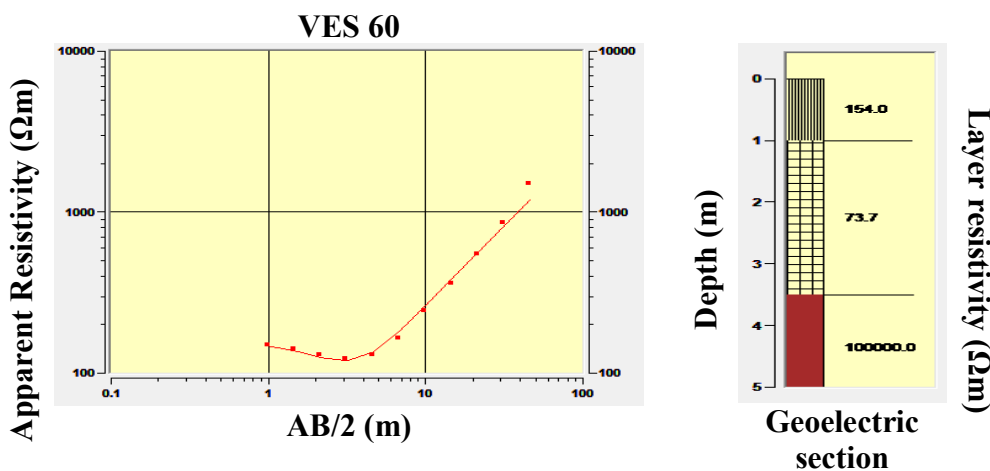
Thickness	Resistivity	Long. Conductance	Trans. Resist.
<hr/>			
0.7	154.4	0.00453	108.1
0.2	1354.1	0.00015	270.8
5.4	62.2	0.08684	335.8
Infinite	597.8		



Thickness	Resistivity	Long. Conductance	Trans. Resist.
1.0	44.4	0.02254	44.4
1.4	34.2	0.04094	47.9
11.3	68.4	0.16513	773.3
Infinite	7385.9		

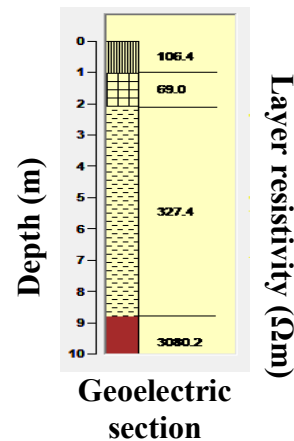
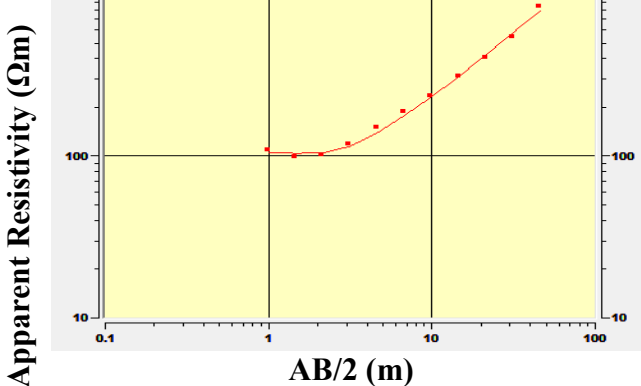


Thickness	Resistivity	Long. Conductance	Trans. Resist.
1.0	154.0	0.00649	154.0
2.5	73.7	0.03393	184.2
Infinite	100000		



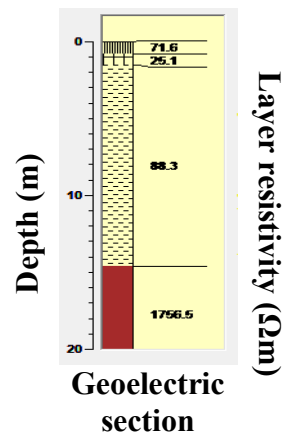
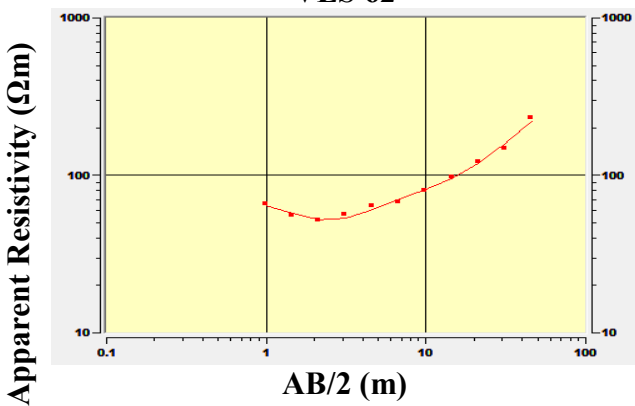
Thickness	Resistivity	Long. Conductance	Trans. Resist.
1.0	106.4	0.0094	106.4
1.1	69.0	0.01594	75.9
6.7	327.4	0.02046	2193.6
Infinite	3080.2		

VES 61

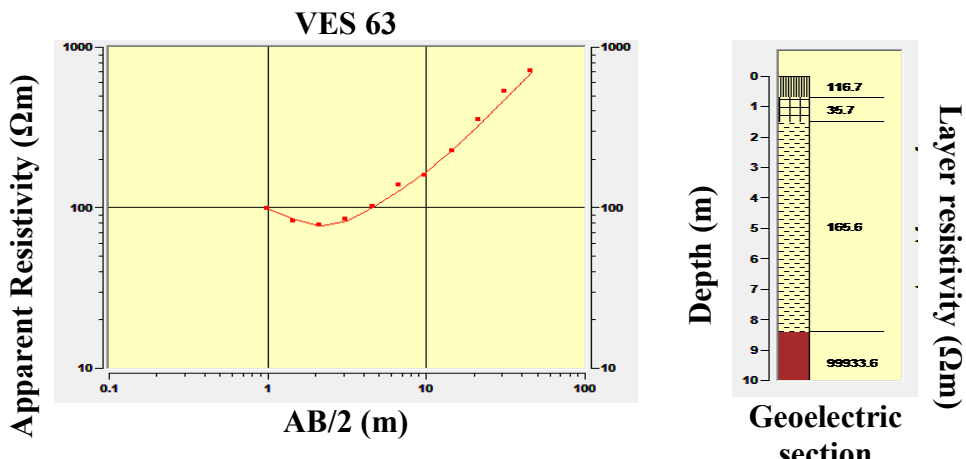


Thickness	Resistivity	Long. Conductance	Trans. Resist.
0.8	71.6	0.01117	57.3
0.7	25.1	0.02792	17.6
13.1	88.3	0.14828	1157.3
Infinite	1756.5		

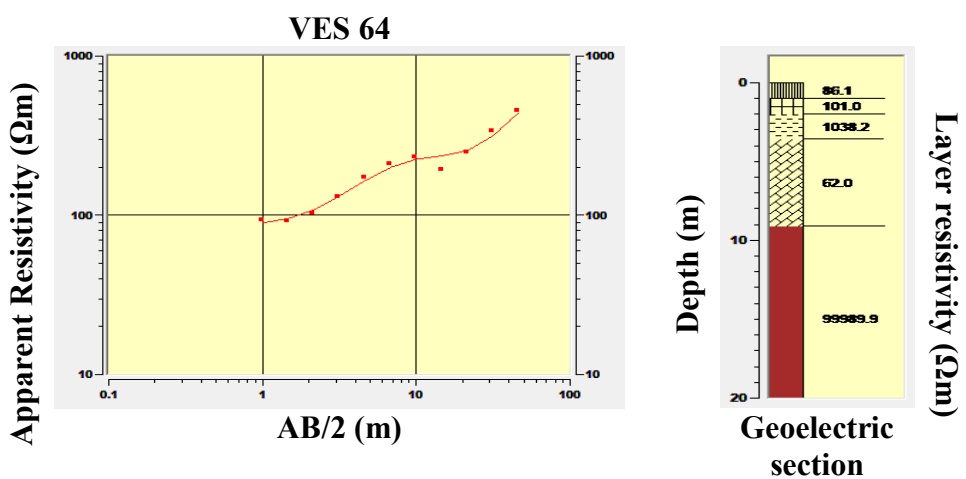
VES 62



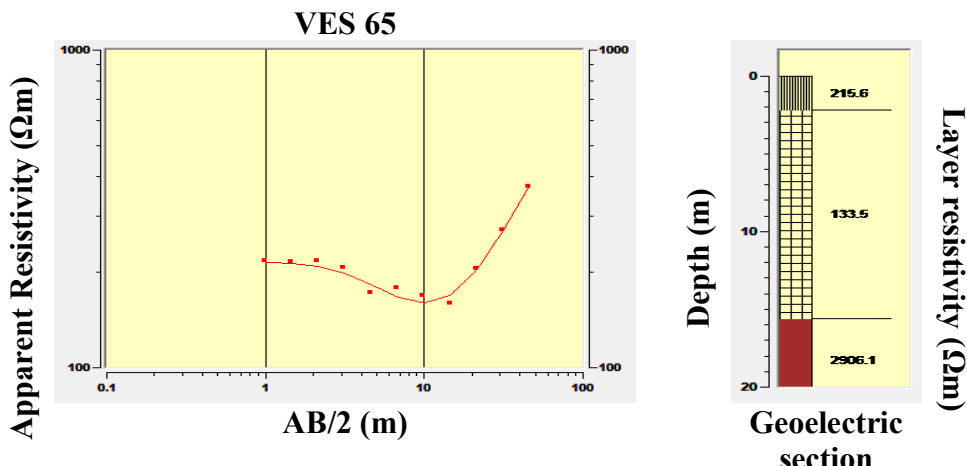
Thickness	Resistivity	Long. Conductance	Trans. Resist.
0.7	116.7	0.006	81.7
0.8	35.7	0.02238	28.6
6.9	165.6	0.04166	1142.8
Infinite	99933.6		



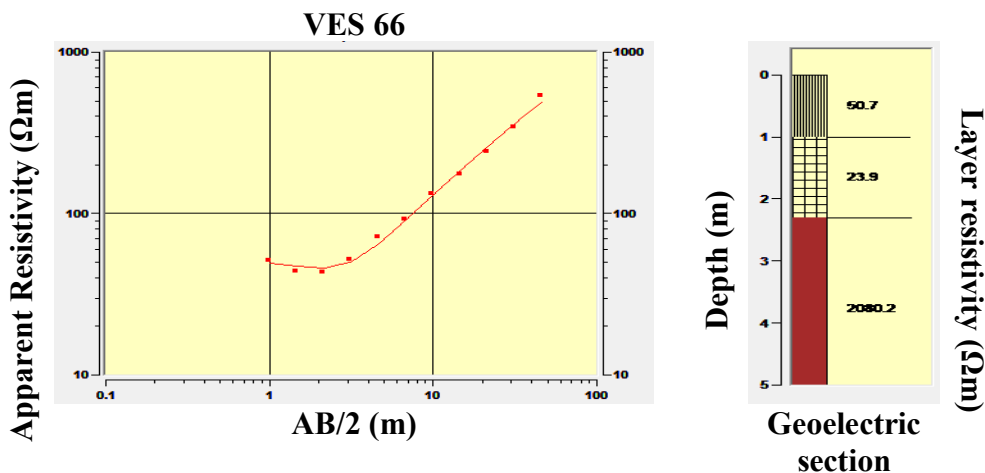
Thickness	Resistivity	Long. Conductance	Trans. Resist.
1.0	86.1	0.01162	86.1
1.0	101.0	0.0099	101.0
1.6	1038.2	0.00154	1661.1
5.5	62.0	0.08865	341.2
Infinite	99989.9		



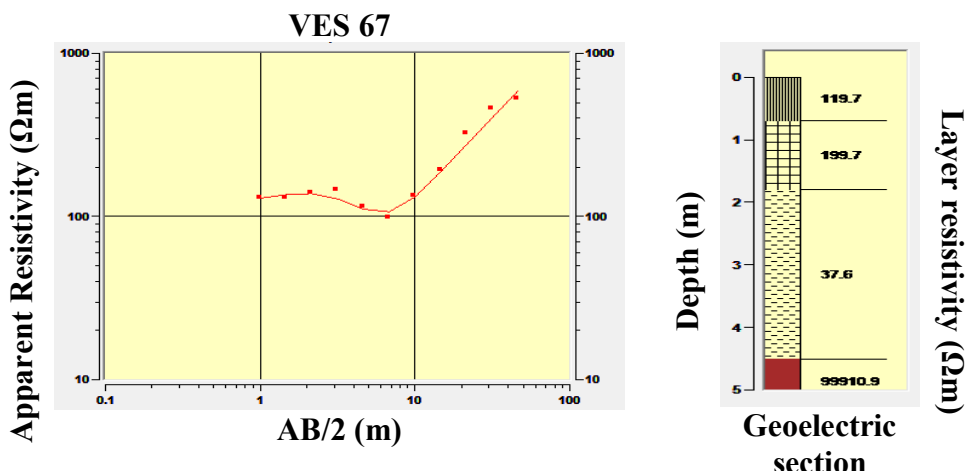
Thickness	Resistivity	Long. Conductance	Trans. Resist.
2.2	215.6	0.01021	474.2
13.4	133.5	0.10041	1788.2
Infinite	2906.1		



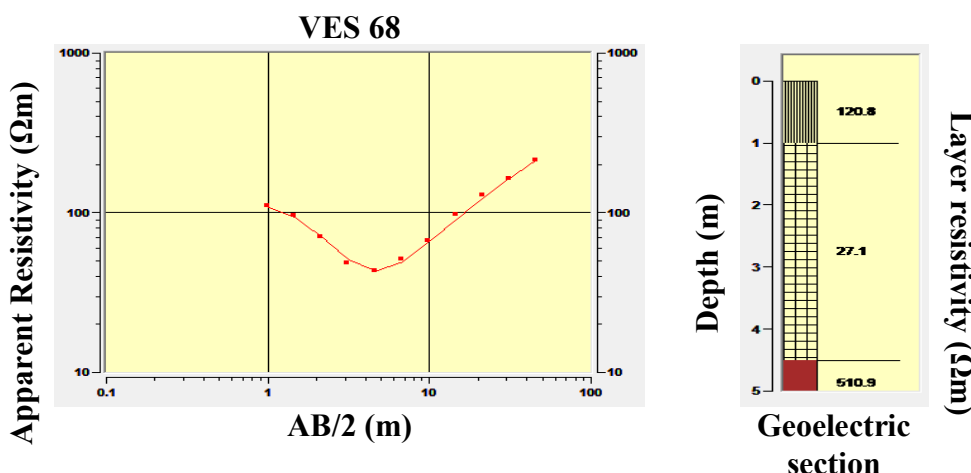
Thickness	Resistivity	Long. Conductance	Trans. Resist.
1.0	50.7	0.01974	50.7
1.3	23.9	0.05438	31.1
Infinite	2080.2		



Thickness	Resistivity	Long. Conductance	Trans. Resist.
<hr/>			
0.7	119.7	0.00585	83.8
1.1	199.7	0.00551	219.7
2.7	37.6	0.07183	101.5
Infinite	99910.9		

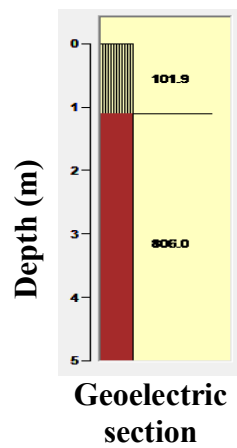
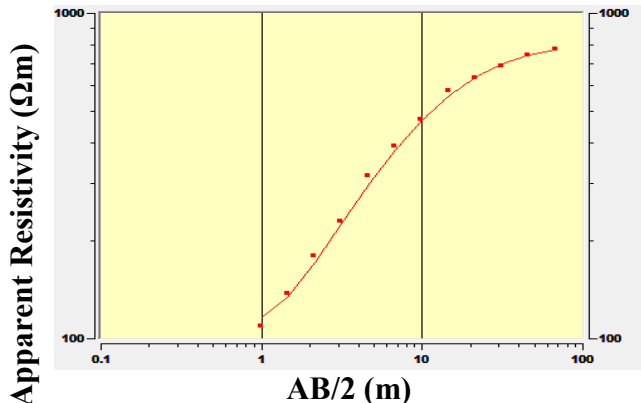


Thickness	Resistivity	Long. Conductance	Trans. Resist.
<hr/>			
1.0	120.8	0.00828	120.8
3.5	27.1	0.1291	94.9
Infinite	510.9		



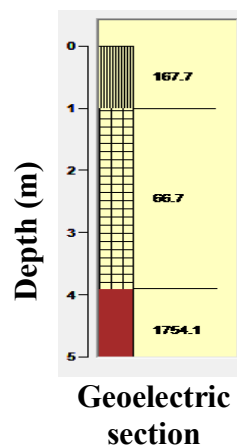
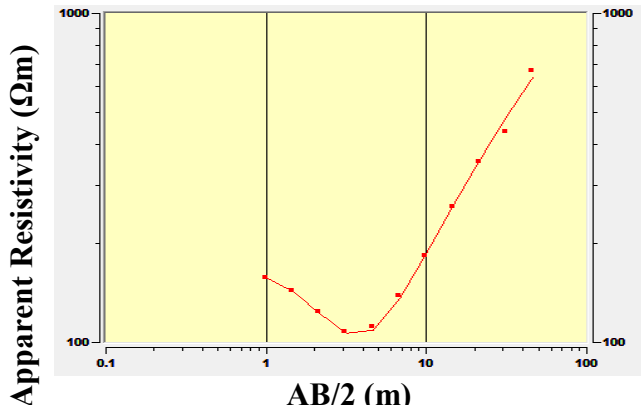
Thickness	Resistivity	Long. Conductance	Trans. Resist.
1.1	101.9	0.0108	
Infinite	806.0		112.1

VES 69

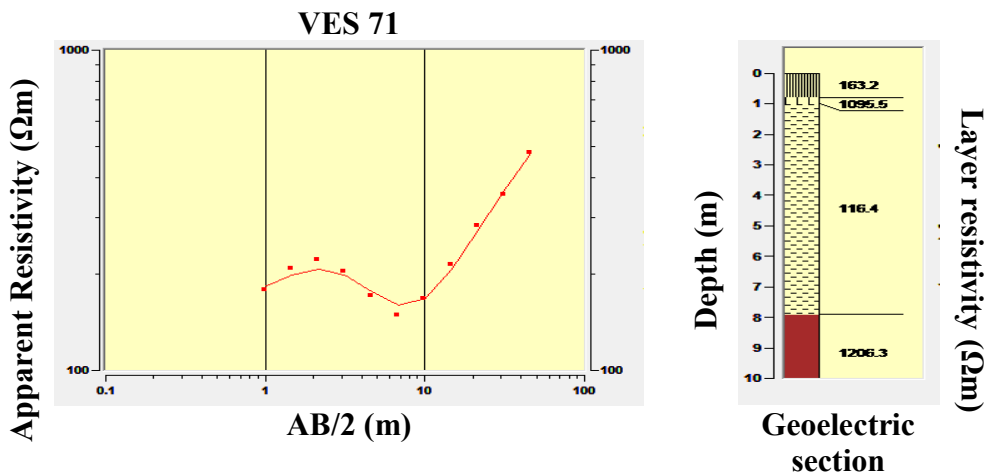


Thickness	Resistivity	Long. Conductance	Trans. Resist.
1.0	167.7	0.00596	
2.9	66.7	0.04346	
Infinite	1754.1		167.7 193.5

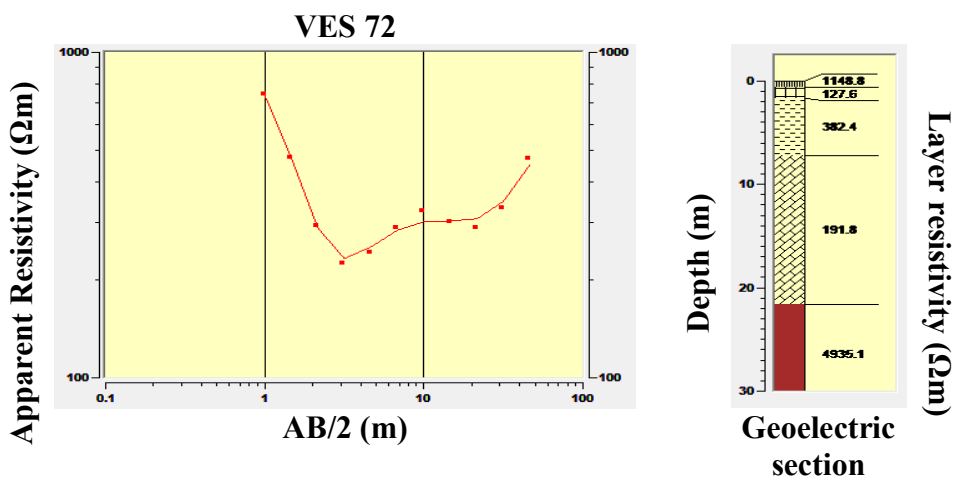
VES 70



Thickness	Resistivity	Long. Conductance	Trans. Resist.
0.8	163.2	0.0049	130.5
0.2	1095.5	0.00018	219.1
6.9	116.4	0.0593	802.9
Infinite	1206.3		

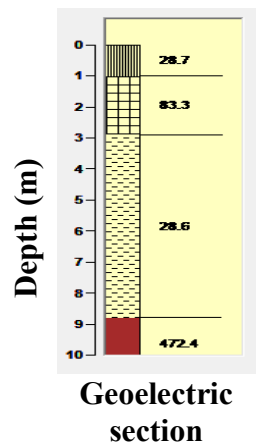
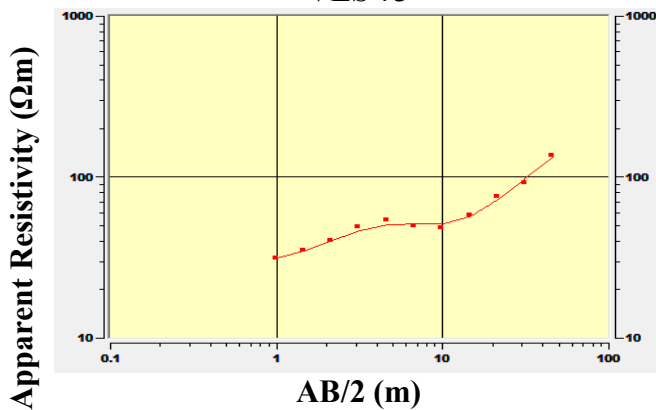


Thickness	Resistivity	Long. Conductance	Trans. Resist.
0.6	1148.8	0.00052	689.3
1.1	127.6	0.00862	140.4
5.5	382.4	0.01438	2103.4
14.4	191.8	0.07506	2762.6
Infinite	4935.1		



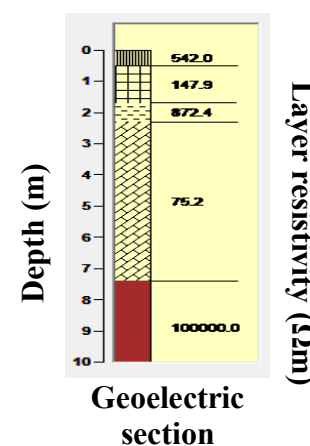
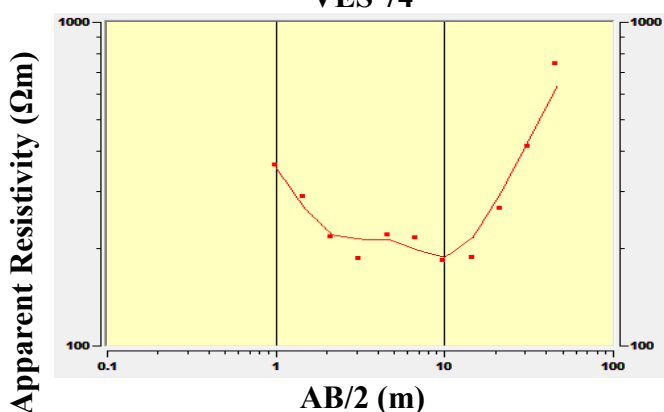
Thickness	Resistivity	Long. Conductance	Trans. Resist.
1.0	28.7	0.03487	28.7
1.9	83.3	0.0228	158.3
5.9	28.6	0.20655	168.5
Infinite	472.4		

VES 73



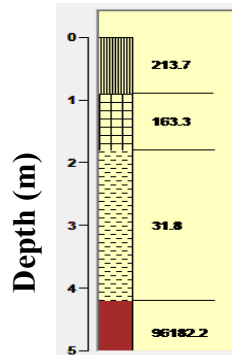
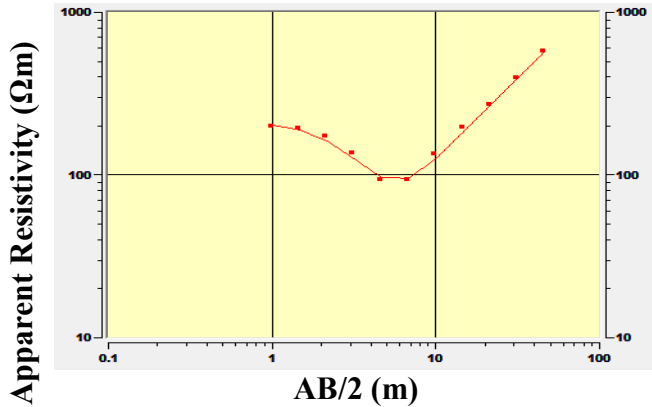
Thickness	Resistivity	Long. Conductance	Trans. Resist.
0.5	542.0	0.00092	271.0
1.2	147.9	0.00811	177.5
0.6	872.4	0.00069	523.4
5.1	75.2	0.06778	383.7
Infinite	100000.		

VES 74



Thickness	Resistivity	Long. Conductance	Trans. Resist.
0.9	213.7	0.00421	192.4
0.9	163.3	0.00551	147.0
2.4	31.8	0.07554	76.3
Infinite	96182.2		

VES 75

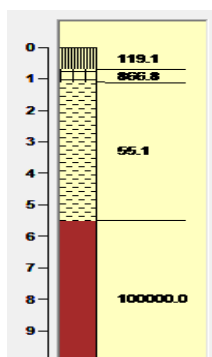
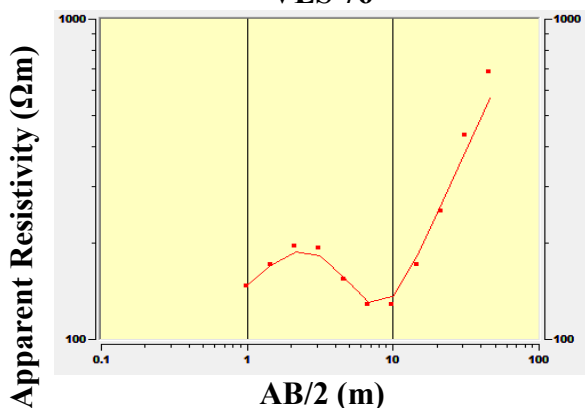


Layer resistivity (Ωm)

Geoelectric section

Thickness	Resistivity	Long. Conductance	Trans. Resist.
0.7	119.1	0.00588	83.4
0.4	866.8	0.00046	346.7
4.4	55.1	0.07992	242.2
Infinite	100000.		

VES 76

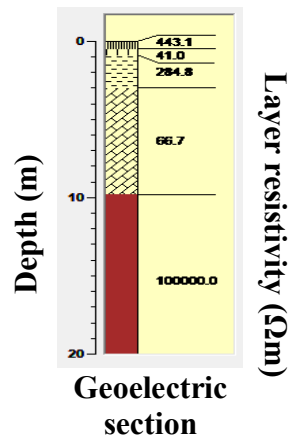
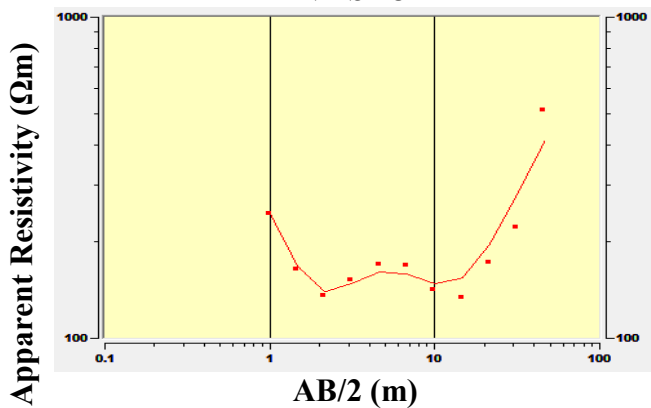


Layer resistivity (Ωm)

Geoelectric section

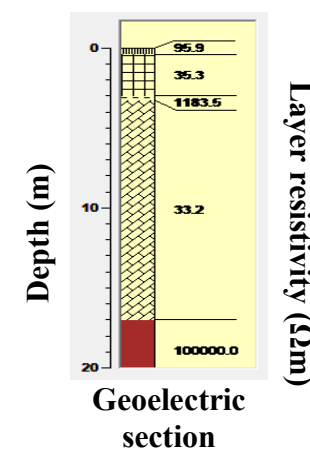
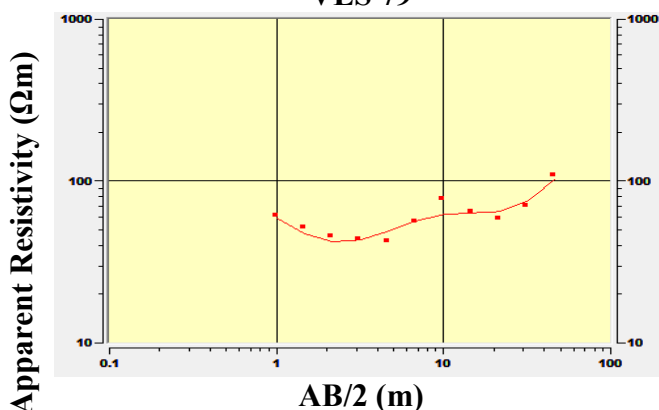
Thickness	Resistivity	Long. Conductance	Trans. Resist.
0.5	443.1	0.00113	221.5
0.4	41.0	0.00976	16.4
2.1	284.8	0.00737	598.0
6.8	66.7	0.10187	453.9
Infinite	100000.		

VES 78



Thickness	Resistivity	Long. Conductance	Trans. Resist.
0.4	95.9	0.00417	38.3
2.6	35.3	0.07357	91.9
0.3	1183.5	0.00025	355.1
13.7	33.2	0.41258	454.9
Infinite	100000.		

VES 79



APPENDIX - MULTIVARIATE REGRESSION ANALYSIS: R Code

R CODE FOR MEAN VALUES

```
names(data1)  
  
[1] "ANISO" "RESIS" "THICK" "YIELD"  
  
> model1 <- lm(YIELD~ANISO+RESIS+THICK, data=data1)
```

> model1

Call:

```
lm(formula = YIELD ~ ANISO + RESIS + THICK, data = data1)
```

Coefficients:

(Intercept)	ANISO	RESIS	THICK
1.229e+00	3.232e-02	1.346e-04	-2.928e-05

```
> summary(model1)
```

Call:

```
lm(formula = YIELD ~ ANISO + RESIS + THICK, data = data1)
```

Residuals:

Min	1Q	Median	3Q	Max
-0.226797	-0.007906	-0.001034	0.007026	0.206298

Coefficients:

	Estimate	Std. Error	t value	Pr(> t)
(Intercept)	1.229e+00	2.656e-03	462.903	<2e-16 ***
ANISO	3.232e-02	1.710e-03	18.903	<2e-16 ***
RESIS	1.346e-04	7.871e-06	17.102	<2e-16 ***
THICK	-2.928e-05	4.521e-05	-0.648	0.517

Signif. codes: 0 ‘***’ 0.001 ‘**’ 0.01 ‘*’ 0.05 ‘.’ 0.1 ‘ ’ 1

Residual standard error: 0.02306 on 8096 degrees of freedom

Multiple R-squared: 0.05751, Adjusted R-squared: 0.05716

F-statistic: 164.7 on 3 and 8096 DF, p-value: < 2.2e-16

99.73%-RCODE

names(data1)

[1] "ANISO" "RESIS" "THICK" "YIELD"

> model1 <-lm(YIELD~ANISO+RESIS+THICK, data=data1)

> model1

Call:

lm(formula = YIELD ~ ANISO + RESIS + THICK, data = data1)

Coefficients:

(Intercept) ANISO RESIS THICK

1.4659919 0.0484777 0.0001542 0.0003285

> summary(model1)

Call:

lm(formula = YIELD ~ ANISO + RESIS + THICK, data = data1)

Residuals:

Min 1Q Median 3Q Max

-0.39554 -0.00834 -0.00049 0.00874 0.13460

Coefficients:

Estimate Std. Error t value Pr(>|t|)

(Intercept) 1.466e+00 3.363e-03 435.907 < 2e-16 ***

ANISO 4.848e-02 1.208e-03 40.140 < 2e-16 ***

RESIS 1.542e-04 7.610e-06 20.255 < 2e-16 ***

THICK 3.285e-04 5.025e-05 6.537 6.64e-11 ***

Signif. codes: 0 ‘***’ 0.001 ‘**’ 0.01 ‘*’ 0.05 ‘.’ 0.1 ‘ ’ 1

Residual standard error: 0.02683 on 8096 degrees of freedom

Multiple R-squared: 0.3432, Adjusted R-squared: 0.343

F-statistic: 1410 on 3 and 8096 DF, p-value: < 2.2e-16

95.45%-RCODE

names(data1)

[1] "ANISO" "RESIS" "THICK" "YIELD"

> model1 <- lm(YIELD ~ ANISO + RESIS + THICK, data = data1)

> model1

Call:

lm(formula = YIELD ~ ANISO + RESIS + THICK, data = data1)

Coefficients:

(Intercept) ANISO RESIS THICK

1.3913410 0.0437027 0.0001594 0.0002502

> summary(model1)

Call:

```
lm(formula = YIELD ~ ANISO + RESIS + THICK, data = data1)
```

Residuals:

Min	1Q	Median	3Q	Max
-0.34403	-0.00741	-0.00016	0.00760	0.14570

Coefficients:

	Estimate	Std. Error	t value	Pr(> t)
(Intercept)	1.391e+00	3.289e-03	423.042	< 2e-16 ***
ANISO	4.370e-02	1.294e-03	33.778	< 2e-16 ***
RESIS	1.594e-04	7.106e-06	22.432	< 2e-16 ***
THICK	2.502e-04	4.711e-05	5.312	1.11e-07 ***

Signif. codes: 0 ‘***’ 0.001 ‘**’ 0.01 ‘*’ 0.05 ‘.’ 0.1 ‘ ’ 1

Residual standard error: 0.02472 on 8096 degrees of freedom

Multiple R-squared: 0.2258, Adjusted R-squared: 0.2255

F-statistic: 787.1 on 3 and 8096 DF, p-value: < 2.2e-16

68.37%-RCODE

```
names(data1)
```

```
[1] "ANISO" "RESIS" "THICK" "YIELD"
```

```
> model1 <- lm(YIELD~ANISO+RESIS+THICK, data=data1)
```

```
> model1
```

Call:

```
lm(formula = YIELD ~ ANISO + RESIS + THICK, data = data1)
```

Coefficients:

(Intercept)	ANISO	RESIS	THICK
-------------	-------	-------	-------

1.319e+00	3.625e-02	1.509e-04	9.555e-05
-----------	-----------	-----------	-----------

```
> summary(model1)
```

Call:

```
lm(formula = YIELD ~ ANISO + RESIS + THICK, data = data1)
```

Residuals:

Min	1Q	Median	3Q	Max
-----	----	--------	----	-----

-0.290841	-0.007082	-0.000249	0.007026	0.168997
-----------	-----------	-----------	----------	----------

Coefficients:

Estimate	Std. Error	t value	Pr(> t)
----------	------------	---------	----------

(Intercept)	1.319e+00	3.273e-03	402.903	<2e-16 ***
-------------	-----------	-----------	---------	------------

ANISO	3.625e-02	1.520e-03	23.849	<2e-16 ***
-------	-----------	-----------	--------	------------

RESIS	1.509e-04	7.101e-06	21.257	<2e-16 ***
-------	-----------	-----------	--------	------------

THICK	9.555e-05	4.584e-05	2.084	0.0372 *
-------	-----------	-----------	-------	----------

Signif. codes: 0 ‘***’ 0.001 ‘**’ 0.01 ‘*’ 0.05 ‘.’ 0.1 ‘ ’ 1

Residual standard error: 0.02339 on 8096 degrees of freedom

Multiple R-squared: 0.1064, Adjusted R-squared: 0.106

F-statistic: 321.2 on 3 and 8096 DF, p-value: < 2.2e-16

31.63%-RCODE

names(data2)

[1] "ANISO" "RESIS" "THICK" "YIELD"

> model2 <-lm(YIELD~ANISO+RESIS+THICK, data=data2)

> model2

Call:

lm(formula = YIELD ~ ANISO + RESIS + THICK, data = data2)

Coefficients:

(Intercept) ANISO RESIS THICK

1.119e+00 4.399e-02 1.631e-04 4.566e-07

> summary(model2)

Call:

lm(formula = YIELD ~ ANISO + RESIS + THICK, data = data2)

Residuals:

Min 1Q Median 3Q Max

-0.166245 -0.009008 -0.001369 0.007124 0.263069

Coefficients:

Estimate Std. Error t value Pr(>|t|)

(Intercept) 1.119e+00 1.210e-03 924.69 <2e-16 ***

ANISO 4.399e-02 1.452e-03 30.29 <2e-16 ***

RESIS 1.631e-04 8.315e-06 19.61 <2e-16 ***

THICK 4.566e-07 4.358e-05 0.01 0.992

Signif. codes: 0 ‘***’ 0.001 ‘**’ 0.01 ‘*’ 0.05 ‘.’ 0.1 ‘ ’ 1

Residual standard error: 0.0239 on 8096 degrees of freedom

Multiple R-squared: 0.1161, Adjusted R-squared: 0.1158

F-statistic: 354.4 on 3 and 8096 DF, p-value: < 2.2e-16

4.55%-RCODE

names(data3)

[1] "ANISO" "RESIS" "THICK" "YIELD"

> model3 <- lm(YIELD ~ ANISO + RESIS + THICK, data = data3)

> model3

Call:

lm(formula = YIELD ~ ANISO + RESIS + THICK, data = data3)

Coefficients:

(Intercept) ANISO RESIS THICK

1.0249312 0.0530104 0.0001950 -0.0000729

> summary(model3)

Call:

lm(formula = YIELD ~ ANISO + RESIS + THICK, data = data3)

Residuals:

Min 1Q Median 3Q Max

-0.131997 -0.009854 -0.000544 0.007262 0.315148

Coefficients:

	Estimate	Std. Error	t value	Pr(> t)
--	----------	------------	---------	----------

(Intercept)	1.025e+00	4.960e-04	2066.208	<2e-16 ***
-------------	-----------	-----------	----------	------------

ANISO	5.301e-02	1.205e-03	43.984	<2e-16 ***
-------	-----------	-----------	--------	------------

RESIS	1.950e-04	8.524e-06	22.873	<2e-16 ***
-------	-----------	-----------	--------	------------

THICK	-7.290e-05	4.435e-05	-1.644	0.1
-------	------------	-----------	--------	-----

Signif. codes: 0 ‘***’ 0.001 ‘**’ 0.01 ‘*’ 0.05 ‘.’ 0.1 ‘ ’ 1

Residual standard error: 0.02554 on 8096 degrees of freedom

Multiple R-squared: 0.2396, Adjusted R-squared: 0.2393

F-statistic: 850.4 on 3 and 8096 DF, p-value: < 2.2e-16

0.3%-RCODE

```
names(data4)
```

```
[1] "ANISO" "RESIS" "THICK" "YIELD"
```

```
> model4 <- lm(YIELD ~ ANISO + RESIS + THICK, data = data4)
```

```
> model4
```

Call:

```
lm(formula = YIELD ~ ANISO + RESIS + THICK, data = data4)
```

Coefficients:

(Intercept)	ANISO	RESIS	THICK
-------------	-------	-------	-------

0.9398210	0.0582666	0.0002138	-0.0002317
-----------	-----------	-----------	------------

```
> summary(model4)
```

Call:

```
lm(formula = YIELD ~ ANISO + RESIS + THICK, data = data4)
```

Residuals:

Min	1Q	Median	3Q	Max
-0.13654	-0.01055	0.00009	0.00821	0.36468

Coefficients:

	Estimate	Std. Error	t value	Pr(> t)
(Intercept)	9.398e-01	7.717e-04	1217.835	< 2e-16 ***
ANISO	5.827e-02	1.120e-03	52.027	< 2e-16 ***
RESIS	2.138e-04	8.990e-06	23.778	< 2e-16 ***
THICK	-2.317e-04	4.708e-05	-4.922	8.76e-07 ***

Signif. codes: 0 ‘***’ 0.001 ‘**’ 0.01 ‘*’ 0.05 ‘.’ 0.1 ‘ ’ 1

Residual standard error: 0.02782 on 8096 degrees of freedom

Multiple R-squared: 0.3546, Adjusted R-squared: 0.3543

F-statistic: 1483 on 3 and 8096 DF, p-value: < 2.2e-16